Transport Canada / Transports Canada
Library and Information Centre /
Centre de Documentation GSLA
Ottawa, Canada K1A 0N5

TP 3405E

FINAL REPORT

CONCEPTS FOR ICEBREAKERS WITH INTEGRAL FLUID CUSHION BOW

Prepared For The:

TRANSPORTATION DEVELOPMENT CENTRE,
TRANSPORT CANADA

Prepared By:

MR. F.R. LIVINGSTONE
DR. M. F. GEORGE
DAVIS ENGINEERING LIMITED
CONSULTING ENGINEERS
OTTAWA, CANADA

DECEMBER 1981

"The contents of this report reflect the view of the Contractor and not necessarily the official views or policies of the Transportation Development Centre".

REPORT DOCUMENTATION FORM

1. Transport Canada Report No.	2. TDC Project No.	3. Recipient's Catalogue No.
TP 3405E	4293	

4. Title and Subtitle	5. Report Date
Concepts for Icebreakers with Integral Fluid Cushion Bow	December 1981
	6. Performing Organization Report No.

7. Author(s)	8. Transport Canada File No.
F.R. Livingstone Dr. M.F. George	D1460-149

9. Performing Organization Name and Address	10. DSS File No.
Davis Engineering Limited, 1481 Cyrville Road, Ottawa, Ontario K1B 3L7	T8200-1-1502
	11. DSS or Transport Canada Contract No. OSD81-00047

12. Sponsoring Agency Name and Address	13. Type of Report and Period Covered
Transportation Development Centre (TDC) 1000 Sherbrooke Street West Montreal, P.Q. H3A 2R3	Final, July-October 1981
	14. Sponsoring Agency Code 4293

15. Supplementary Notes	16. TDC Project Officer
	J.E. Laframboise

17. Abstract

The results from the Transportation Development Centre program on Air Cushion Icebreaking Bow (ACIB) are briefly reviewed. The limitations of a separate air cushion vehicle placed in front of a ship are identified and the concept of an Integrated Fluid Cushion Bow (IFCB) introduced.

Three concepts for an Integrated Fluid Cushion Bow are then presented and their major features and limitations discussed. Finally a work plan is outlined for the investigation of the technical feasibility of the proposed concepts.

18. Key Words	19. Distribution Statement
Icebreakers, Air Cushion Bow Integrated Air Cushion Icebreakers Air Cushion, Fluid Cushion	Limited number of copies available at TDC

20. Security Classification (of this report)	21. Security Classification (of this page)	22. No. of Pages	23. Price
Nil	Nil	85	-

FORMULE DE DOCUMENTATION POUR RAPPORT

1. Nº du rapport Transports Canada	2. Nº de l'étude — CDT	3. Nº de catalogue du destinataire
TP3405E	4293	

4. Titre et sous-titre	5. Date du rapport
Concepts For Icebreakers With Integral Fluid Cushion Bow	Décembre 1981
	6. Nº du rapport de l'organisme exécutant

7. Auteur(s)	8. Nº de dossier Transports Canada
F.R. Livingstone, Dr. M.F. George	D1460-149

9. Nom et adresse de l'organisme exécutant	10. Nº de dossier — ASC
Davis Engineering Limited 1481 Cyrville Road Ottawa, Ontario K1B 3L7	T8200-1-1502
	11. Nº de contrat — ASC ou Transports Canada OSD81-00047

12. Nom et adresse de l'organisme parrain	13. Genre de rapport et période visée
Centre de développement des transports (CDT) 1000 ouest, rue Sherbrooke C.P. 549, Place de l'aviation Montréal, Québec H3A 2R3	Final, juillet-octobre 1981
	14. Code de l'organisme parrain 4293

15. Remarques additionnelles	16. Agent de projet — CDT
	J.E. Laframboise

17. Résumé

Les résultats du programme du Centre de développement des transports sur les proues brise-glaces à coussin d'air sont revus sommairement. Les limites opérationnelles d'un véhicule séparé placé à l'avant d'un navire sont identifiées et le concept d'un coussin fluide intégré à la proue est introduit.

Trois concepts pour un coussin fluide intégré sont présentés par la suite et leurs caractéristiques et leurs limites sont évaluées.

Finalement, un plan de travail est proposé pour une évaluation de la faisabilité technique des concepts proposés.

18. Mots-clés	19. Diffusion
Brise-glace, Proue à coussin d'air, Brise-glace à coussin d'air intégré, coussin d'air, coussin fluide	Un nombre limité de copie est disponible au CDT

20. Classification de sécurité (de ce rapport)	21. Classification de sécurité (de cette page)	22. Nombre de pages	23. Prix
Nil	Nil	85	-

SUMMARY

The objective of this study is to define preliminary concepts for integration of a fluid cushion (air or water) into the bow of an icebreaker, and to provide a work plan for the theoretical and experimental analysis of the recommended concept.

The general objective is to achieve a reduction of the energy required by icebreakers when breaking an ice cover.

This report presents three conceptual designs for integrating the fluid cushion icebreaking principles into a ship. These concepts are:

Concept I:	Extended Bow with Air Cushion/Water Curtain
Concept II:	Twin-Bow Arrangement
Concept III:	Conventional Bow with Air Cushion/Water Curtain Principles

Analogy is then made between the Air Cushion Icebreaker Bow (ACIB) configurations and the proposed concepts for preliminary evaluation. The idea of using water jets for ice cutting is also pursued and the limitations are identified.

A preliminary dynamic analysis of a "water curtain" is carried out and the parameters affecting both the structure of the jet stream and its configuration, under static condition, are outlined.

Finally, a work plan is presented for the follow-on study which includes both the theoretical and experimental analysis for the three concepts. As a result of this proposed follow-on study, Davis Engineering will be in a position to recommend a particular concept to the Transportation Development Centre (TDC). Meanwhile, in light of the present limited study, Concept I is likely to be recommended for Arctic operations, while Concept II may be suitable for icebreaking in light ice conditions, and Concept III for enhancing the icebreaking capabilities of existing vessels in their prospective classes.

The present study is the first in a six-step program being considered by TDC. The investigation, when completed, will ultimately result in a trial of an Arctic icebreaker using the recommended system.

SOMMAIRE

L'objectif de l'étude est la définition préliminaire de concepts pour l'intégration dans une proue de brise-glace d'un coussin fluide (air ou eau) et de présenter un plan de travail pour l'analyse théorique et expérimentale du concept recommandé.

L'objectif primordial est la réduction de l'énergie requise par un brise-glace pour réduire un couvert de glace.

Ce rapport présente trois concepts d'intégration:

Concept I: Proue allongée avec coussin d'air et voile d'eau
Concept II: Proue à redan et jupes frontales
Concept III: Proue conventionnelle avec coussin d'air et voile d'eau

L'évaluation préliminaire compare la plateforme brise-glace à coussin d'air aux trois concepts proposés. Pour référence on étudie le découpage de la glace à l'aide d'eau à haute pression.

Une analyse préliminaire d'un voile d'eau pour contenir le coussin d'air, plutôt que d'utiliser des jupes souples, conduit à déterminer les paramètres d'importance pour sa réalisation.

Finalement, un plan de travail est présenté pour étude subséquente, incluant l'analyse théorique et expérimentale des trois concepts proposés. Par la suite, Davis Engineering serait en mesure de recommander au Centre de développement des transports (CDT) un concept particulier. Présentement il semble que le Concept I soit recommandable pour les opérations dans l'arctique tandis que le Concept II serait utilisable pour les glaces moins ardues, et que le Concept III pourrait être utilisé pour améliorer les performances de brise-glaces existants de diverses catégories.

Cette étude est la première phase d'un programme en six phases envisagé par le CDT. L'essai d'un brise-glace de classe Arctique serait le point culminant de ce programme.

TABLE OF CONTENTS

SUMMARY			v
1.	INTRODUCTION		1
	1.1	General	1
	1.2	Ice Resistance	3
	1.3	Power Prediction	8
2.	AIR CUSHION ICEBREAKING PLATFORMS (ACIB)		12
	2.1	General	12
	2.2	Performance Evaluation of ACIB	14
	2.3	Icebreaking Mechanisms	21
	2.3.1	High Speed	21
	2.3.2	Low Speed	21
	2.4	ACIB Limitations and Practicality	22
3.	INTEGRATED FLUID CUSHION BOW (IFCB)		27
4.	DESIGN CRITERIA FOR ARCTIC CLASS ICEBREAKERS WITH IFCB		29
	4.1	Evaluation Criteria	29
	4.2	Design Parameters of Arctic IFCB	31
5.	PROPOSED CONCEPTUAL DESIGNS		32
	5.1	Concept I: Extended Bow with Air Cushion/Water Curtain	32
	5.2	Concept II: Twin-bow Arrangement	34
	5.3	Concept III: Conventional Bow with Air Cushion/Water Curtain Principles	36
6.	WATER JETS		41
	6.1	Ice Cutting with Water Jets	41
	6.2	Water Curtain	45
	6.2.1	Air Curtain Roof - "Dynamic Structure"	46
	6.2.2	Dynamics of Water Curtain	47
7.	GENERAL EVALUATION OF THE PROPOSED CONCEPTS		58
	7.1	Energy Requirements	58
	7.2	Limitations and Technical Difficulties	61
	7.2.1	Skirts	62
	7.2.2	Stability of Jet Sheets (Water Curtain)	62
	7.2.3	Noise Radiation	63
	7.2.4	Spray	63
	7.3	Preliminary Assessment of the Recommended Concept (CONCEPT I)	63
	7.3.1	Ice Fracture with Air Bubble Formation	64
	7.3.2	Ice Fracture without Air Bubble Formation	70

TABLE OF CONTENTS
(Cont'd)

8. PROPOSAL FOR A FEASIBILITY STUDY OF AN ICEBREAKER WITH AN INTEGRAL FLUID CUSHION BOW 74
8.1 Work Plan 74
8.2 Project Team 82
8.3 Estimated Project Cost 84

REFERENCES 85

Appendix A Estimation of Water Jet Velocity and Power Required for Water Curtain 86

LIST OF FIGURES

Figure 1	Icebreaker Speed of Advance as a Function of Ice Thickness, Showing Relative Importance of Icebreaking Modes (1)	2
Figure 2	Mean Predicted Value of Resistance per Unit Width as a Function of Ice Thickness (Existing Icebreakers Operating at 3 Knots)	5
Figure 3	Process Specific Energy as a Function of Ice Thickness (Existing Icebreakers for Operation at 3 Knots)	6
Figure 4	Thrust Power Vs. Volumetric Icebreaking Rate (Existing Icebreakers for Operation at 3 Knots)	7
Figure 5	Available Thrust as a Function of Shaft Power (Existing Icebreakers for Operation at 3 Knots)	9
Figure 6	Shaft Power Vs. Volumetric Icebreaking Rate (Existing Icebreakers Operating at 3 Knots)	11
Figure 7	Air Cushion Platform Configurations and Resultant Ice Rupture in Cavity at Low Speed	15
Figure 8	Thrust Required and Thrust Available at Various Horsepower Vs. Speed (1)	20
Figure 9	Comparison of Crack Analysis Procedures	24
Figure 10	Low Speed Icebreaking Parameters (4)	25
Figure 11	Low Speed Icebreaking Mechanisms	26
Figure 12	Concept I: Extended Bow with Air Cushion/Water Curtain Integral Fluid Cushion Bow	33
Figure 13	Concept II: Twin-Bow Arrangement Integral Fluid Cushion Bow	35
Figure 14	Concept III: Conventional Bow with Air Cushion/Water Curtain Integral Fluid Cushion Bow	37
Figure 15	Preliminary Sketch of Structural Arrangement	39
Figure 16	Concept I: Extended Bow with Air Cushion/Water Curtain Structural Arrangement	40
Figure 17	Required Nozzle Pressure and Power as a Function of Nozzle Diameter for Two Different Performance Specifications	42
Figure 18	Polar Icebreaker Required Nozzle Pressure and Power Vs. Nozzle Diameter (6 ft of ice(3))	44
Figure 19	An Element of the Water Curtain	50
Figure 20	Continuity for Elemental Control Volume within the Water Curtain	51

LIST OF FIGURES
(Cont'd)

Figure 21	Forces on a Fluid Element of the Water Curtain	54
Figure 22	Jet Inclination	57
Figure 23	Sketch for Ice Fracture with Air Bubble Formation	64
Figure 24	Ice Failure Ahead of the Bubble Leading Edge	65
Figure 25	Simplified Sketch for the Cushion Bow in the Proposed Concept (I)	66
Figure 26	Perimeter/Beam Ratio Vs. Chord/Beam Ratio for the Cushion Bow as a Swept Module	68
Figure 27	Wave Drag of Three ACV Planforms	69
Figure 28	Ice Wedge with Uniform Load (No Air Bubble Formation)	71
Figure 29	Proposed Work Plan for Follow-on Study	83

LIST OF TABLES

Table 1	Main Particulars of Tested Vessels	17
Table 2	Energy Requirements for a Vessel with IFCB	58

1. INTRODUCTION

1.1 General

Icebreakers break ice by virtue of their weight and power. Therefore, the conventional approach to improve icebreaking capability is to increase these parameters. In addition, improvements to hull form and bow shape have been made.

This approach obviously has its own limitations, such as hull strength requirements, material specifications, and the rapid increase in propulsion required to break thicker ice covers.

In the last few years a great deal of testing and analysis has been done to substantiate the hypothesis that an air cushion vehicle (ACV) will progress continually through intact uniform ice cover, breaking it as an icebreaker, provided that certain design conditions are met.

Before we study the icebreaking mechanisms under an ACV, it is advisable to outline first the modes of icebreaking of conventional icebreakers and to assess the ice resistance and powering of existing icebreakers as a basis for comparison and evaluation of any new concept.

Icebreaking by conventional icebreakers may be envisioned to take place in two distinct modes. The first is that commonly referred to as the "continuous" mode. The ice in this mode is relatively thin and forward motion is maintained after ice failure; power is predominant in this mode. The second mode of icebreaking is "ramming", where the ship rams very thick ice at the highest possible velocity; momentum is predominant in this mode. Between these two modes, there is the transition region.

Figure 1 shows the relative importance of icebreaking modes, assuming full power is always employed for a typical icebreaker. The measure of effectiveness was obtained from the product of ice thickness and speed through the ice. This product, with units of metre-kilometre of ice broken per hour, indicates the amount of ice broken per unit time. From Figure 1, it is clear that the measure of effectiveness is maximum in the "continuous" mode icebreaking. For this reason, the "continuous" icebreaking mode should receive more attention and consideration than the "ramming" mode in the development of new icebreaking concepts.

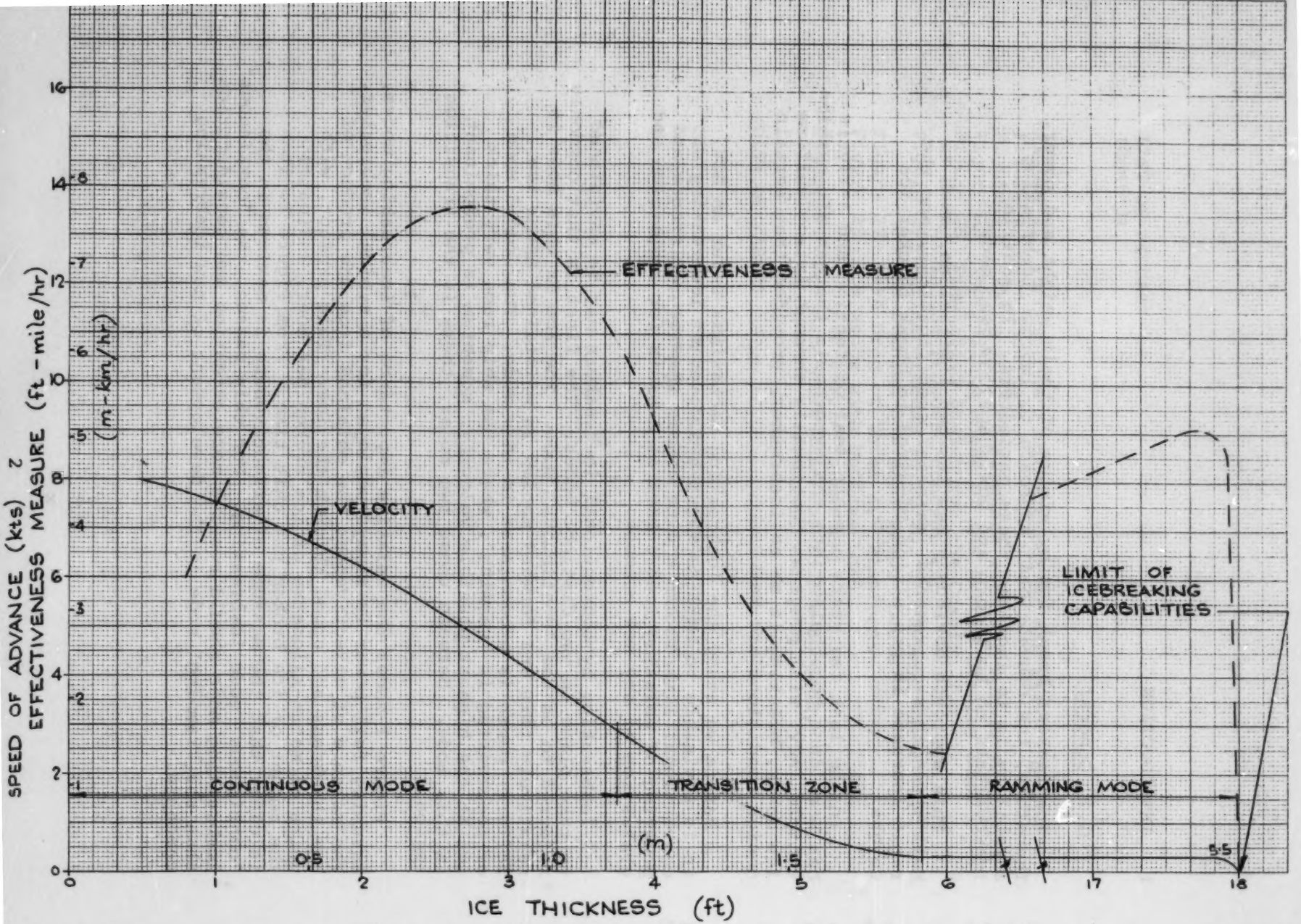

Figure 1 Icebreaker Speed-of-Advance as a Function of Ice Thickness, Showing Relative Importance of Icebreaking Modes (1)

Another point of interest is the icebreaking mechanism itself. Icebreaking by the bow of a ship is a smooth mechanical process. The icebreaker rides onto the ice sheet and breaks it under its weight. The vertical force created by the forebody is a function of the angles of the stem, waterline and station flare. The ratio between the applied vertical rupture force and the available ship thrust (or total ice resistance) may be taken as an effective criterion in judging the bow performance and, consequently, the icebreaking capability of the vessel. This ratio, which is sometimes referred to as Hull Transform Ratio (HTR), is about 1.0 for conventional icebreakers.

The study of the detailed dynamics of the icebreaking process is, however, complicated. During the "continuous" mode operation, the icebreaking process may be considered discontinuous. The forces needed to break the ice, to accelerate the ice fragment and to move the fragments against hydrodynamic resistance all fluctuate. However, the ship by virtue of its large mass, tends to proceed with approximately constant speed with minimum thrust fluctuation. Under a steady continuous motion, the developed thrust would have to be equal to the total ice resistance.

1.2 Ice Resistance

As mentioned above, the ice resistance R_T can be equated to the summation of four components which are:

a. breaking the ice;
b. submerging the ice fragments;
c. accelerating and moving the ice fragments; and,
d. open water resistance.

The open water resistance is usually negligible in the ice resistance calculation. Furthermore, the force required to break the ice sheet is relatively small (about 15% or so) in comparison with the total ice resistance for a particular ship. Therefore, the resistance components b and c are the most energy dissipative components as far as the total ice resistance is concerned.

There are several analytical techniques and computer programs available to predict the ice resistance of a conventional icebreaker.

Resistance predictions based on Kashteljan equations, on Milano theory and on model test results have been compared in reference (3). The mean resistance (i.e., the mean value obtained by the three approaches) per unit width for 12 classes of ships at 3 knots (~1.5 m/s) continuous speed produced the data band shown in Figure 2 as a function of ice thickness. The mean line drawn through the data band can be represented by:

$$\frac{R_T}{1.1\ B} = 520\ t^{1.55}\ \text{lbf/ft} \qquad (1.1)$$

$$= (366.89\ t^{1.55}\ \text{N/m})$$

where R_T is the time-averaged total resistance in lbf (N)
t is ice thickness in ft (m)
B is beam in ft (m)

Formula 1.1 was obtained as a "best" fit to the existing conventional designs, which by themselves are not optimum or best designs. For a new concept, it may be useful to compare the performance on the basis of the volumetric icebreaker's capability, rather than the resistance. However, it is obvious that for the same available power, a design which would give maximum icebreaking rate is the one which would require minimum thrust or alternatively achieve maximum icebreaking speed.

If one defines the process specific energy, E_s, as the thrust power (=T·U), divided by the icebreaking volumetric rate $\dot{V}$ (=width of the broken channel (1.1B)·ice thickness t·ship speed U), then the compilation of the performances of the existing icebreakers would be as shown in Figure 3 (3). It is clear that E_s increases (i.e., less efficient) with increasing ice thickness t. Therefore, if one considers the ice thickness "t" shown in Figure 3 as the maximum ice thickness that an icebreaker can negotiate at 3 knots, then a light icebreaker would operate at a specific energy (E_s) of about 17 kN/m^2 (2.5 lbf/in^2), while a polar icebreaker (Class 7 for example) would operate at $E_s \approx 70$ kN/m^2 (10. lbf/in^2), and consequently, it can be expected to be less efficient than a light icebreaker. Figure 4 shows the relation between the thrust power versus the breaking rate ($\dot{V}$) for the existing icebreakers for three values of E_s, viz. 10, 5, and 2.5 lbf/in^2, all at 3 knots. For different icebreaking speeds, similar sets of curves can be produced provided that the performance for different classes of icebreakers at those speeds are known.

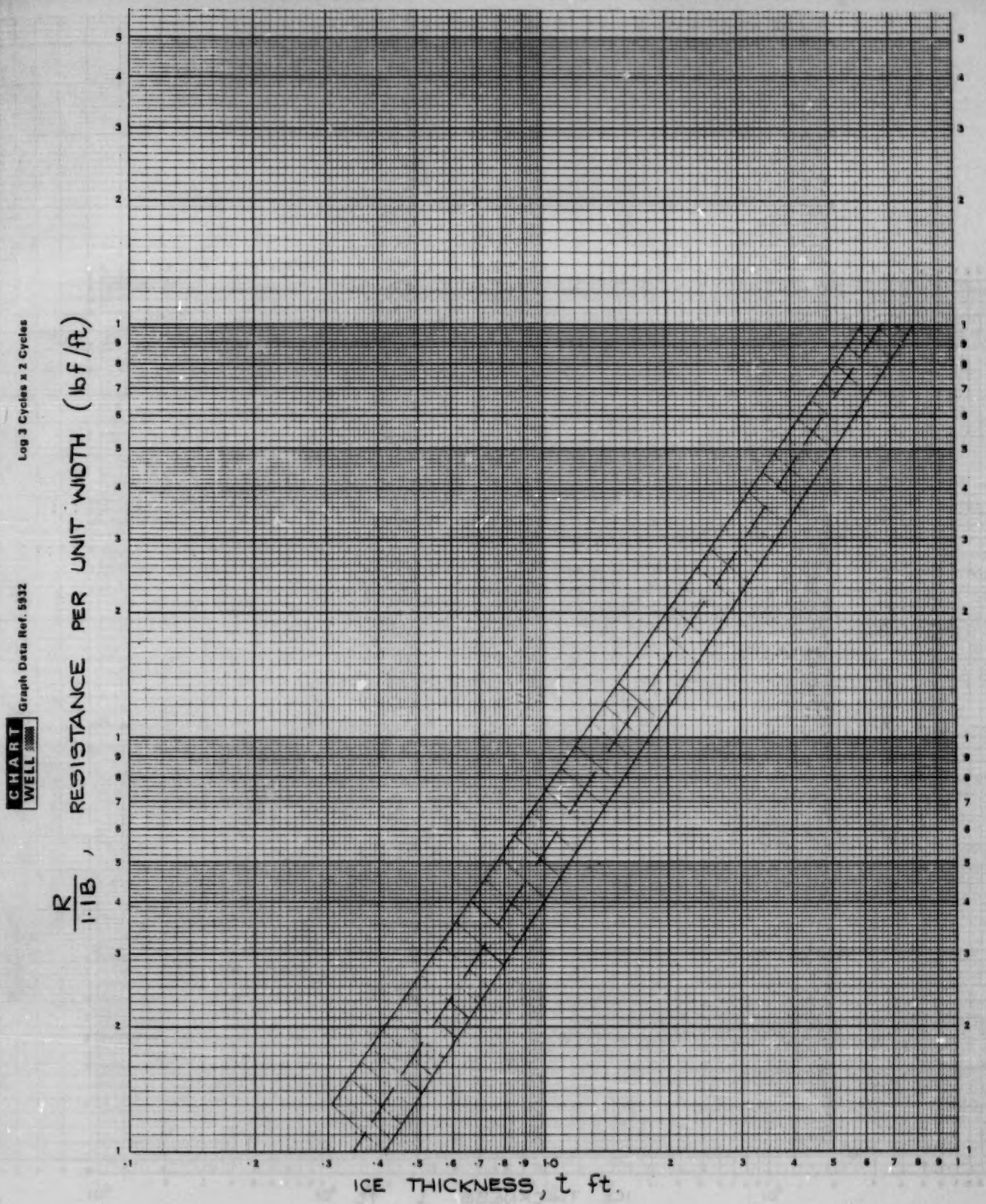

Figure 2 Mean Predicted Value of Resistance Per Unit Width as a Function of Ice Thickness (Existing Icebreakers Operating at 3 Knots)

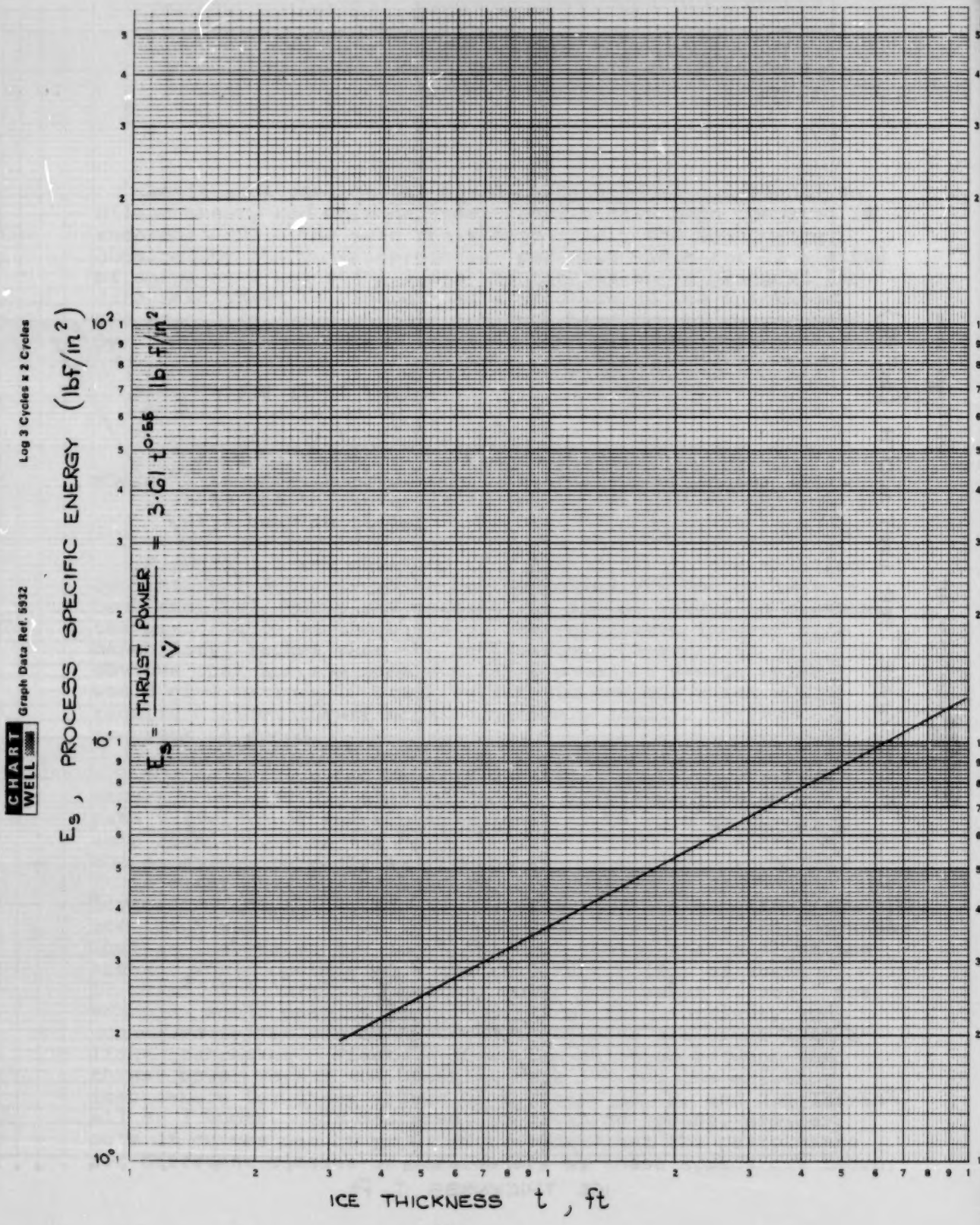
E_s , PROCESS SPECIFIC ENERGY (lbf/in^2)
$E_s = \frac{\text{THRUST POWER}}{\dot{V}} = 3.61\, t^{0.56}$ lb f/in^2
ICE THICKNESS t , ft
CHART WELL Graph Data Ref. 5932
Log 3 Cycles x 2 Cycles

Figure 3 Process Specific Energy as a Function of Ice Thickness (Existing Icebreakers Operating at 3 Knots)

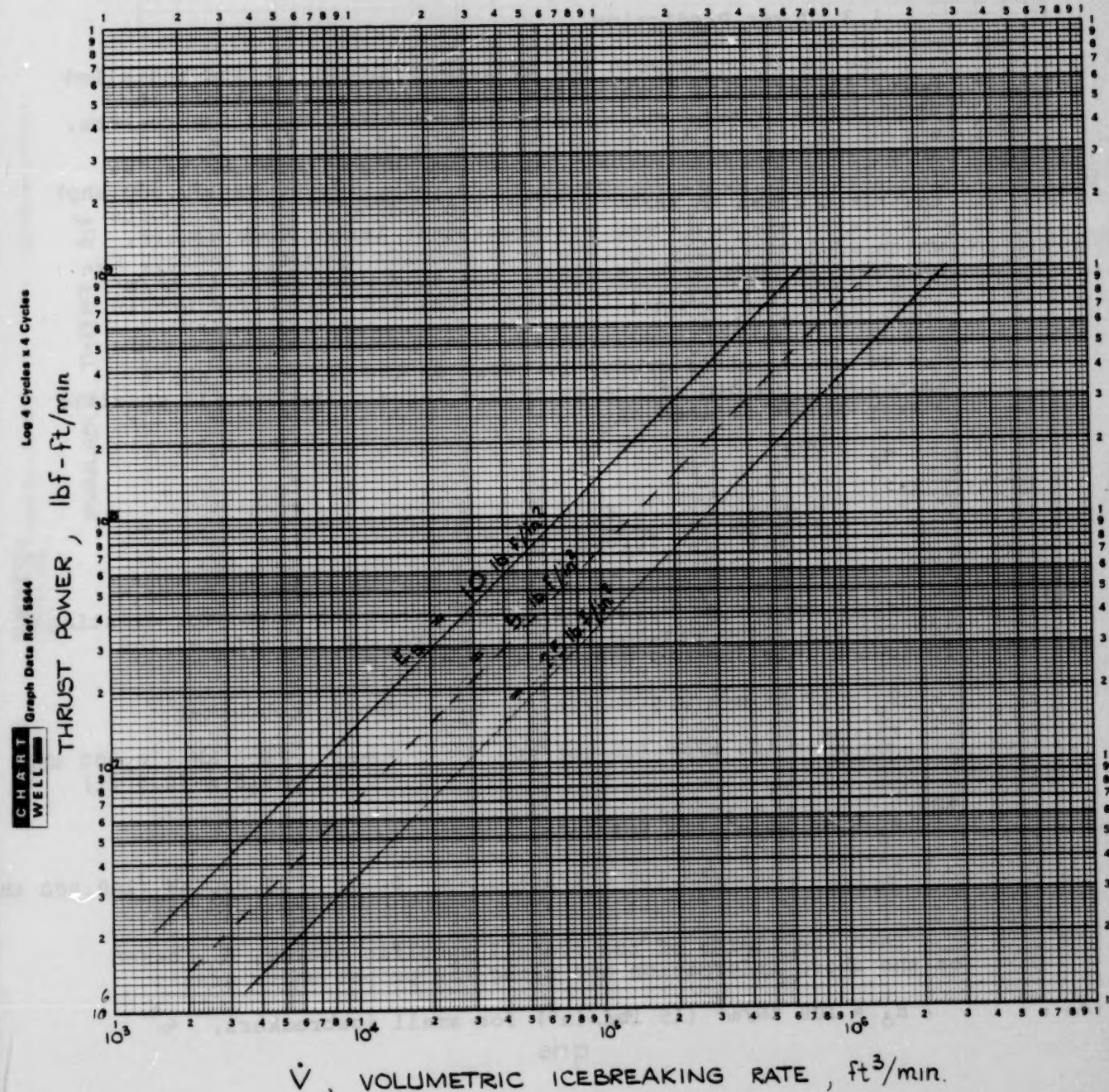

Figure 4 Thrust Power Vs. Volumetric Icebreaking Rate (Existing Icebreakers For Operation at 3 Knots)

For a given horsepower, as the maximum workable ice thickness decreases with increasing ship speed, the process specific energy also decreases.

1.3 Power Prediction

The relation between the available thrust (T) and installed power for existing icebreakers for operation at 3 knots is shown in Figure 5 (3). It is clear that for small icebreakers, say up to 7500 kW (10,000 shp) the thrust power ratio is about 100 N/kW (18 lbf/hp), while for larger icebreakers, as the installed power increases above, say, 22,000 kW (30,000 shp) the ratio drops to about 60 N/kW (10 lbf/hp). This supports the previously mentioned statement that larger icebreakers, which would normally operate at a process specific energy, E_s, of about 70 kN/m^2 (10 lbf/in^2), compared with about 17 kN/m^2 (2.5 lbf/in^2) for smaller icebreakers, are less efficient in breaking ice.

If the specific energy is based on the installed shaft horsepower instead of the available thrust, the overall specific energy can be defined as:

$$E_o = \frac{shp}{\dot{V}}$$

$$= \frac{T \cdot U \cdot shp}{T \cdot U \cdot \dot{V}} = \frac{E_s}{\frac{Thrust}{hp} \cdot U}$$

With the proper values of E_s and thrust/hp ratio for existing icebreakers (from Figures 3 and 5) operating at 3 knots, the following relationship can be derived:

$E_s \approx 17$ kN/m^2 (2.5 lbf/in^2)	Small Icebreaker
$\frac{Thrust}{Power} \approx 100$ N/kW (18 lbf/hp)	Power < 7500 kW (10,000 shp) t ≈ 0.15 m (0.5 ft)

and

$E_s \approx 70$ kN/m^2 (10 lbf/in^2)	Large Icebreaker
$\frac{Thrust}{Power} \approx 60$ N/kW (10 lbf/hp)	Power > 22,000 kW (100,000 shp) t ≈ 2 m (6 ft)

Then the limits of the overall specific energy, E_o, based on the above information and using the proper units are:

$E_o \approx 100$ kN/m^2 (15 lbf/in^2) for small icebreakers,

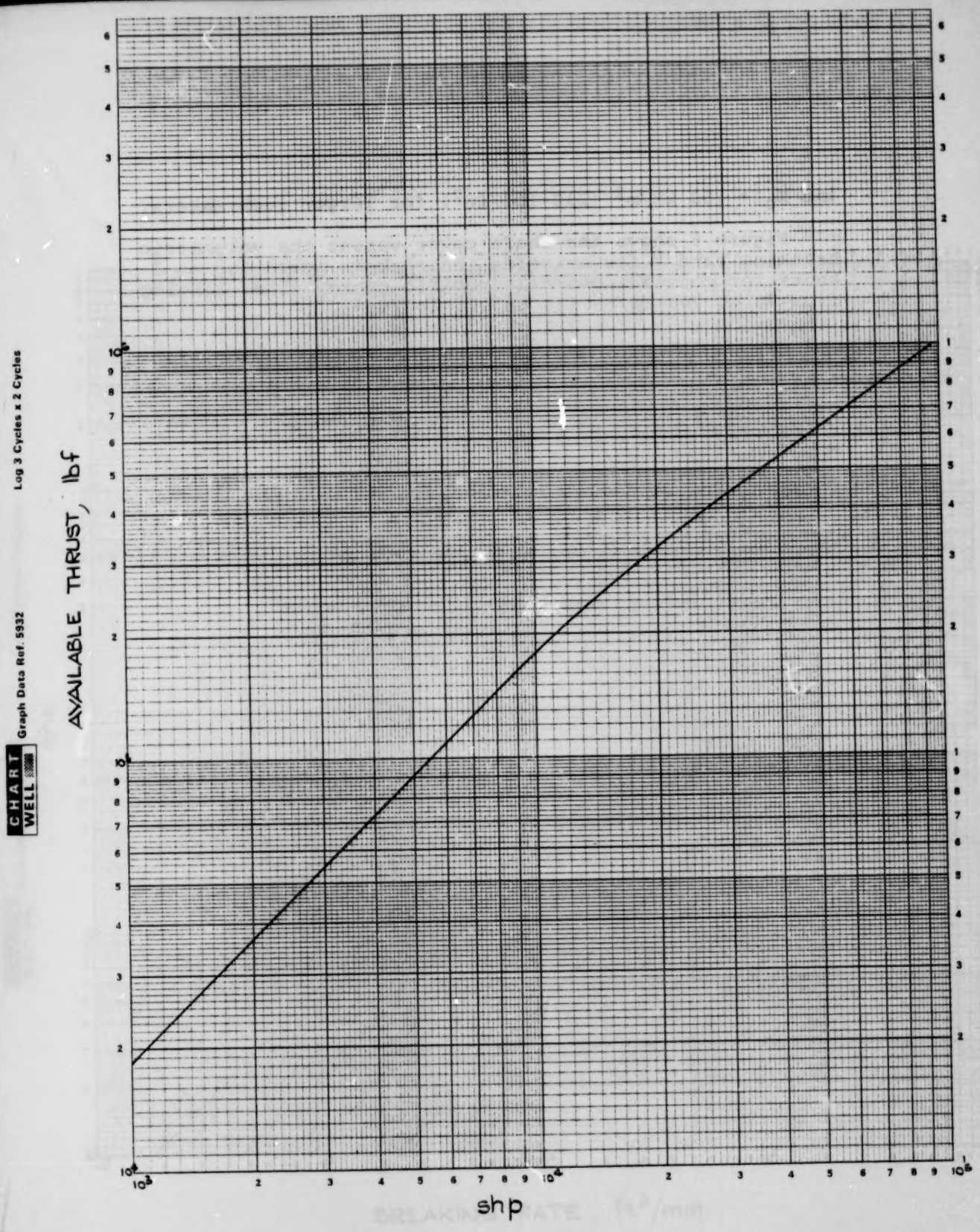

Figure 5 Available Thrust as a Function of Shaft Power (Existing Icebreakers for Operation at 3 Knots)

and $E_o \approx 750$ kN/m^2 (110 lbf/in^2) for larger icebreakers.

Figure 6 shows the shaft power versus the volumetric breaking rate $\dot{V}$ for existing icebreakers operating at 3 knots for constant overall specific energy lines ranging from 70 to 900 kN/m^2 (10 to 125 lbf/in^2).

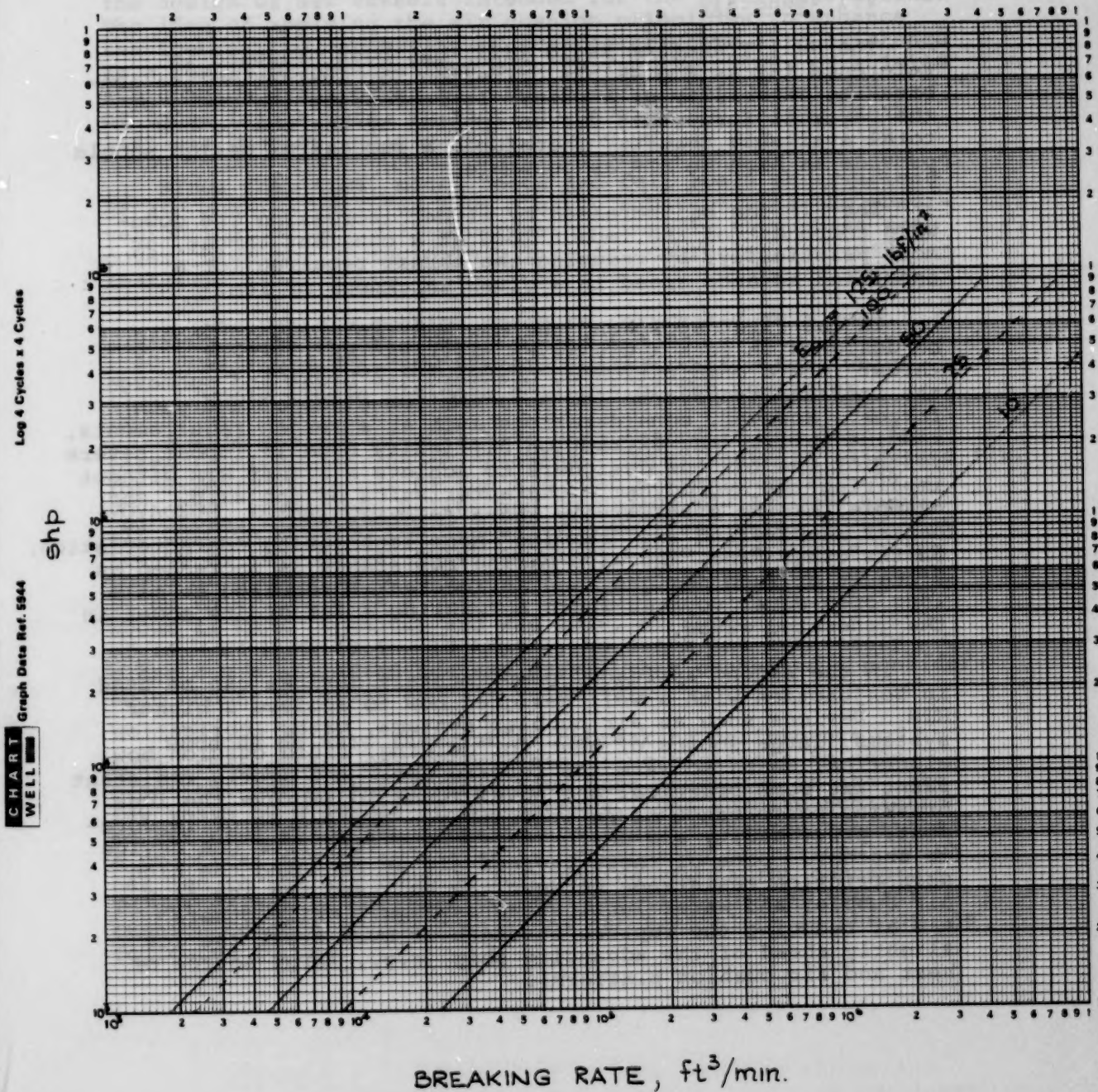

Figure 6 Shaft Power Vs. Volumetric Icebreaking Rate (Existing Icebreakers Operating at 3 Knots)

2. AIR CUSHION ICEBREAKING PLATFORMS (ACIB)

2.1 General

The Hull Transform Ratio (HTR) has been proposed in Reference (8) as a possible criterion for evaluating the ice-breaking capability of a ship. It represents the ratio of the vertical force that can be applied by the bow to the total available thrust. Therefore, a successful design should provide as high an HTR as possible.

The HTR can be increased by either increasing the downward component of the impact load at a constant thrust, or more practically, by reducing the thrust required for a specified advance speed in a given thickness of ice.

In the first approach, the bow and the forebody should be designed in such a way as to maximize the conversion of thrust into a combination of downward (to break and submerge the ice) and transverse (to move the ice clear of the path) forces. However, considerations such as strength requirements, ramming ability and extraction difficulty usually impose severe restrictions for the designers to achieve a higher HTR without impairing the hydrodynamic characteristics of the ship. For example, having a relatively short forebody would result in better maneuvering and "ramming" mode icebreaking characteristics. On the other hand, the wave-making resistance is increased as a result of such designs, and an icebreaker required to make long open-water voyages would be wasting a lot of its power in the generated waves.

In the second approach, complementary devices can be used in conjunction with a well designed bow to achieve a higher HTR. Devices such as air bubbler systems, water lubrication systems, large source of heat for deicing, fluid cushion bow, electrical means to warm the forward shell and arctic resistant paint are some practical and novel ideas to improve the ice-breaking performance of an icebreaker. The degree of improvement, practicality and design difficulty vary from one device to another. Some of these devices aim at reducing the high skin friction resistance between the hull and the ice (e.g., air bubbler and water lubricating systems), while others aim at reducing the rupture strength or even break the ice slightly ahead of the advancing ship (e.g., large source of heat and air cushion platform).

Among the above devices, air cushion platforms are the most promising and practical devices to be incorporated in the design of new vessels intended for the Arctic operations. The idea of applying the air cushion principles to enhance the icebreaking capability of icebreakers came into existance as a result of observations made during the trials of a large air cushion transporter ACT-100 in 1971. The objectives of those trials were, in fact, to develop and extend heavy lift air cushion vehicle (ACV) technology to oil drilling.

Since that time, model tests and full scale observations of air cushion vehicles have clearly substantiated the observation that an ACV will progress continually through an ice cover, breaking it thoroughly like an icebreaker provided that (7):

- the vehicle cushion pressure, expressed as a head, exceeds the ice cover depth; and,
- the weight of the vehicle exceeds that weight which would create ultimate collapse of the ice cover.

A wide variety of ACVs have been tested in the last few years in different ice thicknesses. Experiments in reference (7), for example, made use of the air cushion vehicles ACT-100, VOYAGEUR, TERRACROSS H-110, and HOVERJACK NJ-15. The heavy air cushion ACT-100 continuously broke fresh water first-year ice 68 cm (27 inches) thick on Great Slave Lake, while being towed at speeds up to 3.5 knots. VOYAGEUR was able to clear 24 cm thick ice with a cushion pressure of 25.4 cm water at about 11 km/h (6 knots) and was able, at speeds in the range of 16 - 24 km/h (8.6 - 13 knots), to crack and eventually clear 4.9 m of rafted ice and frazil that contained a considerable amount of slush and air voids (2).

Because of this favourable icebreaking performance of ACVs, theoretical and experimental investigations to make practical use of the concept have been conducted in the last few years by a number of researchers. The results published so far have shown the potential of the air cushion concept as a practical device to assist in icebreaking operations, which has led to the Air Cushion Icebreaking Bow (ACIB) concept. To put things in perspective, the practical use of the air cushion concept in ice conditions can take place in one of the following forms:

a) air cushion vehicles adapted for ice conditions as mode of transportation;
b) air cushion icebreakers assisting navigation in ice-covered waters (self-propelled, limited range, could be located at some strategic points along the route);
c) air cushion icebreaking platforms (ACIB) coupled to the bow of an icebreaker (not suitable for high ice class vessels); and,
d) integral fluid cushion bow (IFCB) (suitable for Arctic class vessels if proved to be effective and structurally sound).

The present investigation deals with the form d) above. It is a logical follow-on study to the ACIB concept. Therefore, a brief review on the ACIB performance evaluation, icebreaking mechanisms, and limitations and practicability is given in the next subsections.

2.2 Performance Evaluation of ACIB

Experience with air cushion icebreaking platforms (ACIB) and with existing icebreakers (IB) has shown that the HTR value (as a possible criterion for the evaluation) of the former concept is about twenty, while the value for IB is approximately one (7,8).

Model tests in smooth level ice of CCGS NORMAN McLEOD ROGERS, fitted with an air cushion device deployed at the bow, showed that the resistance is reduced by 22 - 42% (depending on the ship speed) below the resistance which would be encountered without the ACV (7). Similar results are also indicated in reference (9) with the LOUIS ST. LAURENT model. The resistance force, when towed in broken ice, is about 25% to 40% less than in level ice that had identical thickness and properties. With the LOUIS ST. LAURENT following an ACIB, the resistance is reduced by about 50%. It is estimated that with such a reduction in the total resistance, the icebreaker can move at about 1.5 knots continuously in ice 1.4 metres thick, while without the ACIB, it can only break ice in the "ramming" mode.

One of the configurations of the ACIB used in the model tests is shown in Figure 7. The ACIB is attached to the bow of the ship by a soft-coupled type of attachment so that the platform could pitch and heave, while roll and yaw are limited by the geometry of the platform notch, which accommodates the bow of the host ship.

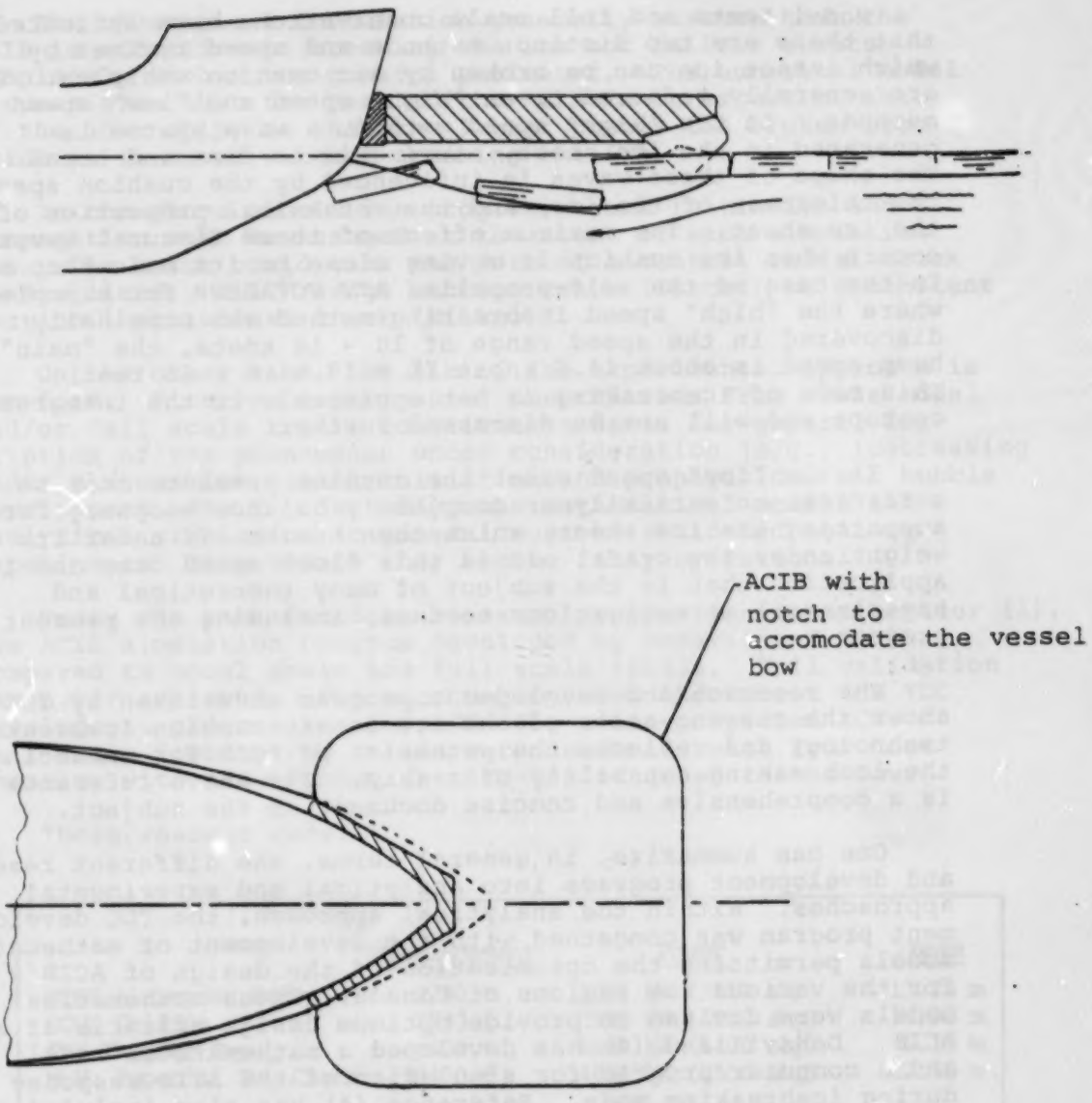

Figure 7 - Air Cushion Platform Configurations and Resultant Ice Rupture in Cavity at Low Speed

Model tests and full scale observations have indicated that there are two distinct methods and speed regimes by which intact ice can be broken by air cushion vehicles. They are generally referred to as "high" speed and "low" speed methods. In the "high" speed method, a wave system is generated in the ice sheet, causing it to flex and break. The shape of these waves is influenced by the cushion speed, the thickness of the ice, and the mechanical properties of the ice sheet. The maximum effect of these flexural waves occurs when the cushion is moving close to its main hump speed. In the case of the self-propelled ACV VOYAGEUR for example, where the "high" speed icebreaking method was originally discovered in the speed range of 10 - 16 knots, the "main" hump speed is about 14.6 knots (L = 19.81 m - 65 feet). This mode of icebreaking is not applicable to the integrated concept and will not be discussed further.

In the "low" speed case, the cushion pressure must be sufficient to partially or completely balance buoyancy forces supporting the ice sheet, which then breaks off under its own weight under the craft. It is this "low" speed case and its application that is the subject of many theoretical and experimental investigations to date, including the present project.

The research and development program undertaken by TDC (1) shows the current state-of-the-art in air cushion icebreaking technology and reflects the potential of ACIB for enhancing the icebreaking capability of a ship. The above reference is a comprehensive and concise document on the subject.

One can summarize, in general terms, the different research and development programs into analytical and experimental approaches. Within the analytical approach, the TDC development program was concerned with the development of mathematical models permitting the optimization of the design of ACIB's for the various ice regions of Canada. These mathematical models were devised to provide optimum design criteria of an ACIB. DeHavilland (4) has developed a mathematical model and a computer program for simulation of the ACIB response during icebreaking mode. Reference (4) has also included a mathematical formulation for predicting the pattern of ice fracture as a function of cushion pressure and vehicle speed, as will be discussed later. To develop such a computer program, Reference (4) adapted a finite element method for ice fracture analysis using ASAS (Atkins Structural Analysis System) computer program. This program has the capability to predict the stress pattern in a finite and infinite ice sheet subjected to a variety of loadings.

The theoretical formulation generally assumes that the ACIB is effective in breaking the ice and failure occurs completely within the cushion perimeter. The numerical model assumes also that the beam of the ACIB is in excess of that of the host ship, so that the latter pushes the broken ice aside as it moves without crushing the ice.

In the above simulation program, crack initiation and propagation must be assumed at the start of each simulation run. The crack could take the form of a central radial crack (DeHavilland), a 60° wedge section crack (Carter), or a constant section longitudinal crack (Milano)*.

On the other hand, the aim of the experimental approach is two-fold. Firstly, experimental observations from scale model and/or full scale trials constitute a basis for general description of the phenomenon under consideration (e.g., icebreaking under air cushion, crack initiation and propagation, air bubble development, etc.). Secondly, the mathematical models and analytical simulation in general must be validated against experimental data before they become fully operational.

Under the same Canadian research program mentioned earlier (1), the ACIB simulation program developed by DeHavilland (4) was compared to model scale and full scale trials. Full validation was never achieved. The air cushion used throughout the TDC development program was the ACT-100, a non-propelled ACV. Full scale icebreaking trials were conducted with four host vessels, with and without the ACT-100 attached to the bow.

These vessels were:

	Displacement	Power	Beam
CCGS Alexander Henry	2240 t	2650 kW (3550 shp)	13.25 m
CCGS Griffon	2793 t	2980 kW (4000 shp)	14.93 m
Tug Thunder Cape	400 t	1040 kW (1400 shp)	6.10 m
M.V. Imperial St. Clair	16450 t	4850 kW (6500 shp)	22.56 m

Table 1 Main Particulars of Tested Vessels

*More on the subject will be discussed later.

These full scale tests were conducted in suitable, uniform sheets ranging in thickness from 30 cm to 75 cm, with an absence of major discontinuities. The flexure strength of the ice varied from 400 to 900 kPa. The depth of local snow cover varied between 0 and 38 cm. Economic studies were conducted after each of the full scale trials. Costs of breaking a given volume of ice with CCGS ALEXANDER HENRY (AH) operating alone were compared to costs of breaking the same volume and thickness of ice with assistance of ACT-100. A significant reduction in costs was achieved by using the combination ACT-100/AH over the cost of operating the Alexander Henry alone. This was a direct function of the speed of the combination, and the significant reduction in time required to break the 6.4 km track through ice 36 cm thick. More important, using the above combination, it was possible to break 75 cm of fresh water ice at a speed over 6 knots. Alone, the Alexander Henry could not cope, except by ramming, with ice thickness exceeding 30 cm (8). Another example is the ACIB/Tug THUNDER CAPE combination, which was able to break a solid ice cover 40 cm thick and of 650 kPa (95 psi) at a steady speed of 5 knots. The tug alone would not normally operate in ice cover exceeding 12 cm (1). This improved icebreaking capability could benefit the existing fleet of the commercial shipping companies by over $10 million as a result of the reduction in time and extended navigation season.

Model tests were carried out afterwards (9) in support of the full scale trials. Difficulties, however, were apparent with the modelling techniques used. For example, it was not possible with model tests in synthetic (wax-based) ice to reproduce consistently the same icebreaking behaviour observed earlier during the full scale tests. It was found necessary to increase the cushion pressure to twice or three times the ice thickness in order for the ice to fail. However, for limited runs in which the ice did fail within the cushion area, the total resistance for the ACIB/ship combination, as compared to that of the ship alone, was reduced from 60% at low speeds to 30% at higher speeds. When the ice did not fail, the reduction in resistance was almost non-existent.

Failure to consistently reproduce the full scale ice-breaking behaviour may be attributed to:

- synthetic ice is certainly unrepresentative of the ice field;

- scale effects with regard to skirt stiffness, longitudinal stiffness of the ACT-100 and coupling arrangement; and,
- each vessel has its own characteristic length since they are not rigidly coupled and, therefore, one scale may not necessarily produce the behaviour of the free floating, soft-coupled two units.

Despite the lack of validation of the mathematical model, an attempt was made (1) to interpolate and extrapolate the results as shown in Figure 8. Curves of thrust required to penetrate ice of various thickness versus speed, and curves of available thrusts at various power levels versus speed are shown for one particular design.

The results of the TDC air cushion icebreaking bow development program (1975 - 1978) indicated that:

I. Attaching an air cushion icebreaking platform to the bow of a ship in intact uniform ice cover substantially enhances the ship's icebreaking capability. By attaching an air cushion platform to the bow of a ship, the resistance can be reduced by at least 30% depending on the speed, ice thickness, and ice mechanical properties.
II. This method of breaking ice achieves considerable savings.

There are other benefits, reported in the same Reference (1), which indirectly resulted in the improved performance of the ship. For example:

III. The ACIB/ship combination contends with less ice resistance than does the ship operating alone.
IV. By allowing the icebreaker to penetrate thicker ice, in which it would otherwise need to adopt a ramming procedure, maintenance costs for the hull and machinery of the vessel would be reduced, compared to those for a ship operating alone.
V. A wider, straighter and cleaner track was produced astern of the icebreaker, which would be of great assistance to a following escorted vessel.
IV. The platform appeared to stabilize the ship and improve its turning ability, except in high winds and with high cushion pressure.

The main advantage of the ACIB is that it can be attached to conventional ships to allow it to break ice without special design or strengthening requirements and without assistance.

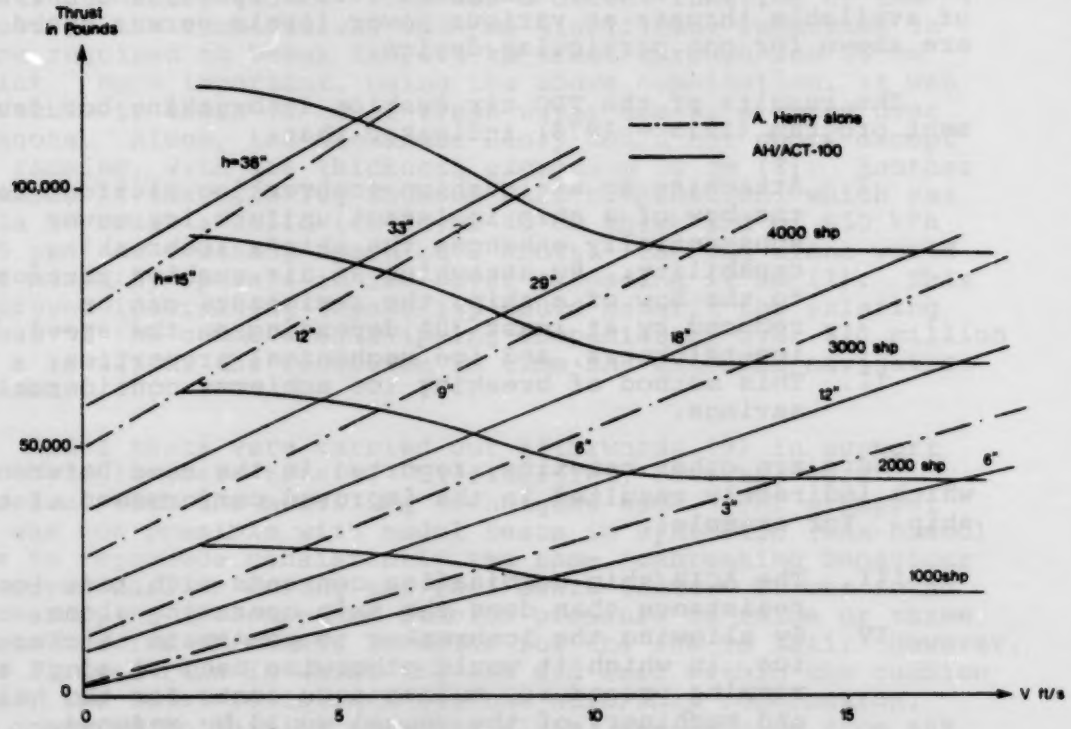

Figure 8 Thrust Required and Thrust Available at Various Horsepower vs Speed (1)

2.3 Icebreaking Mechanisms

As indicated in Section 2.2, observations showed that there are two distinct methods of icebreaking using air cushion technology, namely the high speed and the low speed methods.

2.3.1 High Speed

Moving an air cushion vehicle over a floating ice sheet generates waves in the ice and at a critical vehicle velocity these waves amplify the stress in the ice sufficiently to cause failure. The critical velocity depends upon ice characteristics (thickness and flexural strength) and water depth.

2.3.2 Low Speed

This method depends upon having a patch of open water from which to start. It also depends upon having a cushion pressure head slightly in excess of the ice sheet thickness. As the ACV moves across the edge of the ice, the water is depressed below the lower surface of the ice and an air cavity forms. Part of the ice sheet is then unsupported and fails under its own weight.

The failure ceases if the ice thickness exceeds about 90% of the cushion pressure head or if the speed rises above about 8 to 11 km/h (4 to 6 knots)(7)(2).

The air cavity ensures ice failure regardless of ice strength and modulus, as long as sufficient air cushion length exists on top of the ice to generate the breaking load. An air cavity below the ice surface is not essential for ACV icebreaking (as demonstrated during experiments, provided the ACV is heavy enough). However, model tests and analysis suggest that the presence of the air cavity will ensure the ice fragments break away cleanly imparting momentum which can facilitate dispersal.

It has been established (2) that the high speed method is a very powerful method of icebreaking compared to the slow speed method. However, since its effective speed range is outside that of conventional icebreakers the applicability of air cushion principles will be limited to that of the low speed method.

A number of attempts have been made by Carter, Milano, and more recently by DeHavilland (DHC) to predict ice fracture (4). Taking into account cushion pressure, simplified vehicle geometry, and ice properties, Carter's theory was based on a wedge shaped structural element, whereas Milano's was based on a constant section cantilever beam. DeHavilland on the other hand considered the crack initiation as shown in Figure 9. In all cases, prior cracks defining the structural shape of the ice element were presumed in the analytical simulation.

Based on their research, DHC (4) were able to formulate, in very simple terms, the basic mechanisms of low speed ice-breaking as shown in Figures 10 and 11.

The mathematical model developed by DHC was based on the "bubble propagation theory". This theory was established to understand the static and the dynamic bubble behaviours. Discussion and review of "bubble propagation theories" are considered outside the scope of the present limited study.

2.4 ACIB Limitations and Practicality

Despite the promising icebreaking performance of ACIB/ship combination in level ice, there are nevertheless some practical structural and operation problems.

1. The ACIB must operate coupled to a host ship because it is not practical to provide it with propulsion devices. Consequently, relative movements between the two units are unavoidable.
2. The ACIB stops breaking ice once the ice thickness exceeds its pressure draft (head) and the ship has to resort to the "ramming" mode. An ACIB in this instance is undesirable and should be uncoupled and removed.
3. The handling of the separate air cushion platform presents great difficulty.
4. The connection between the ACIB and the host ship is generally of a soft-coupled type, with movement constraints depending on the geometry of the platform notch. The configuration of the notch makes it impracticable to accommodate all host ship bow configurations. A rigid connection has never been tried for obvious reasons (e.g., design and construction difficulties).

5. Operational experience (1) has indicated that excessive spray occurs, reducing visibility.
6. Flexible skirts are very vulnerable to damage in ice operations.
7. Fluctuations in propeller rpm when penetrating thicker ice have been observed. These could be the result of large fragments of ice striking the propeller*, a phenomenon which was not observed when the host ship operated alone in thinner ice (1).
8. Satisfactory sealing between the ship and the platform has never been achieved. This results in an inefficient pumping system. A 50% margin for the design cushion pressure is common practice.

From the foregoing observations, it is a logical follow-on to consider an integrated air cushion as part of the ship's bow. By doing so, the relative movements between the platform and the host ship can be eliminated and, therefore, most of the problems and difficulties mentioned above will disappear, which makes the Integral Fluid Cushion Bow (IFCB) a more practical concept for Arctic operations.

---

* Although not considered alarming for light ice operations, it is certainly a cause for concern in the case of Arctic vessels with unprotected propellers.

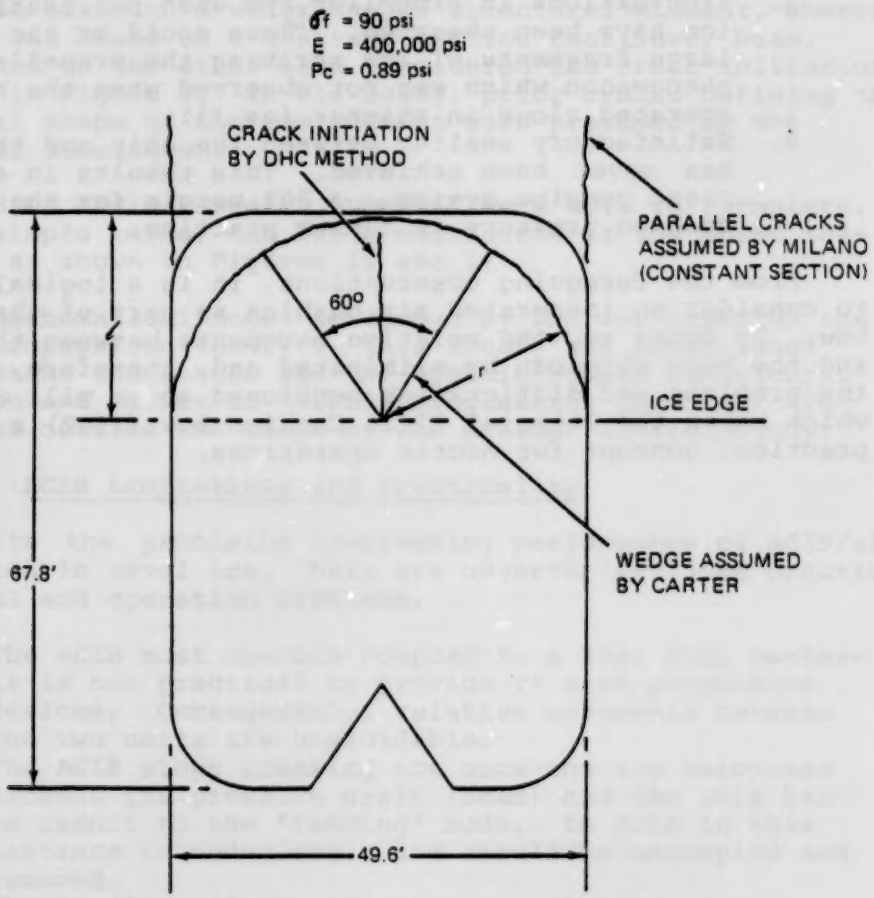

CARTER'S METHOD: PREDICT MAXIMUM THICKNESS BROKEN = 2.75' @ r = 24.8' (REF. 3, PAGE 58)

MILANO'S METHOD: PREDICT MAXIMUM THICKNESS BROKEN = 8.0' @ ℓ = 24.8' (REF. 4, PAGE D-23)

DHC METHOD: PREDICT CRACK INITIATION AT ℓ = 2.5' @ h = 10" (.83')
ℓ = 5.17' @ h = 20" (1.67')
ℓ = 8.0' @ h = 40" (3.33')

Figure 9 COMPARISON OF CRACK ANALYSIS PROCEDURES

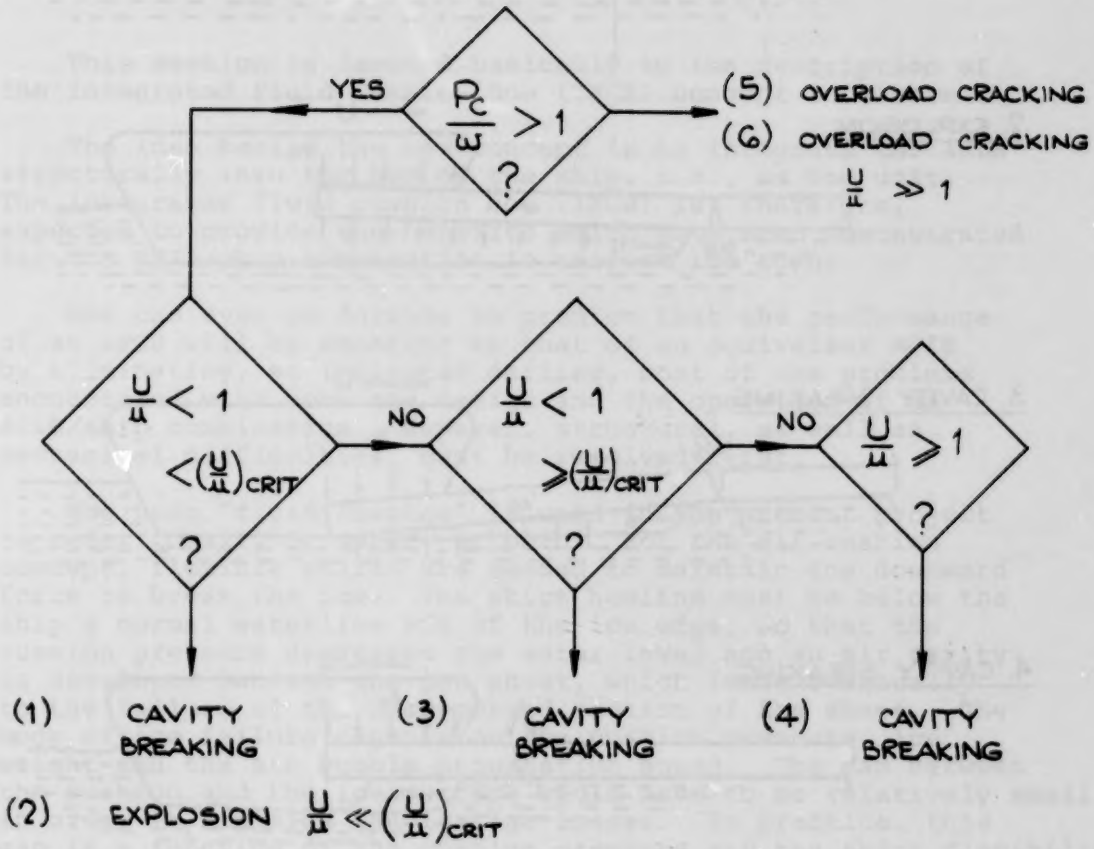

WHERE: U = vehicle speed

u = air bubble propagation speed*

p_c = cushion pressure

w = ice weight

$$\left(\frac{U}{u}\right)_{crit} = \left(1 - \frac{w}{p_c}\right)^n, \quad n = 1 \text{ for constant section}, \quad n = \tfrac{1}{2} \text{ for wedge section}$$

* The air bubble propagation speed increases with increasing cushion pressure, ice thickness, and stem angle at the ice edge.

Figure 10 Low Speed Icebreaking Parameters (4)

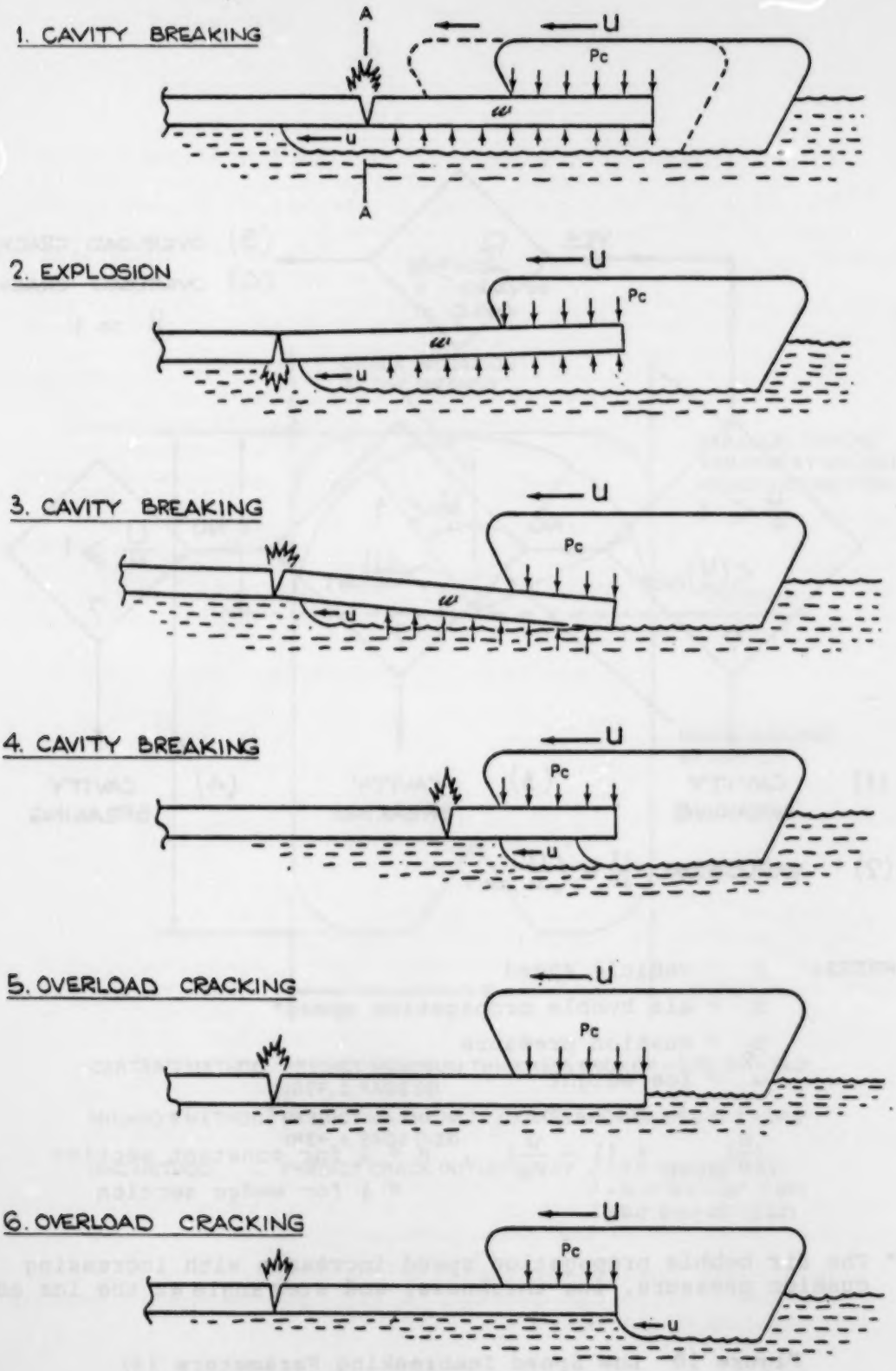

Figure 11 LOW SPEED ICEBREAKING MECHANISMS

3. INTEGRATED FLUID CUSHION BOW (IFCB)

This section is devoted basically to the description of the Integrated Fluid Cushion Bow (IFCB) concept in general.

The idea behind the new concept is to integrate the ACIB structurally into the bow of the ship, i.e., as one unit. The integrated fluid cushion bow (IFCB) is, therefore, expected to provide the benefits which have been demonstrated for the ACIB/ship combination in uniform ice cover.

One can even go further to predict that the performance of an IFCB will be superior to that of an equivalent ACIB by eliminating, as indicated earlier, most of the problems encountered with both the design and the operation of an ACIB/ship combination. However, structural, as well as mechanical difficulties, must be resolved first.

The term "fluid cushion" is used in the present project to refer to air, or water, or both. For the air cushion concept, flexible skirts are needed to maintain the downward force to break the ice. The skirt hemline must be below the ship's normal waterline aft of the ice edge, so that the cushion pressure depresses the water level and an air cavity is developed beneath the ice sheet, which leads eventually to the failure of the unsupported section of the sheet. The mode of ice failure depends on the cushion pressure, ice weight and the air bubble propagation speed. The gap between the cushion and the ice surface would have to be relatively small in order to minimize the leakage losses. In practice, this gap is a function of the cushion pressure and the skirt flexibility (heave and roll stiffness in particular) which by itself is a major design problem.

If, however, water is substituted for air, it is possible to eliminate the flexible skirts. Moreover, under the same pressure, water flows at a much lower velocity, so that for the same pumping power, a much greater gap can be maintained. This is, of course, to the advantage of Arctic operations and an advantage in the case of heavy or uneven ice formations. Obviously, there will be no air cavity, and the ice sheet breaks only when the vertical rupture load exceeds the bearing capacity of the ice sheet.

A combination of both systems (i.e., air cushion/water curtain) will be discussed later as the recommended concept among the three proposed ones. This concept consists of a high water jet pressure on the outside, enclosing high air pressure cushion inside. The water jet stream replaces the flexible skirts, thus eliminating a very vulnerable item from the design; and with the high air pressure cushion, the air cavity is developed and ice is broken under its own weight.

Clearly, the suitability of the proposed IFCB concept(s) for icebreakers in the Canadian Arctic will strongly depend on the results of extensive analytical and comprehensive experimental studies, which have to be carried out to determine the most effective design and hydrodynamic parameters.

4. DESIGN CRITERIA FOR ARCTIC CLASS ICEBREAKERS WITH IFCB

4.1 Evaluation Criteria

In order to formulate general criteria for designing an IFCB, one has to understand the ice failure mechanisms. Criteria such as hull transform ratio HTR (i.e., the ratio between the vertical rupture load and the available thrust), measure of effectiveness (i.e., multiplication of maximum ice thickness which would be broken and the ship speed), or process specific energy E_s (i.e., the ratio between the useful thrust and volumetric icebreaking rate) may be suitable for judging the performance of different units of the same concept, but certainly not for comparing different concepts.

The above statement needs some clarification. It is a well known fact that most of the resistance to motion in ice comes not from actually breaking the ice but from submerging it and pushing aside the floes once it is broken. The substantial improvement in the icebreaking capability of the ACIB/ship combinations, for example, comes partially from breaking the ice clearly but mostly from submerging the broken fragments to the depressed water level before the ship bow contacts it. The cushion in fact starts the ice fragments moving so that the ship has just to add to the momentum of the floes. There is no reason to indicate differently in the case of IFCBs.

Two conventional icebreakers could have the same HTR in the same ice condition but one may consume less power as a result of a lower icebreaking velocity. On the other hand, a conventional IB may have the same process specific energy as a ship with IFCB under the same ice condition but require more power at a given speed.

Therefore, a more proper criteria for the evaluation should include the total power, P, as well. The fan power required for the air cushion and the power required for the water jet circulating pumps must be added to the main machinery power to obtain the total power, P.

The icebreaking efficiency of the IFCB concept may be defined in such a way as to include:

- ability to break given ice thickness;
- ability to create small ice fragments; and,
- ability to disperse ice fragments.

This efficiency is determined by the cushion configuration, size and shape, cushion pressure, total power, and net forward thrust, speed of advance, and ice properties (thickness, strength, and modulus).

Therefore a possible definition of the suggested evaluating criteria could be written in very simple terms as:

$$\text{Icebreaking Efficiency } \eta = f\left[\frac{TU}{P},\ \left(\frac{t\ b}{\ell_c b_c}\right),\ \left(\frac{\sigma_F}{E}\right)\right]$$

$$\text{or} \qquad \eta = f_1\left(\frac{TU}{P}\right) + f_2\left(\frac{t\ b}{\ell_c b_c}\right) + f_3\left(\frac{\sigma_F}{E}\right)$$

where T = thrust
= total resistance
= ice resistance + aerodynamic drag + pressure drag + ... etc.
σ_F = flexural strength
E = Young's modulus
t = ice thickness
b = clear channel width
ℓ_c = air cushion length
b_c = air cushion maximum beam
U = ship speed
P = total power

Regression analysis based on experimental observations of limited parametric series can determine the functions f_1, f_2, and f_3 and their mutual interaction. It is likely that there will be a combined term for f_2 and f_3 for example. The first term in the regression equation represents basically the operating efficiency, which is the ratio between the required power and the total resistance at a given speed.

The second term is related to the configuration design of the IFCB. It is very important to develop a structural analysis technique to avoid unnecessary and costly tests with model scale and full scale configurations.

The third term is concerned with the ice properties. The ability of an IFCB to break the ice sheet depends on the two critical properties of ice, namely strength and modulus. Ice thickness is already included in the second term of the regression equation. However, due to the fact that when it comes to ice failure, the thickness and the mechanical properties of the ice are interrelated, as stated previously, an

additional term combining the two functions f_2 and f_3, in the final analysis, will be of no surprise. In support of this argument, it is worth noting that thick and brittle ice makes the icebreaking prediction relatively easy, whereas thin and soft ice which sustains large deflection without failure can severely limit the air cavity penetration due to the possible air supply cut-off.

4.2 Design Parameters of Arctic IFCB

Mathematical models and computer simulation programs are usually limited to level ice. For Arctic applications one must always bear in mind the real ice condition since it influences the selection of the cushion height and pressure.

For a high Arctic Class IFCB (POLAR IFCB), the feasibility of the design is governed by the practicality of resolving numerous problems such as skirt/seal problems (if applicable), water curtain stability, and of course, structural and mechanical problems associated with the Arctic environment.

The following parametric ranges must be considered in the design of an IFCB:

a) ice thickness varies between 0.5 and 2.5 m (1.5 and 8 ft);
b) cushion pressure: 6.0 to 24 kPa (0.9 to 3.5 psi) (plus margin);
c) ice flexural strength: 275 to 1030 kPa (40 to 150 psi);
d) speed of advance: 0 to 6 knots;
e) probable air cushion to ship beam ratio: 0.5 to 1.0; and,
f) reasonable clearing efficiency.

The "best" design of an icebreaker with IFCB should resemble a number of features of which the overall objective is to provide an energy-efficient means of icebreaking. Maximum average speed at a given power, maximum reliability and maintainability, structural integrity, and low cost are the main features of a successful design.

5. PROPOSED CONCEPTUAL DESIGNS

Three conceptual designs, reflecting the integrated fluid cushion bow (IFCB), are provided in this section. The general features of the IFCBs have been already outlined in the previous sections. However, additional features and limitations concerning each concept will be mentioned whenever appropriate.

The practical feasibility of each concept will have to be assessed through numerical simulation and the predicted performance must then be validated by experimental data. The work plan for this extensive numerical and comprehensive experimental analysis is the subject of Section 8. The actual study is the objective of the second phase in the six-phase research and development program being considered by TDC of which the present project is the first phase to provide preliminary conceptual designs for the IFCB.

5.1 Concept I: Extended Bow with Air Cushion/Water Curtain

Figure 12 shows a typical arrangement for the proposed concept. The main features of the concept can be summarized as follows:

a) water jet stream replaces the flexible skirts thus eliminating a very vulnerable item from the design; this will reduce the maintenance requirements due to the removal of the skirts;
b) with the high air pressure cushion, the air cavity is developed and ice is broken under its own weight. As indicated in the literature, air cavity icebreaking is the most efficient icebreaking mechanism (4,1,2,7);
c) there is no direct contact between the cushion bow and the ice and therefore does not require special strengthening;
d) the cushion does not interfere with the conventional icebreaking bow, and therefore, can be considered as an adjunct to a good bow design; and,
e) the IFCB does not interfere with the ramming operation.

Clearly, the last feature is essential in Arctic operations and this, combined with the above favourable features, makes the concept quite attractive.

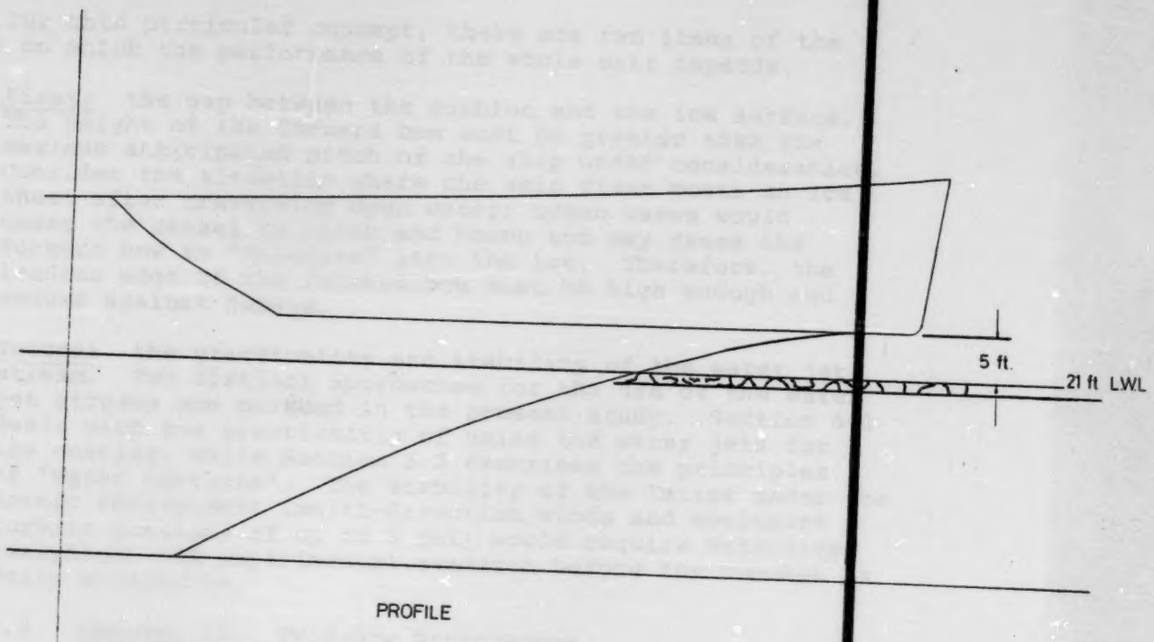

PROFILE

STN 16 STN 17 STN 18 STN 19 STN 20 A B

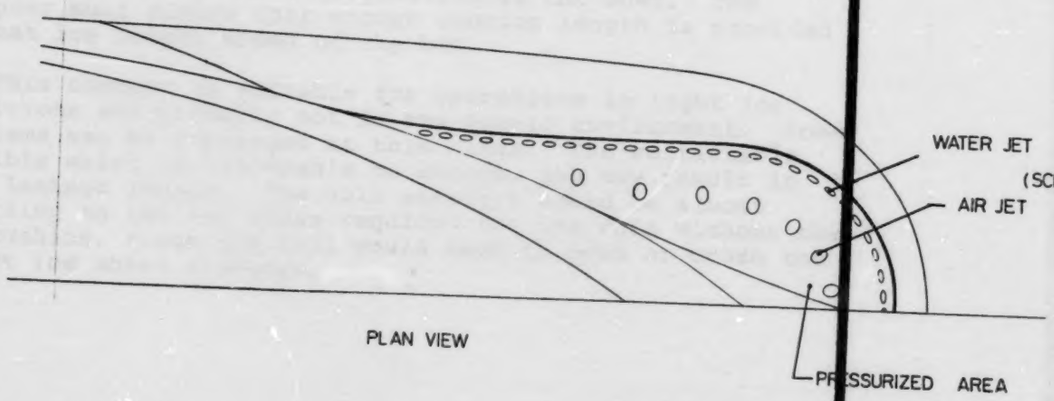

PLAN VIEW

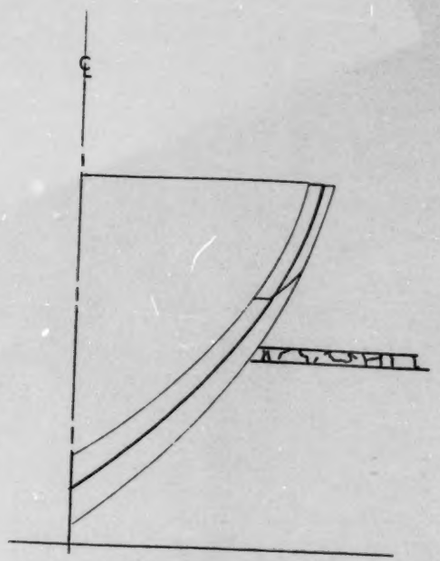

SECTION AT STNS 17, 17½, 18

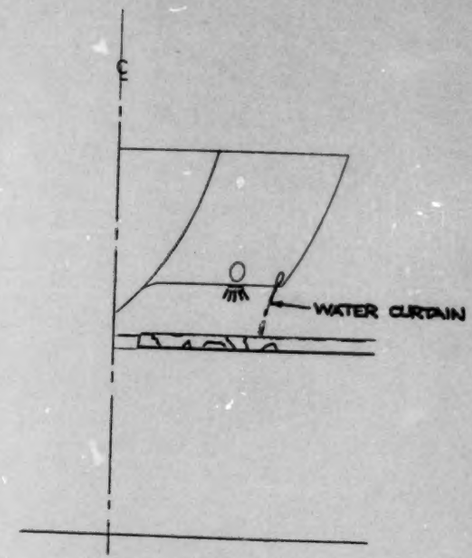

SECTION AT 'A'

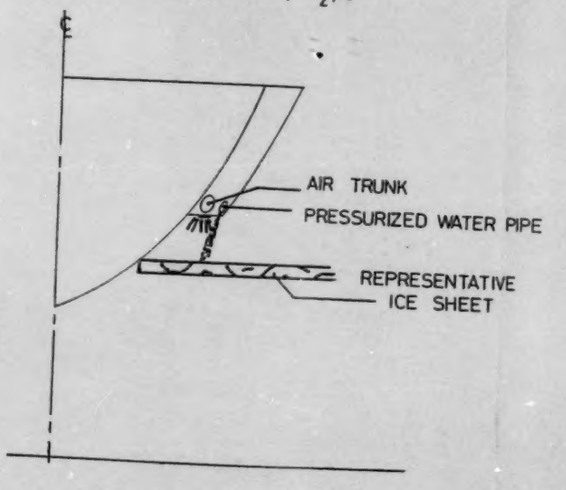

SECTION AT STN 19

Figure 12

GENERAL NOTE: REMOVE BURRS & SHARP EDGES

APPROVAL

DRAWN G.B.C. CHECKED M.G. METRIC

SCALE 1 cm : 3M DATE 12/10/91 INCHES

GEN. DIM.: DECIMALS HOLES .XX: SHAFTS .XXX: ANGLES:

NEXT ASSY USED ON CODE IDENT. NO.

ITEM QTY. PART NO. DESCRIPTION NOTES

Davis Engineering CONSULTING ENGINEERS OTTAWA CANADA

CONCEPT I - EXTENDED BOW WITH AIR CUSHION/ WATER CURTAIN INTEGRAL FLUID CUSHION BOW

CLIENT DRAWING NUMBER

MATERIAL TECHNICAL DATA LIST ENG SIZE A1 PART NO. DE 1654 SHEET 1 OF 1

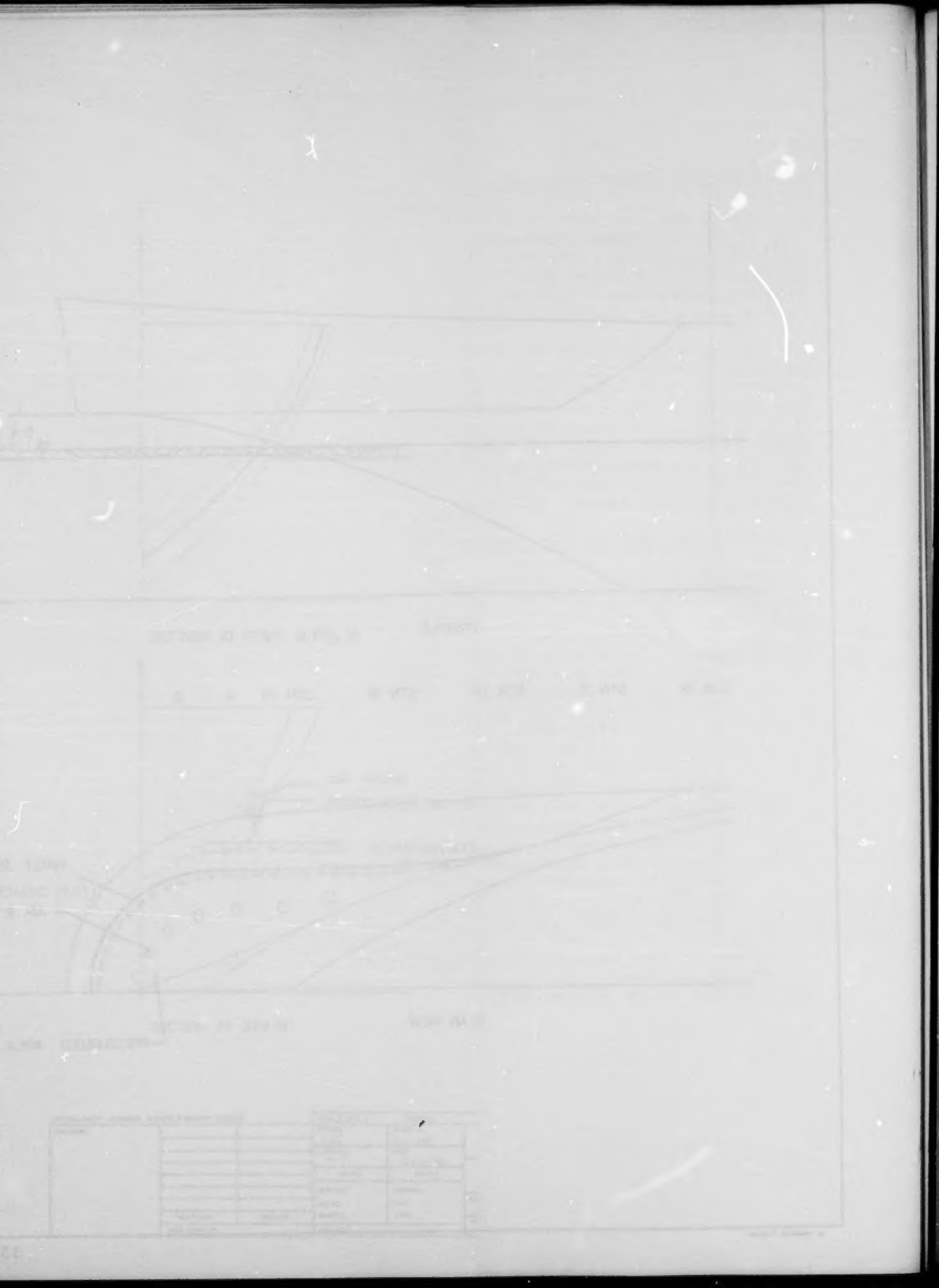

For this particular concept, there are two items of the IFCB on which the performance of the whole unit depends.

First: the gap between the cushion and the ice surface. The height of the forward bow must be greater than the maximum anticipated pitch of the ship under consideration. Consider the situation where the ship first meets an ice sheet after traversing open water; ocean waves would cause the vessel to pitch and heave and may cause the forward bow to "nosedive" into the ice. Therefore, the leading edge of the forward bow must be high enough and secure against damage.

Second: the practicality and stability of the water jet stream. Two distinct approaches for the use of the water jet streams are pursued in the present study. Section 6.1 deals with the practicality of using the water jets for ice cutting, while Section 6.2 describes the principles of "water curtains". The stability of the latter under the Arctic environment (multi-direction winds and enclosure cushion pressure of up to 5 psi) would require extensive analytical and experimental research before the concept is fully acceptable.

5.2 Concept II: Twin-Bow Arrangement

Figure 13 shows an arrangement of the concept. The distance between the centerlines of the two bows must be kept as large as the ship lines permit. Air cushion icebreaking performance improves by increasing the beam. The configuration of the cushion depends on the configuration of the bows. The designer must ensure that enough cushion length is provided so that ice breaks ahead of the bow.

This concept is suitable for operations in light ice conditions and probably not in the Arctic environment. Some problems can be envisaged at this stage. The retractable flexible skirt is vulnerable to damage, and may result in high leakage losses. The hull strength would be almost according to the ice class required for the ship without the air cushion, since the hull would have to push or crush the intact ice sheet sideways.

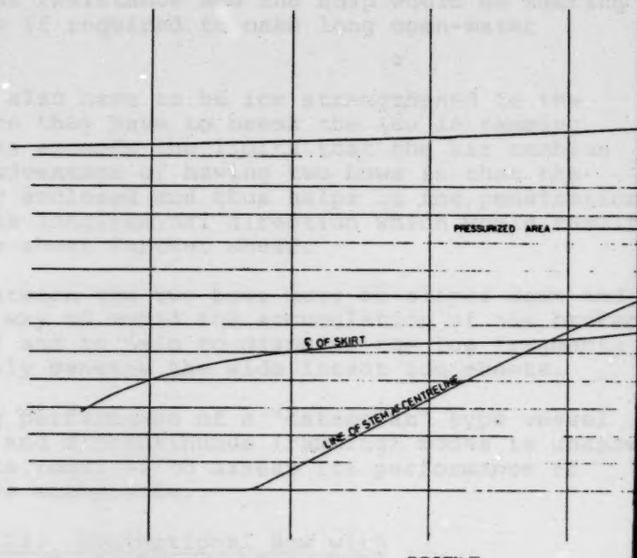

PROFILE

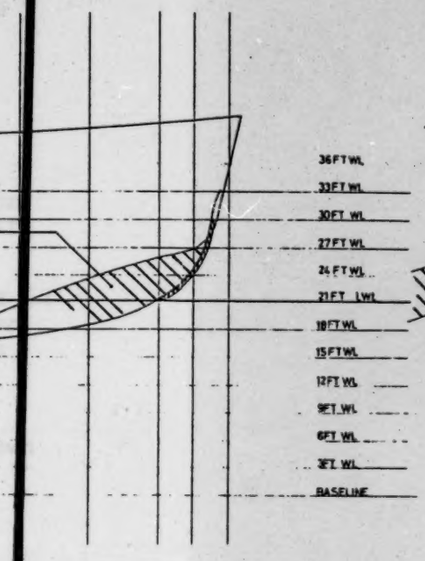

ALTERNATIVE ARRANGEMENTS

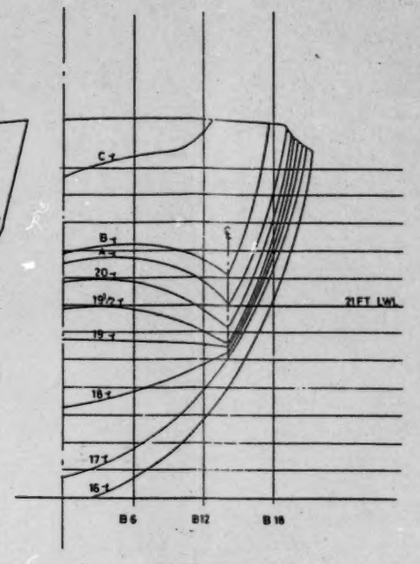

PART BODY PLAN

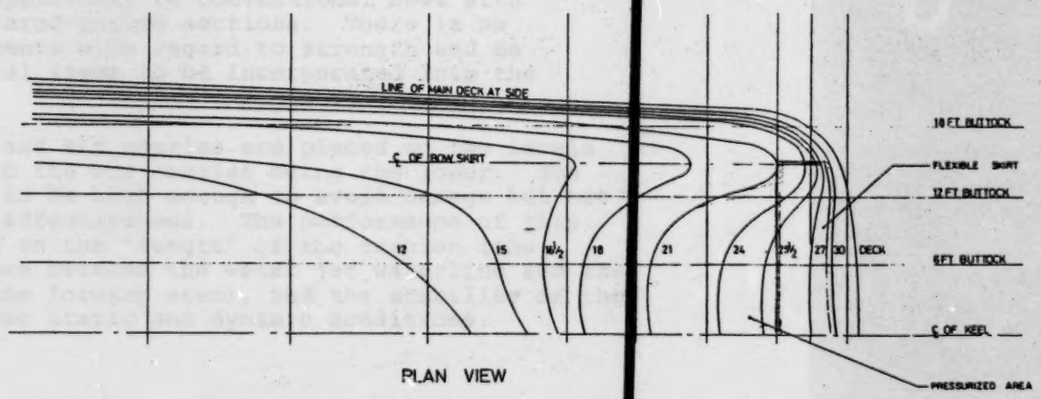

PLAN VIEW

ARRANGEMENT I

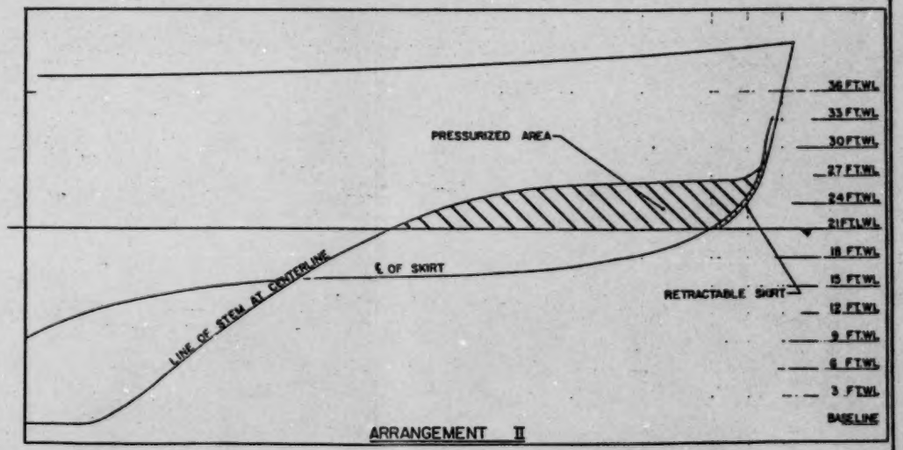

ARRANGEMENT II

Figure 13

GENERAL NOTE: REMOVE BURRS & SHARP EDGES

APPROVAL

NEXT ASSY | USED ON

CODE IDENT. NO.

ITEM | QTY. | PART NO. | DESCRIPTION | NOTES

DRAWN GF | SCALE 1cm: 3ft

CHECKED M G | DATE 11th Dec 81

METRIC | INCHES

GEN. DIM.: | DECIMALS .XX: | .XXX:

HOLES | SHAFTS | ANGLES:

Davis Engineering CONSULTING ENGINEERS OTTAWA CANADA

CONCEPT II – TWIN BOW ARRANGEMENT
INTEGRAL FLUID CUSHION BOW

CLIENT | DRAWING NUMBER

MATERIAL | TECHNICAL DATA LIST | SIZE A1 | PART NO. DE 1655 | SHEET 1 OF 1

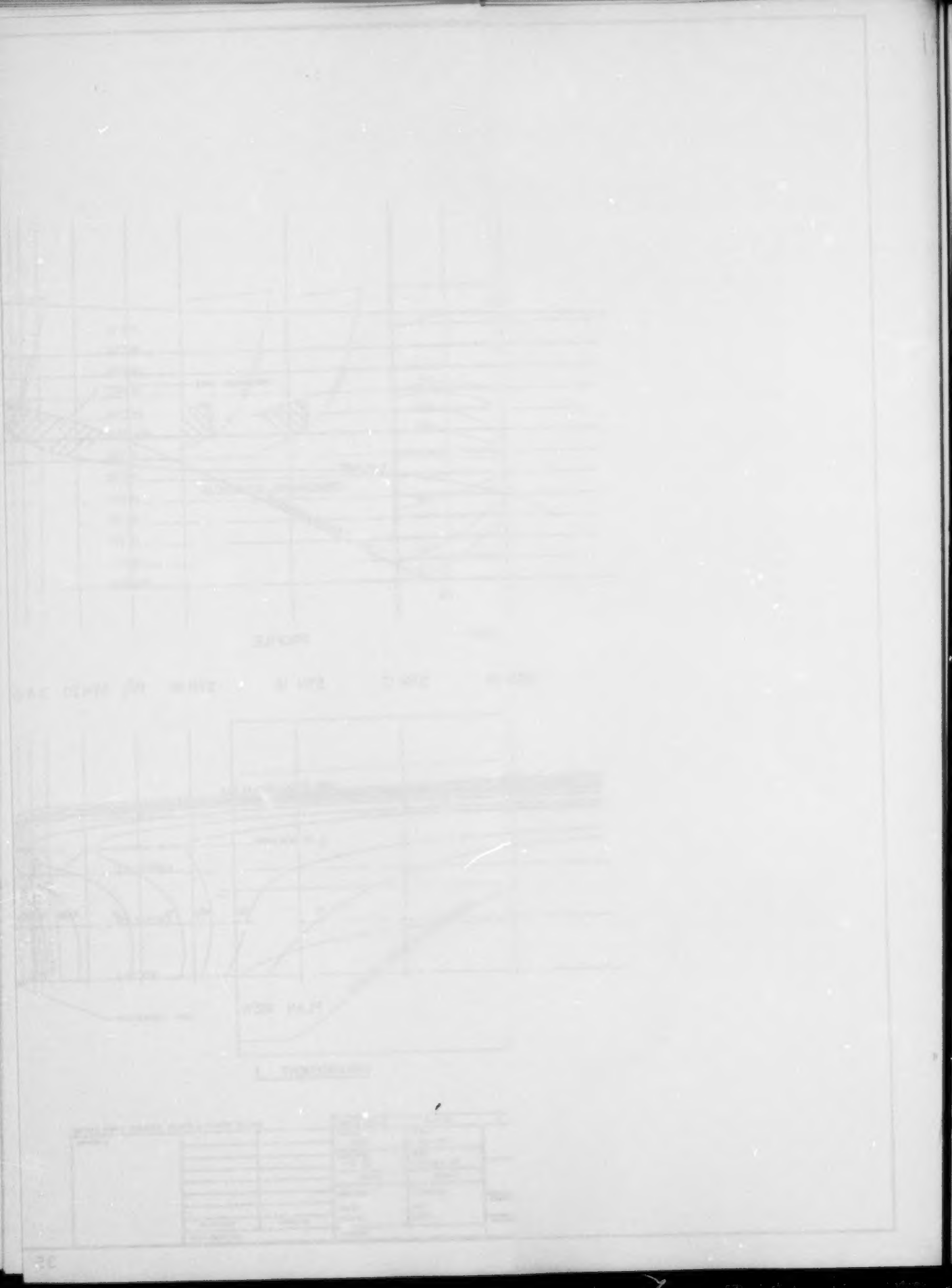

The flat bow sections would result in substantially increased open water resistance and the ship would be wasting a lot of its energy if required to make long open-water voyages.

The bows would also have to be ice strengthened to the required class since they have to break the ice in ramming if the ice thickness exceeds the limits that the air cushion could break. The advantage of having two bows is that the air cavity is fully enclosed and thus helps in the penetration of the cavity in the longitudinal direction which would result in breaking the ice sheet further ahead.

The sections between the two bows must be sloped down and outwards in such a way to avoid the accumulation of the broken ice pieces in front and to help to disperse the ice fragments sideways and possibly beneath the side intact ice sheets.

The icebreaking performance of a "catamaran" type vessel in both continuous and discontinuous (ramming) modes is unknown and investigation is required to assess its performance if the concept is to be acceptable.

5.3 Concept III: Conventional Bow with Air Cushion/Water Curtain Principles

Figure 14 shows schematic plans of the concept. It resembles most of the features mentioned for Concept I except that it is applicable to conventional bows with preferably large flared-angled sections. There is no additional requirements with regard to strength and no additional structural items to be incorporated into the bow.

The water jets and air nozzles are placed on two levels in the forebody with the air nozzles being the lower. The nozzles would have to be high enough to avoid damage but not too high to ensure effectiveness. The performance of this concept will depend on the "length" of the cushion (the longitudinal distance between the water jet waterline and the load waterline at the forward stem), and the stability of the "water curtain" under static and dynamic conditions.

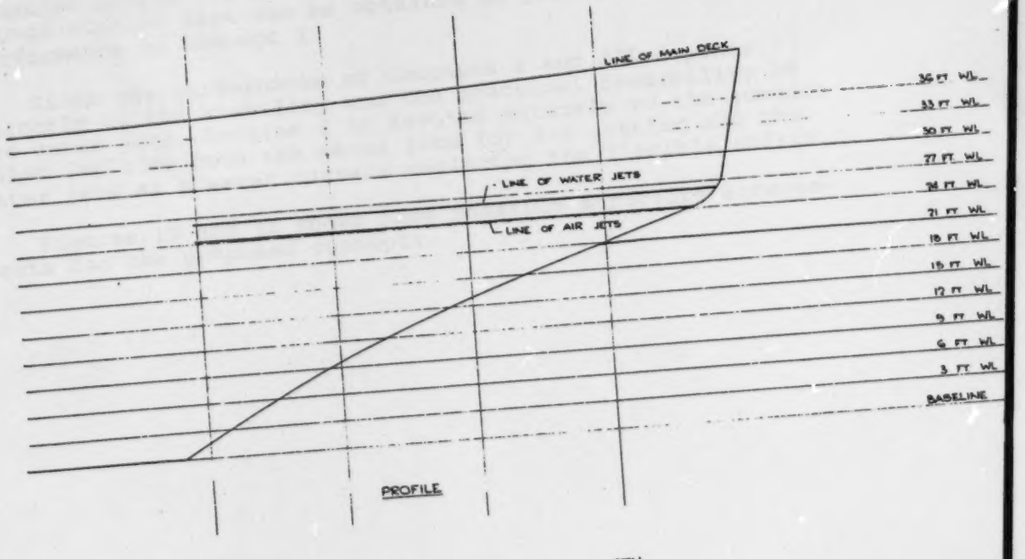

PROFILE

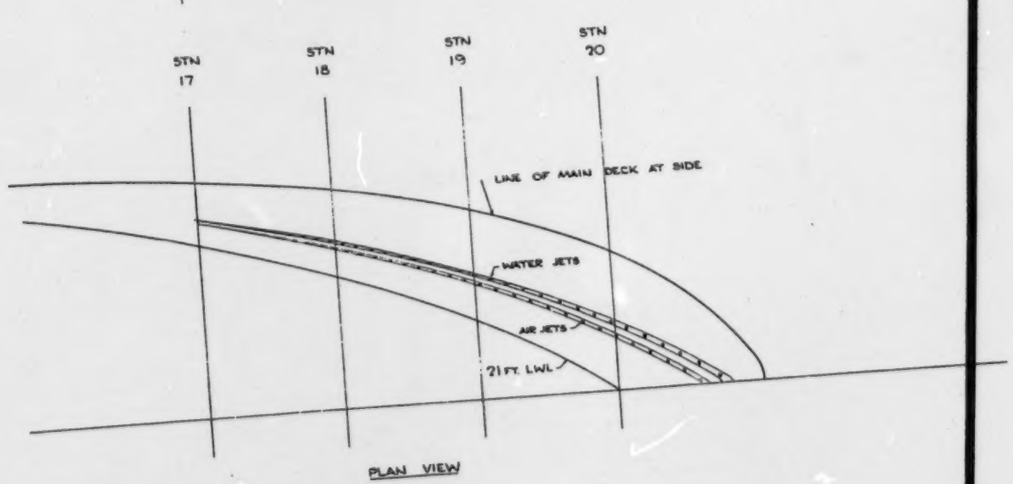

PLAN VIEW

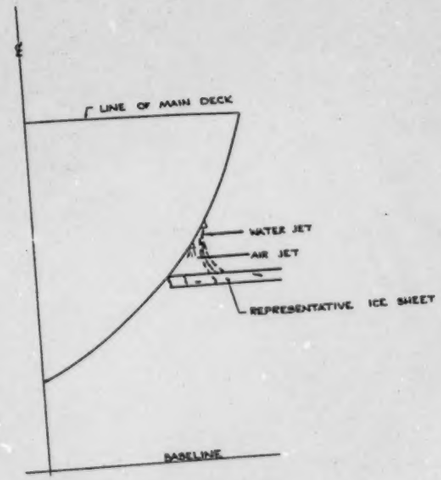

SECTION AT STATION 18

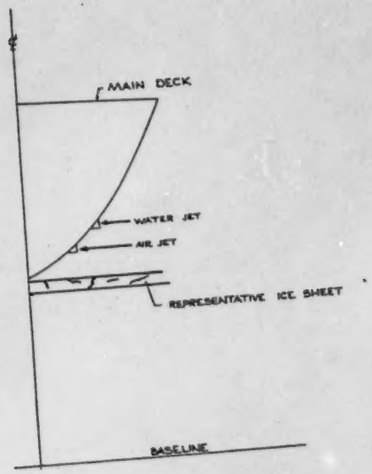

SECTION AT STATION 20

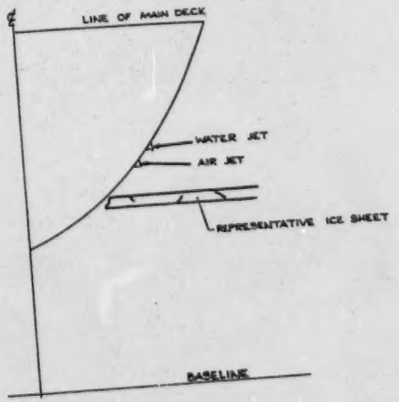

SECTION AT STATION 19

Figure 14

GENERAL NOTE: REMOVE BURRS & SHARP EDGES

APPROVAL

NEXT ASSY | USED ON

CODE IDENT NO.

ITEM	QTY	PART NO.	DESCRIPTION	SHEET

DRAWN C.S.C. | SCALE 1cm = 3½

CHECKED M.G. | DATE 13th Oct 1981

METRIC | INCHES

GEN. DIM'L? | DECIMALS

HOLES .XX? | .XXX?

SHAFTS

ANGLES?

Davis Engineering — CONSULTING ENGINEERS OTTAWA CANADA

TITLE: CONCEPT III - CONVENTIONAL BOW WITH AIR CUSHION/WATER CURTAIN INTEGRAL FLUID CUSHION BOW

CLIENT

MATERIAL | TECHNICAL DATA LIST

DRAWING NUMBER

DWG SIZE | PART NO. DE 1656

SHEET 1 OF 1

The performance of this concept is expected to be less than that of Concept I, unless investigations showed that "cushion length" is not a critical parameter. In that case, enough cushion area can be obtained to produce a comparable performance to Concept I.

Since the performance of Concepts I and III depends strongly on the stability and the practical feasibility of the water jets, Section 6 is devoted entirely to the subject which includes both the water jets for ice cutting and the water jets as a water curtain replacing the flexible skirts.

Figures 15 and 16 shows some possible structure arrangements for the proposed concepts.

SYM	REVISION	AUTH	DATE	APP'D

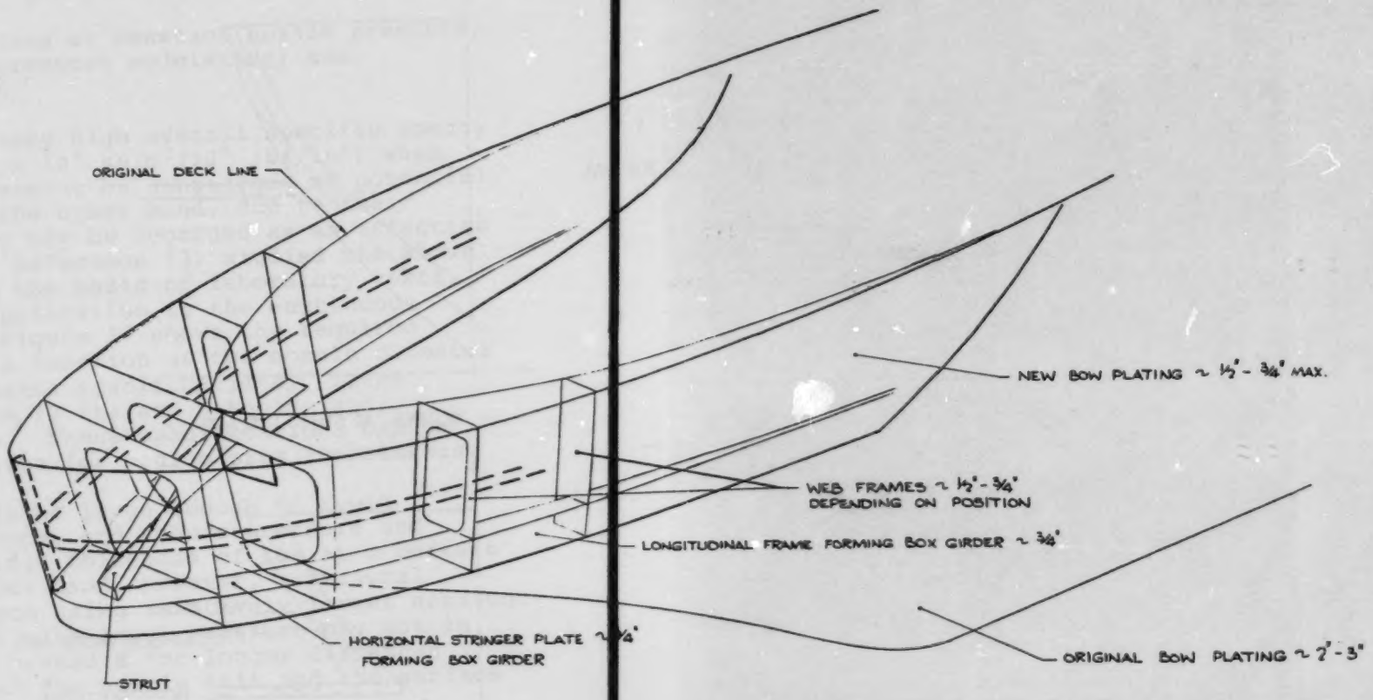
ORIGINAL DECK LINE
NEW BOW PLATING ~ ½" - ¾" MAX.
WEB FRAMES ~ ½" - ¾"
DEPENDING ON POSITION
LONGITUDINAL FRAME FORMING BOX GIRDER ~ ¾"
HORIZONTAL STRINGER PLATE ~ ¾"
FORMING BOX GIRDER
ORIGINAL BOW PLATING ~ 2" - 3"
STRUT

NOTE : ONLY A REPRESENTATIVE SAMPLING OF WEB FRAMES ARE SHOWN

Figure 15

GENERAL NOTE: REMOVE BURRS & SHARP EDGES

APPROVAL					
			NEXT ASSY	USED ON	
			CODE IDENT. NO.		

ITEM	QTY.	PART NO.	DESCRIPTION	NOTES

DRAWN GG	SCALE N.T.S.
CHECKED M.G.	DATE NOV. 1, 1981
METRIC	INCHES
GEN. DIM.:	DECIMALS
HOLES	.XX:
SHAFTS	.XXX:
ANGLES:	

Davis Engineering CONSULTING ENGINEERS OTTAWA CANADA

TITLE: PRELIMINARY SKETCH OF STRUCTURAL ARRANGEMENT

CLIENT

MATERIAL | TECHNICAL DATA LIST

DRAWING NUMBER: DWG SIZE | PART NO. DE 1657 | SHEET OF

K+E

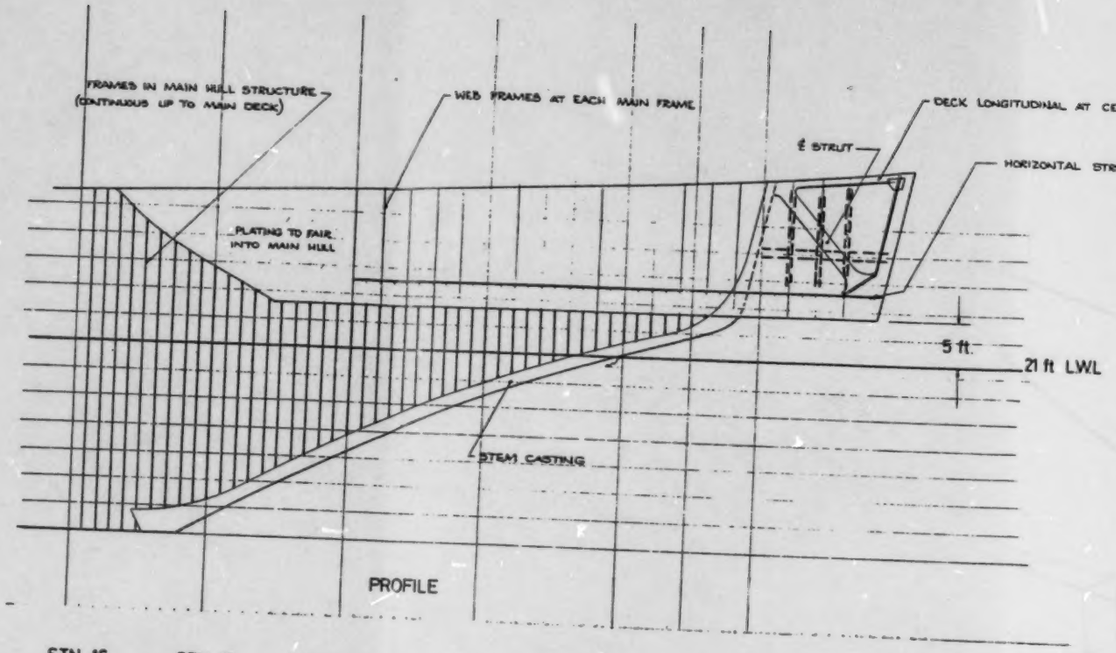

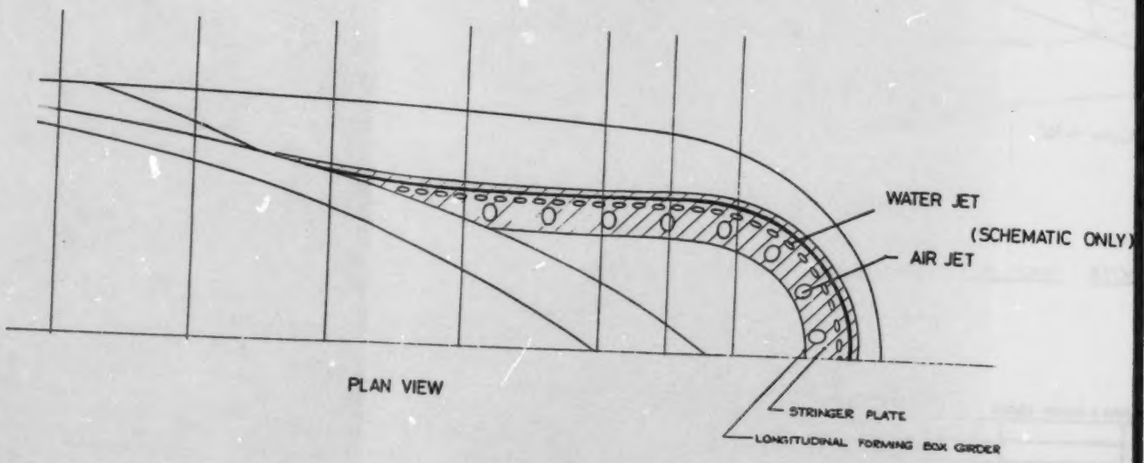

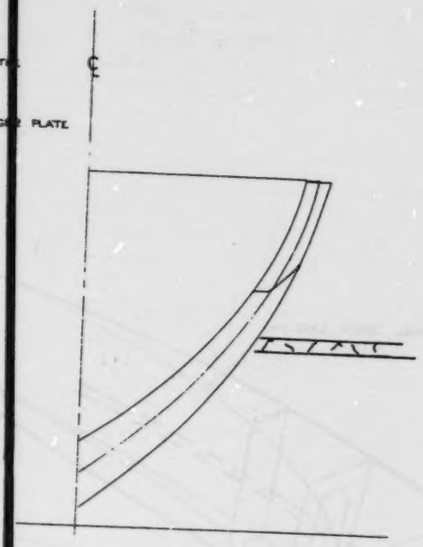

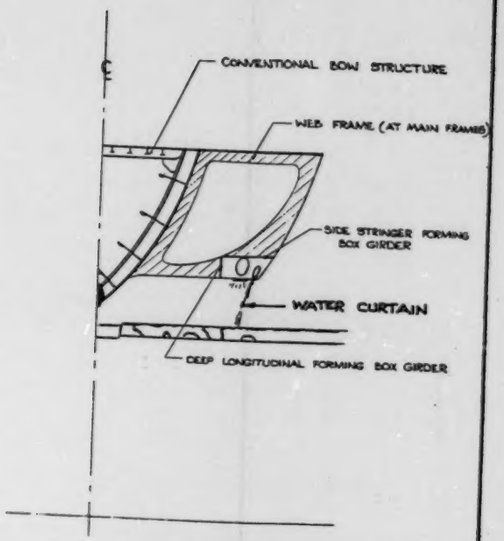

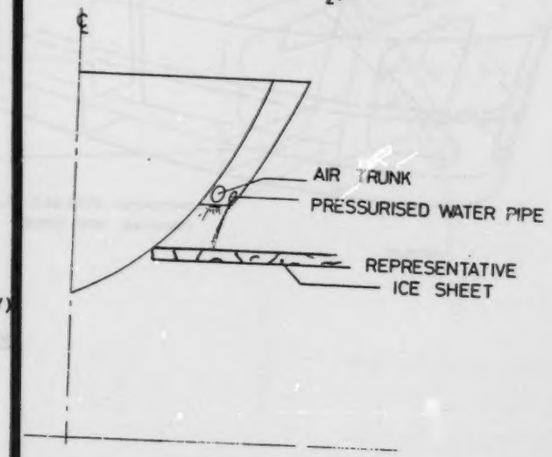

Figure 16

DRAWN G.BC	SCALE 1 in : 3ft	Davis Engineering		CONSULTING ENGINEERS OTTAWA CANADA	
CHECKED M.G.	DATE 12/10/71	TITLE CONCEPT I – EXTENDED BOW WITH AIR CUSHION / WATER CURTAIN STRUCTURAL ARRANGEMENT			
METRIC	DECIMAL	CLIENT			
GEN. DIM'S ±.1	DECIMALS .xx ±.01 .xxx ±.005	MATERIAL		PART NO. DE 1658	
HOLES				SHEET OF	
SHAFTS					
ANGLES ±					

6. WATER JETS

6.1 Ice Cutting with Water Jets

High velocity water jets are capable of cutting ice. There are three types which might be considered (3):

a) continuous jets operating at constant nozzle pressure;
b) continuous jets with pressure modulation; and,
c) pulsed jets.

All the above types have very high overall specific energy (Power/$\dot{V}$) in the order of 7.0×10^4 kN/m^2 (10^4 lbf/in^2) when cutting ice; therefore, they cannot be considered as potential means for bulk breaking. On the other hand, due to their enormous power densities, they may be regarded as an effective tool for cutting thin slots. Reference (3) studied the above three types and concluded, on the basis of laboratory tests, that the only contender for application is the continuous jets at constant pressure. Figure 17 shows the required nozzle pressure and power as a function of the nozzle diameter to meet two different performance specifications. These specifications are: a) 61 cm (2 ft) and 5 knots; and, b) 46 cm (1.5 ft) and 3 knots. These specifications can be regarded as operating conditions for medium size icebreakers.

The nozzle diameter has to be large enough to avoid clogging, facilitate maintenance, and reduce pressure and power required to cut a specific thickness of ice at a certain traversing speed. On the other hand, however, structural complications might result from using relatively larger nozzles. More importantly, a water jet with lower pressure may not in fact be able to maintain its pressure for longer distances represented by the gap between the nozzle exit and the surface of the ice sheet.

This gap parameter was not considered in the results shown in Figure 17. However, one can assume that, for light and medium icebreakers, the motion response (heave and pitch in particular) occur with relatively small amplitudes and therefore the water jets can be placed close to the ice sheet without the risk of damaging the nozzles. A gap of up to 60 cm (approximately 2 ft) or so may not impair the laminar jet flow, provided that the structual requirements of such an arrangement are met.

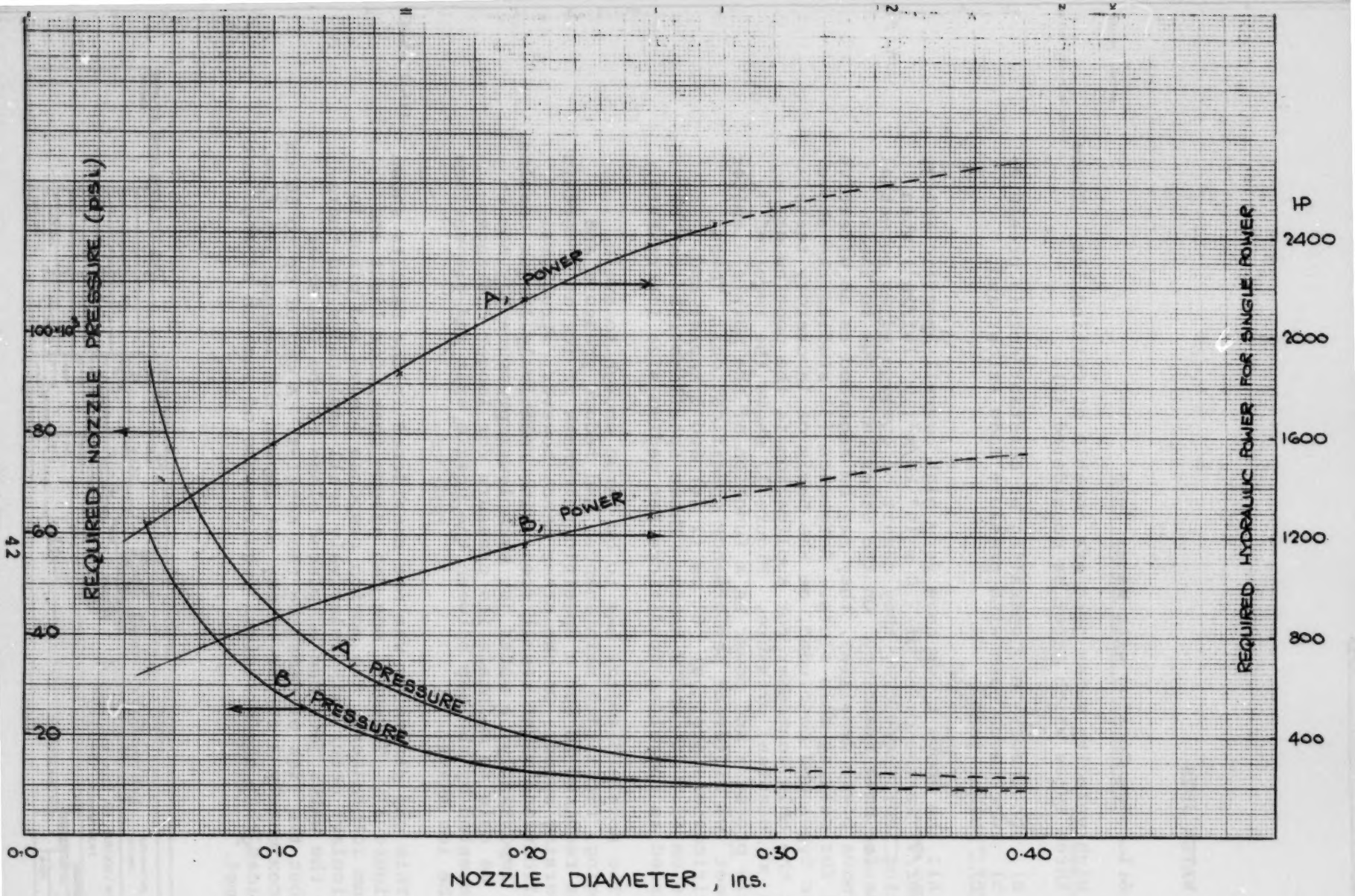

Figure 17 Required Nozzle Pressure and Power as a Function of Nozzle Diameter for Two Different Performance Specifications
A, 2 ft ice, 5 knots; B, 1.5 ft ice, 3 knots

From Figure 17, with a 10 mm (0.4 in) nozzle diameter, a jet pressure of 7 x 10^4 kPa (10^4 psi) and power of about 1550 hp per nozzle is required to cut 46 cm (1.5 ft) ice at a traversing speed of 3 knots.

Figure 18 shows the results (3) of ice cutting with water jets applicable to polar icebreakers. Due to the severe environmental conditions for Arctic operations, the nozzles fitted to a polar icebreaker will probably have to be 1 to 1.5 m (4 to 5 ft) above the ice surface to reduce the risk of damage. As a result of these structural requirements, the nozzle diameter will be kept relatively small so that the jet flow would maintain its high pressure and high penetration velocity. From Figure 18, (again not considering the effect of the gap on the nature of the jet flow), with a 10 mm (0.4 in) nozzle, the required nozzle pressure is about 10^5 kPa (15,000 psi) and the power required for a single nozzle is about 4500 hp. This enormous power requirement makes the idea of adapting water jet techniques to cut ice impracticable.

Moreover, cutting ice sheets (within limits) is by no means a problem in icebreaking. It is the submergence and dispersing of the ice fragments that consumes most of the energy. There is no clear indication in the literature that cutting a slot in the ice sheet would enhance the icebreaking capability of the ship. In fact, one can even go further to say that, under certain circumstances, it may seriously interfere with the ship's continuous motion and bring it to a halt. This may be explained as follows. Although cutting a slot in the ice would weaken the ice sheet, larger slabs of ice could be created. As a result, more of the ship's energy would be dissipated in submerging and dispersal of these slabs, with an overall effect of reducing the icebreaking capability of the ship.

It might be possible to improve the ice cutting performance of water jets by heating the feedwater, but the improvement is expected to be only marginal.

From the foregoing discussion, it is clear that for polar icebreakers, ice cutting with water jets is not of much interest for a variety of reasons: low efficiency; enormous power requirements; unnecessary structural complications; vulnerability to damage; unpredictable icebreaking performance; and possible simpler alternatives.

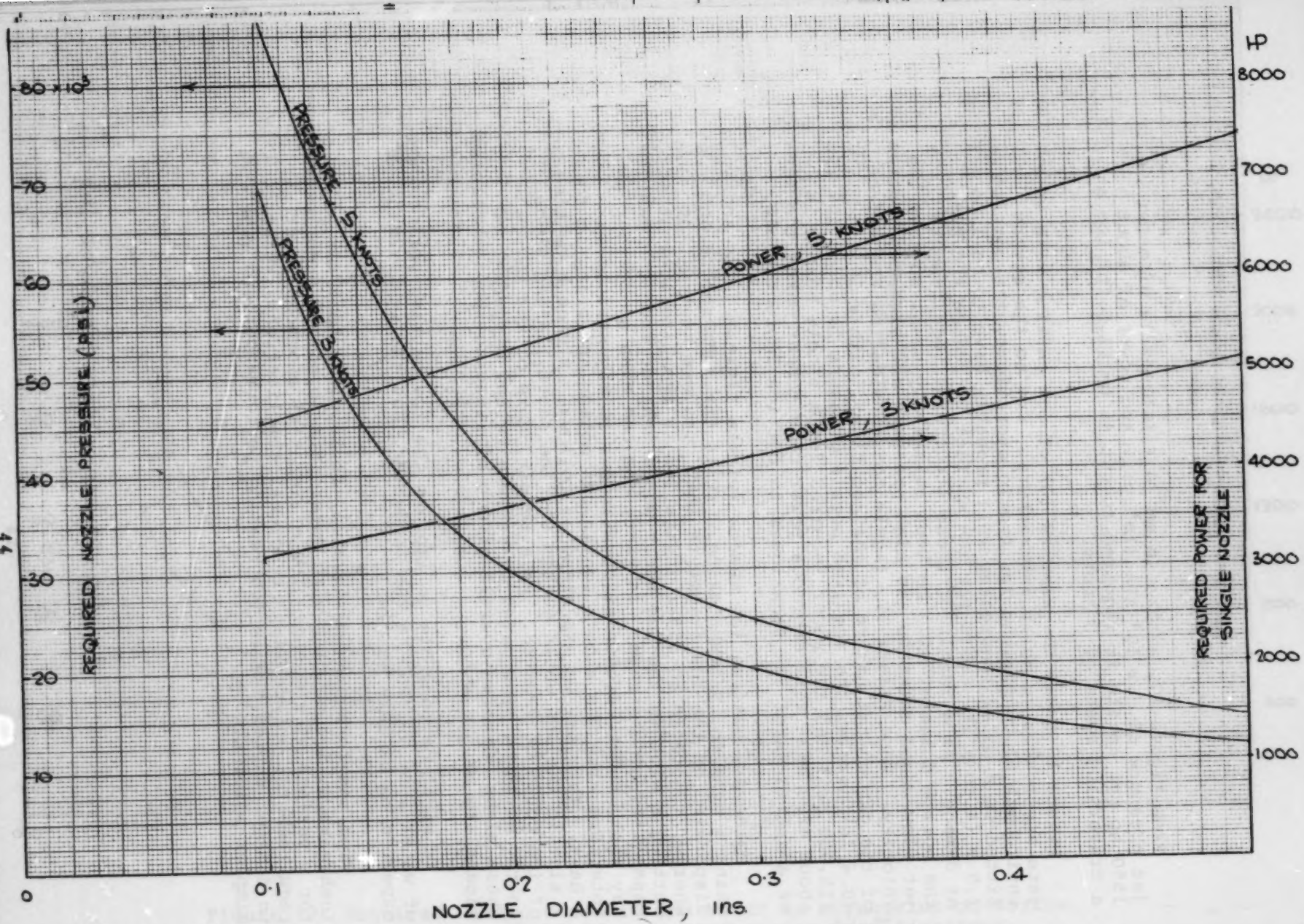

Figure 18 Polar Icebreaker Required Nozzle Pressure and Power Vs. Nozzle Diameter 6 ft of ice (3)

For light and medium icebreakers, the performance with the water jets versus the expected performance of the icebreaker with increased installed power appears to be the decisive factor upon which the designer will have to decide whether to implement the water jet device, increase the power instead, or look for simpler alternatives. However, there is no reason to believe that water jets with nozzle pressure in the order of 7×10^4 kPa (10^4 psi) and power of more than 1500 hp per nozzle are either economical or practically feasible. Water jets, however, can be used with much reduced pressure as a water curtain. This is discussed in the following section.

6.2 Water Curtain

As indicated in Section 3, integrated air cushion bow requires skirts to create the downward force to break the ice. The skirt's hemline must be below the ship's normal waterline so that the air cavity in front of the bow can be enclosed and allowed to propagate in the forward direction.

For Arctic operations, the skirt's vulnerability to damage constitutes a major design problem. Flexible, segmented, and retractable skirts have been suggested recently. However, due to the harsh Arctic environment, their practicability, maintenance, and replacement are major tasks which affect the overall performance of the cushion. In addition, skirts at very low temperature tend to loose their flexibility and consequently become subject to damage by the rough and uneven ice surface, and also by the broken slabs of ice within the perimeter of the cushion. Considerable leakage of cushion pressure can be expected in such applications either due to the uncontrolled relative movements between the adjacent segments of the skirt, or due to unfit seal lines between the cushion and the bow. As a result, an air pumping system with a very low efficiency can be expected.

From the foregoing discussion, it can be concluded that skirts are likely to be damaged if used in Arctic operations, and the air pumping system, as a result, will be extremely inefficient. Therefore a device is required to provide an identical air cavity icebreaking performance and at the same reduce the system leakage and eliminate some of the design problems. In this section, a preliminary investigation is made into the possibility of replacing the skirts by a "water curtain". An analogy is made first of all with the "air curtain" techniques to outline the principles behind the proposed concept.

6.2.1 Air Cushion Roof - Dynamic Structure

Ordinarily, certain environmental variables such as temperature, pressure, or contaminant concentration can be maintained within some prespecified ranges in a prescribed space by means of a solid structure. The form of such a structure is dictated by its protective function. "Dynamic Structure" on the other hand accomplishes this protection function by means of air walls and roofs without any solid structure.

Reference (10), for example, investigated the possibility of protecting a portion of space by means of an annular air jet. In such a device, the region to be protected from rain is surrounded by an annular jet nozzle. Due to entrainment, the annular air sheet issuing from the nozzle folds in upon itself to completely enclose the region within the annulus.

This study has been extended in Reference (11) in two ways: firstly, to include the effect of a side wind, and secondly, to properly achieve dynamic scaling by using fine glass beads instead of actual water drops so that requirement of Froude number and Reynolds number can be met simultaneously.

In Reference (5), a laboratory simulation with a scaled-down model of the Ontario Science Centre was performed in order to study the effectiveness of an air-cushion roof in preventing rain and snow from entering the courtyard at the Ontario Science Centre. The power requirement and the jet parameters are functions of the area to be protected and the specified fraction of the particles (e.g., rain drops) penetrating the air curtain.

Another application of the "air curtain" is "air curtain" doors.

The principle of the "air curtain" is relatively simple. The moving sheet of air, if its thickness and speed are high enough, prevents mixing of the interior and exterior, providing an effective barrier. When the pressure on the inside of the curtain is not the same as on the outside, then the curtain has to resist a force tending to push it one way or the other. Owing to its momentum, the curtain has a certain "stiffness" with which it can resist this force. If the inside pressure is the higher one, then the jet nozzles will have to be angled so that the jet momentum vector is initially directed inward. Owing to the outward force, the air velocity changes its direction with distance. The limit

to the "load" the curtain can withstand depends on the momentum of the jet and on the injection angle. The momentum increases both with jet thickness and with speed. The former is more economical while the latter is more effective.

6.2.2 Dynamics of a Water Curtain

6.2.2.1 General

In order to study the trajectory of a fluid particle in the water curtain under a prescribed condition, two approaches may be followed. In the first approach, emphasis can be placed on an individual fluid particle for all times; which is the familiar Lagrangian approach in dynamics. The particle velocity is obtained by differentiating the particles's position vector with respect to time. In the Cartesian coordinate system, the position vector is expressed as:

$$r(t) = x\bar{I} + y\bar{j} + z\bar{k} \tag{6.1}$$

where $\bar{I}$, $\bar{j}$, and $\bar{k}$ are the unit vectors in the x, y, and z directions. Differentiating with respect to time, the velocity of the fluid particle is given by:

$$V(t) = u\bar{I} + v\bar{j} + w\bar{k} \tag{6.2}$$

where u, v, and w are the velocity components in their respective coordinate direction. The motion of the flow field is obtained, in this approach, by solving the equation of motion of all fluid particles simultaneously. This approach is most suited for solid bodies, whereas for a fluid motion the relative positions of the particles in the flow field continuously change with time. Consequently, to keep track of the positions of all particles is an enormous task.

The second approach known as Eulerian approach, is to focus on a certain point on space and consider the motion of fluid particles that pass that point as time goes on. In this case the fluid particle velocity depends on the point in space and time, i.e.,

$$\left.\begin{aligned} u &= f_1(x,y,z,t) \\ v &= f_2(x,y,z,t) \\ w &= f_3(x,y,z,t) \end{aligned}\right] \tag{6.3}$$

or $V = V(s,t)$ (6.4)

where "s" refers to the position of a particle along the streamline.

From the above observations, it is clear that the Eulerian approach is more appropriate in the study of the water curtain dynamics.

6.2.2.2 The Water Curtain Configuration

In order to study the configuration of the water curtain, we must study first the accelerations and forces on an element of the curtain (see Figure 19).

By the Eulerian approach, the velocity components at a point in the flow are functions of both space and time as given by equation (6.3), i.e.,

$$V = u\bar{i} + v\bar{j} + w\bar{k}$$

$$u = f_1(x,y,z,t)$$

$$v = f_2(x,y,z,t)$$

$$w = f_3(x,y,z,t)$$

The acceleration components in the three directions are given by:

$$a_x = \frac{du}{dt} \, , \; a_y = \frac{dv}{dt} \, , \; a_z = \frac{dw}{dt} \tag{6.5}$$

Equation (6.5) can be expressed as a summation of the partial changes as follows:

$$\left.\begin{aligned} a_x &= \frac{\partial u}{\partial x}\frac{dx}{dt} + \frac{\partial u}{\partial y}\frac{dy}{dt} + \frac{\partial u}{\partial z}\frac{dz}{dt} + \frac{\partial u}{\partial t} \\ a_y &= \frac{\partial v}{\partial x}\frac{dx}{dt} + \frac{\partial v}{\partial y}\frac{dy}{dt} + \frac{\partial v}{\partial z}\frac{dz}{dt} + \frac{\partial v}{\partial t} \\ a_z &= \frac{\partial w}{\partial x}\frac{dx}{dt} + \frac{\partial w}{\partial y}\frac{dy}{dt} + \frac{\partial w}{\partial z}\frac{dz}{dt} + \frac{\partial w}{\partial t} \end{aligned}\right\} \tag{6.6}$$

Since $u = \frac{dx}{dt}$, $v = \frac{dy}{dt}$, and $w = \frac{dz}{dt}$

then

$$\left.\begin{aligned} a_x &= u\frac{\partial u}{\partial x} + v\frac{\partial u}{\partial y} + w\frac{\partial u}{\partial z} + \frac{\partial u}{\partial t} \\ a_y &= u\frac{\partial v}{\partial x} + v\frac{\partial v}{\partial y} + w\frac{\partial v}{\partial z} + \frac{\partial v}{\partial t} \end{aligned}\right\} \qquad (6.7)$$

and

$$a_z = u\frac{\partial w}{\partial x} + v\frac{\partial w}{\partial y} + w\frac{\partial w}{\partial z} + \frac{\partial w}{\partial t}$$

Each of the above components consists of two different types. Terms of the first type are called convective accelerations and include the changes of velocity with respect to position. The second type include terms that are associated with velocity changes with respect to time. These are called local accelerations.

Obviously, local accelerations result when the flow is unsteady, whereas convective accelerations occur when the flow is nonuniform, that is, if the velocity changes along a streamline.

As mentioned previously, individual fluid particles are not generally easily identified and one has to isolate and focus attention on a small space through which the fluid flows. The Reynold's transport theorem, known as the control volume approach, can be utilized in this instance to study the continuity and momentum equilibrium of such an infinitesimal volume $d\Psi$ of the water curtain. For a general unsteady and compressible flow the control volume continuity equation can be written as:

$$\Sigma\rho A.V = -\int_{cv} \frac{\partial \rho}{\partial t}\, d\Psi \qquad (6.8)$$

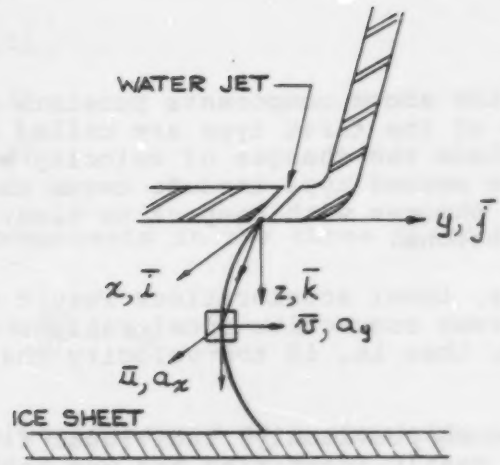

Figure 19 An Element of a Water Curtain

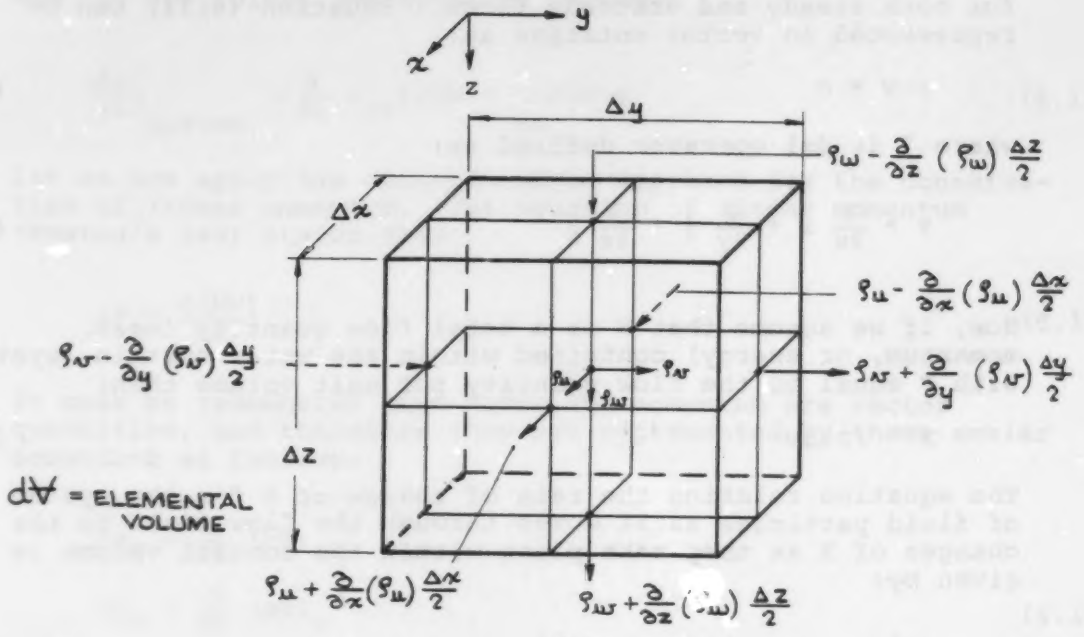

Figure 20 Continuity for Elemental Control Volume within the Water Curtain

Using the mass flux on the six faces of the above representative cubical element, then one obtains:

$$\frac{\partial}{\partial x}(\rho u) + \frac{\partial}{\partial y}(\rho v) + \frac{\partial}{\partial z}(\rho w) = -\frac{\partial \rho}{\partial t} \qquad (6.9)$$

If the flow is steady, equation (6.9) reduces to:

$$\frac{\partial}{\partial x}(\rho u) + \frac{\partial}{\partial y}(\rho v) + \frac{\partial}{\partial z}(\rho w) = 0 \qquad (6.10)$$

and if the flow is incompressible, it reduces further to:

$$\frac{\partial u}{\partial x} + \frac{\partial v}{\partial y} + \frac{\partial w}{\partial z} = 0 \qquad (6.11)$$

for both steady and unsteady flows. Equation (6.11) can be represented in vector notation as:

$$\nabla \cdot V = 0 \tag{6.12}$$

where ∇ is del operator defined as:

$$\nabla = \frac{\partial}{\partial x} i + \frac{\partial}{\partial y} j + \frac{\partial}{\partial z} k \tag{6.13}$$

Now, if we assume that X is a total flow quantity (mass, momentum, or energy) contained within the water curtain (system) with P equal to the flow quantity per unit volume then:

$$X = \int P\rho d\Psi \tag{6.14}$$

The equation relating the rate of change of X for the system of fluid particles as it moves through the flow field to the changes of X as they take place within the control volume is given by:

$$\left.\frac{dX}{dt}\right|_{\substack{\text{system of fluid} \\ \text{particles}}} = \left.\frac{\partial X}{\partial t}\right|_{cv} + \int_{cs} P\rho V_n dA \tag{6.15}$$

or in vector notation:

$$\left.\frac{dX}{dt}\right|_{\text{system}} = \left.\frac{\partial X}{\partial t}\right|_{cv} + \int_{cs} P\rho V \cdot dA$$

$$= \frac{d}{dt} \int_{cv} X\rho d\Psi + \int_{cs} P\rho V \cdot dA \tag{6.16}$$

Equation (6.16) is usually referred to as the control-volume equation in a general form. If, however, the velocity is uniform across the section (one-dimensional flow), then the second term in the right hand side of equation (6.16) can be replaced by:

$$\Sigma_{cs} P\rho V \cdot A$$

and the control-volume equation becomes:

$$\left.\frac{dX}{dt}\right|_{system} = \frac{d}{dt}\int_{cv} P\rho d\forall + \sum_{cs} P\rho V\cdot A \qquad (6.17)$$

Let us now apply the control-volume approach for the conservation of linear momentum. The equation of linear momentum (Newton's law) states that:

$$\Sigma F = \frac{d(MV)}{dt} \qquad (6.18)$$

It must be remembered that force and momentum are vector quantities, and therefore they are represented by three scaler equations as follows:

$$\begin{aligned} \Sigma F_x &= \frac{d}{dt}(MV)_x \\ \Sigma F_y &= \frac{d}{dt}(MV)_y \\ \Sigma F_z &= \frac{d}{dt}(MV)_z \end{aligned} \qquad (6.19)$$

Applying equation (6.16) to each equation with X = MV and P = V_x (≡u), v, w respectively, then:

$$\left.\begin{aligned} \Sigma F_x &= \frac{d}{dt}\int_{cv} u\rho d\forall + \sum_{cs} u\rho V.A \\ \Sigma F_y &= \frac{d}{dt}\int_{cv} v\rho d\forall + \sum_{cs} v\rho V.A \\ \Sigma F_z &= \frac{d}{dt}\int_{cv} w\rho d\forall + \sum_{cs} w\rho V.A \end{aligned}\right\} \qquad (6.20)$$

The left hand side represents the sum of all externally applied forces on the fluid within the control volume. These forces may include pressure forces, viscous forces, gravity forces, surface tension, and so on. The first term of the right hand side represents the rate at which linear momentum is stored in

the control volume, and the second term represents the net rate of efflux of linear momentum from the control volume. Note that the form of equation of conservation of linear momentum (Newton's law) as given above applies only in an inertial reference frame. Therefore, the equations derived so far apply only to a non-accelerating control volume, that is, a non-moving control volume, or moving with constant velocity.

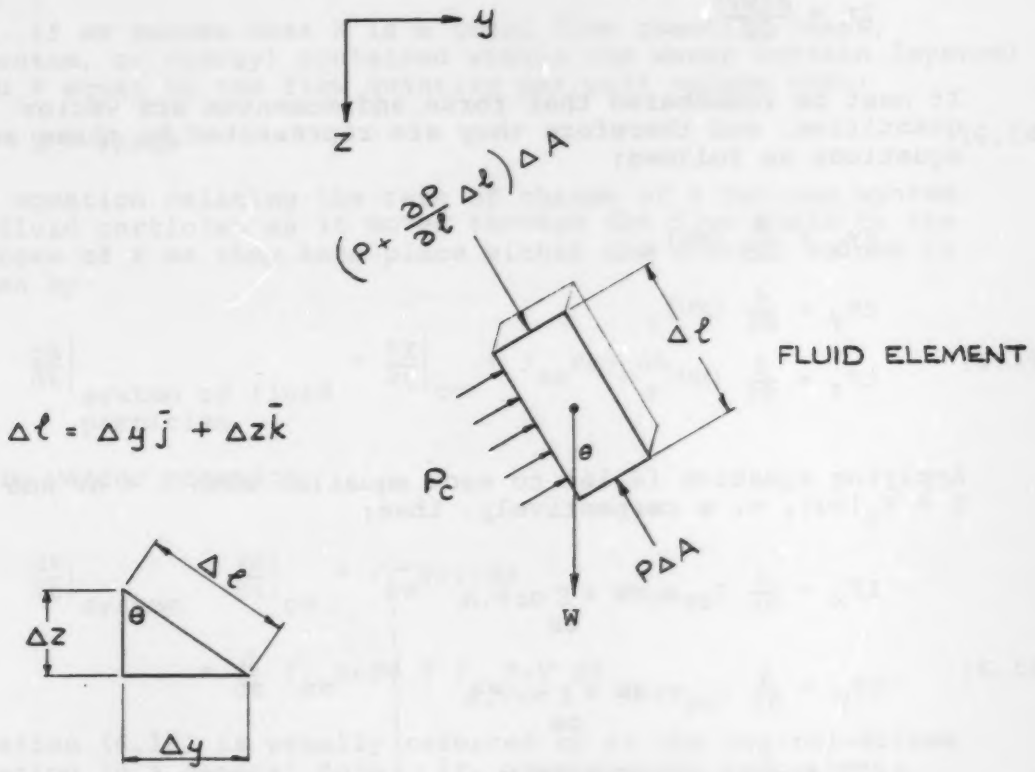

Figure 21 Forces on a Fluid Element of the Water Curtain

Consider an element of the water curtain as shown above. Here the element is being accelerated in the y and z directions and is acted upon by pressure and weight forces only. Assume that the fluid pressure varies with the length of the element, then:

$$\Sigma F_y = M a_y$$

or $$\left[\left(p + \frac{\partial p}{\partial \ell} \Delta\ell\right)\Delta A - p\Delta A\right] \sin\theta + p_c \Delta\ell \cos\theta = M a_y \qquad (6.21)^*$$

and

$$\left[\left(p + \frac{\partial p}{\partial \ell} \Delta\ell\right)\Delta A - p\Delta A\right] \cos\theta + W - p_c \Delta\ell \sin\theta = M a_z \qquad (6.22)$$

$$W = \gamma \Delta\ell \Delta A \ , \ M = \rho \Delta\ell \Delta A$$

(where γ = specific weight, ρ = density)

Then:

$$\frac{\partial p}{\partial \ell} \Delta\ell . \Delta A \sin\theta + p_c \Delta\ell \cos\theta = \rho \Delta\ell \Delta A \, a_y \qquad (6.23)$$

and

$$\frac{\partial p}{\partial \ell} \Delta\ell \Delta A \cos\theta + \gamma \Delta\ell \Delta A - p_c \Delta\ell \sin\theta = \rho \Delta\ell \Delta A a_z$$

From the trigonometric relations, (Figure 21) then:

$\sin\theta = \frac{\partial y}{\partial \ell}$ and $\cos\theta = \frac{\partial z}{\partial \ell}$, in the limiting condition as

Δy and Δz approach zero.

---

* The partial derivative of p with respect to ℓ, $\partial p/\partial \ell$, is used here because pressure may also vary with time.

$$\text{Therefore } \frac{\partial p}{\partial \ell} \cdot \Delta A \cdot \frac{\partial y}{\partial \ell} + p_c \frac{\partial z}{\partial \ell} = \rho \Delta A a_y$$

$$\text{and } \frac{\partial p}{\partial \ell} \cdot \Delta A \frac{\partial z}{\partial \ell} + \gamma \Delta A - p_c \frac{\partial y}{\partial \ell} = \rho \Delta A a_z \qquad (6.24)$$

Assume that the water curtain thickness is S which is a function of y, z, and t, i.e.,

$$S = f(y,z,t)$$

The third dimension of the fluid element is taken as a unit length since we are dealing basically with a 2-dimensional flow in the y-z plane. Therefore $\Delta A = S$, and from equation (6.7) for a steady flow (i.e., zero local acceleration terms) and from equation (6.24), then:

$$\frac{\partial p}{\partial \ell} S \frac{\partial y}{\partial \ell} + p_c \frac{\partial z}{\partial \ell} = \rho S(v \frac{\partial v}{\partial y} + w \frac{\partial v}{\partial z})$$

and (6.25)

$$\frac{\partial p}{\partial \ell} \cdot S \cdot \frac{\partial z}{\partial \ell} + \gamma S - p_c \frac{\partial y}{\partial \ell} = \rho S(v \frac{\partial w}{\partial y} + w \frac{\partial w}{\partial z})$$

The continuity equation will read (from equation 6.1):

$$\frac{\partial v}{\partial y} + \frac{\partial w}{\partial z} = 0 \qquad (6.26)$$

With the boundary conditions defined as (see Figure 22):

$$v = V_{jet} \cos \alpha \text{ at } y = 0, z = 0$$

$$w = V_{jet} \sin \alpha \text{ at } y = 0, z = 0 \qquad (6.27)$$

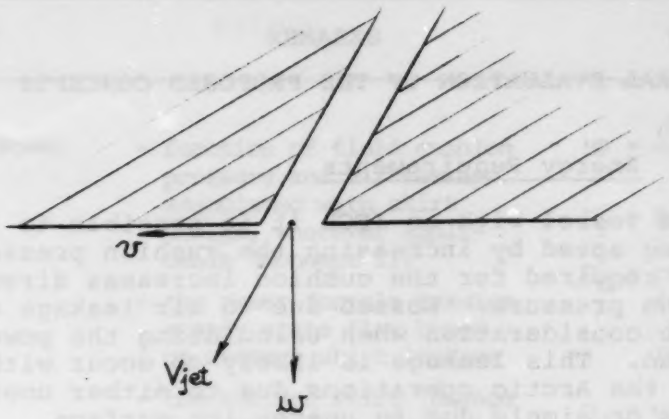

Figure 22 Jet Inclination

and the elementary length is defined as:

$$\partial \ell = \partial y \bar{j} + \partial z \bar{k}$$

then it is possible to solve the above set of partial differential equations to obtain the shape of the water curtain under steady two-dimensional state.

Obviously, the effects of ship speed and wind speed (co-flowing, counter-flowing, and cross wind) will have to be considered in a more realistic three-dimensional analysis of the water curtain dynamics.

In addition, a more accurate prediction of the dynamics and shape of the water curtain may be obtained by a quantitative analysis of the detailed structure of the jet flow field. The effects of the cushion pressure on the deformation of the water curtain can be studied by utilizing the line-source technique in the space enclosed by the curtain. The interaction between the water curtain and the solid ice sheet can be simulated by using the singularity image technique and then by studying the behaviour of the whole flow field.

Estimations of jet velocity* and power required for the water jets are given in Appendix A.

---

* Jet velocity V_{jet} is required as a boundary condition in the analysis of the water curtain dynamics (see expression 6.27)).

7. GENERAL EVALUATION OF THE PROPOSED CONCEPTS

7.1 Energy Requirements

For a vessel with an IFCB it is possible to increase the icebreaking speed by increasing the cushion pressure. However, the power required for the cushion increases directly with the cushion pressure. Losses due to air leakage should be taken into consideration when calculating the power required for the fan. This leakage is likely to occur with flexible skirts in the Arctic operations due to either unexpected ice formations or simply due to uneven ice surface.

The energy requirements for a vessel with an integral fluid cushion bow (IFCB) may be summarized as follows:

a) cushion auxiliary systems;
b) cushion power;
c) propulsion power:
   - cushion resistance
   - ship resistance
d) ice dispersal energy

CATEGORY	REMARKS	FORMULA
(a) Cushion Auxiliary Power	- required for supporting the fluid cushion bow. Devices such as de-icing or anti-icing provisions may require appreciable power and should be accounted for in detail energy analysis.	
		to be continued

Table 2 Energy Requirements for a Vessel with IFCB

CATEGORY	REMARKS	FORMULA
(b) Cushion Power	- function of fluid cushion pressure and air leakage associated with skirt design, wherever applicable (Concept II) - the power formula assumes steady state flow based on average skirt leakage - the average skirt leakage is governed by the choice of skirt type and the operating clearance (seal depth); larger clearance can reduce the skirt drag, but it will require more pressure power - the cushion perimeter is related to the pressure energy, whereas the cushion beam is related to the icebreaking capability - the air flow and pressure fluctuations caused by the variation in the skirt leakage due to either icebreaking or uneven ice sheets, imply the need for a power margin; a general trend is to use about 50% margin in the actual installed power of the fan	$HP = \frac{(P_f/P_c)\ P_c Q_c}{75\ \eta_f}$ P_f = fan pressure (kg/m^2) P_c = cushion pressure (including a margin for leakage) (kg/m^2) Q_c = volumetric fluid flow (including a margin for leakage) (m^3/sec) η_f = fan efficiency
(c) Propulsion Power	- the horsepower required for the icebreaker is based on the total resistance of the design	$HP = TU/75\,\eta$ T = thrust (kg) = total resistance U = ship speed (m/s) η = propulsion coefficient

to be continued

Table 2 Energy Requirements for a Vessel with IFCB

CATEGORY	REMARKS	FORMULA
(c) Propulsion Power (cont'd)	- to determine the propulsive power, the overall propulsive efficiency should be taken into account	
	- in open water, the integrated bow will contribute very little to the total resistance of the ship if it is well above water level; it will only affect the aerodynamic drag component	
	- for Concept II, with solid side skirts, the frictional and wave making resistance of the ship will be affected; model tests may be required to assess the increase in the resistance	
	- in icebreaking mode, the total resistance consists of ship ice resistance, aerodynamic drag, DA momentum drag, DM, skirt drag on ice, DI (if applicable), and pressure drag D_p.	$DA = \frac{1}{2}\rho_A U^2 S_A C_{DA}$ $DM = \rho_C \cdot Q_{Fan} \cdot U$ $DI = \mu_I \cdot \Sigma A_{CIi} + \mu_I \Sigma R_i$ $D_p = \Sigma D_i + \Sigma D_j$ where: C_{DA} = aerodynamic drag coefficient S_A = aerodynamic drag reference area Q_{Fan} = fan intake flow

to be continued

Table 2 Energy Requirements for a Vessel with IFCB

CATEGORY	REMARKS	FORMULA
(c) Propulsion Power (cont'd)		μ_I = ice to skirt friction coefficient A_{CIi} = ice contact area of i^{th} skirt segment R_i = ice edge reaction force $D_{i,j}$ = pressure drag component, front and rear skirt segment ρ_A = air density at atmospheric pressure ρ_C = cushion air density
(d) Ice Dispersal Area	- using the ACV icebreaking principles, a considerable savings in the ship dissipated energy in submerging and dispersing the broken ice fragments can be achieved	

Table 2 Energy Requirements for a Vessel with IFCB

7.2 Limitations and Technical Difficulties

Most of the technical difficulties encountered with the proposed concepts were outlined in the previous sections. The nature of each concept determines to a large extent the problems requiring investigation. Four specific problems were isolated, however, and readdressed in the next subsections, namely: skirts, stability of jet sheets, noise radiation, and spray.

7.2.1 Skirts

Losses due to air leakage must be taken into consideration when calculating the power required for the fan. This leakage is likely to occur with flexible skirts in the Arctic operations due to either unexpected ice formations or simply due to uneven ice surface.

Skirt damage is a major problem with serious consequences on the overall performance of the whole unit. Material used for model and prototype skirts are usually of nylon fabric polyurethane. Reference (4) indicated that two grades of the materials were used in the indoor and outdoor model and prototype testings, namely #15381 black Neoprene at 0.36 kg/m^2 (10.5 oz. per square yard) and #5944 black Neoprene at 0.54 kg/m^2 (16.0 oz. per square yard) for rear skirts only. Both materials were obtained from Reeves Brothers Inc., (Industrial and Coated Fabrics Division). The maximum operating conditions for these tests with the ACT-100 were: cushion pressure equivalent to about 61 cm (2 ft) of water in ice thickness of about 52 cm (1.7 ft), with ultimate strength of about 620 kPa (90 psi).

The material and seal design required for polar sized IFCB are certainly outside the current state-of-the-art. The design pressure of over 35 kPa (5.25 psi), (e.g., 2.5 m (8 ft) of water x 1.5 margin) and possible seal depth of between 6 and 9 m (20 and 30 ft) are untried requirements (4). Skirt leakages are likely to be unacceptably high which would have a deleterious effect on the icebreaking performance of the integrated bow.

7.2.2 Stability of Jet Sheets (Water Curtain)

Thin jet sheets have a strong tendency to adhere to adjacent surfaces (the Coanda effect), and if there are two such surfaces, the jet may have difficulty in choosing to which one it should attach. In fact, a small change in the environmental condition could cause the jet sheet to flip from one surface to the other. This flow instability must be carefully taken into account in designing the jets and the shapes of all nearby surfaces. On the other hand, the Coanda effect can be put to good use as a control device or scoop at the jet exit.

7.2.3 Noise Radiation

For air and water jets, noise will emanate from motors, blowers, fans, pumps, and the jet itself. Conventional acoustical techniques can be used to silence all but the last of these noise sources. The noise generated by the jet flow can be estimated by semi-empirical formulas.

Whether the level of noise would be acceptable or not depends on the presence of other noises. However, it is anticipated that for the proposed concept the additional noise will not be too hazardous to jeopardize its application.

7.2.4 Spray

The spray generated by ACVs is a recognized problem area as it affects visibility, and for applications in low temperature regions, results in icing of the craft. Spray suppression skirts have been developed and tested in a variety of craft and have met with considerable success.

For icebreakers with a fluid cushion bow, research at the model stage will be required to investigate spray and icing, particularly in the case of the water curtain where ice formation could be severe.

Use of de-icing systems such as electric heating low adhesion coatings or other specialized coatings will be investigated.

7.3 Preliminary Assessment of the Recommended Concept - CONCEPT I

As clearly indicated in this report, extensive analytical and comprehensive experimental investigations are required to assess the performance of the proposed concepts. However, it can be envisaged at this stage that CONCEPT I (Extended Bow with Air Cushion/Water Curtain) will show the most promising performance in a simulated Arctic environment, provided that the "water curtain" technique is feasible and the curtain can withstand an inward-outward force resulting from an air cushion pressure of about 5 psi. In this section, a preliminary assessment is given to indicate the potentiality of the concept under consideration.

The ice fracture can be studied either with or without the formation of the cavity beneath the ice sheet, as discussed in detail in the following sections.

7.3.1 Ice Fracture with Air Bubble Formation

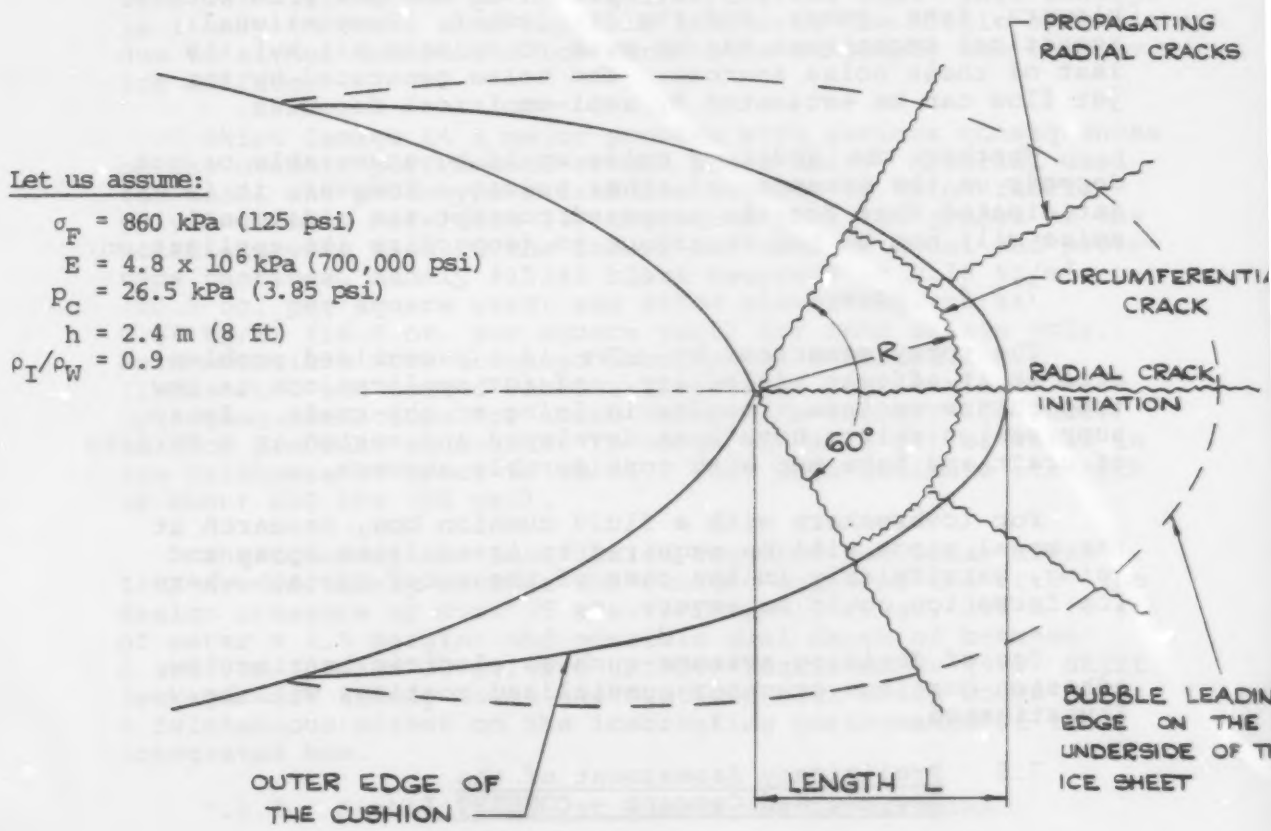

Let us assume:

σ_F = 860 kPa (125 psi)

E = 4.8 x 10^6 kPa (700,000 psi)

p_c = 26.5 kPa (3.85 psi)

h = 2.4 m (8 ft)

ρ_I/ρ_W = 0.9

Figure 23 Sketch for Ice Fracture with Air Bubble Formation

Since the water curtain will be more effective in reducing the leakage, then one can assume that the ratio

$$\frac{p_c}{\rho_w g h}$$ is about 1.1 instead of 1.5 or even more.

The theoretical bubble propagation speed (at the ice surface) can be calculated from reference (4) as:

$$u = \sqrt{\frac{2}{3}\left(\frac{p_c}{\rho_w gh} - \frac{\rho_I}{\rho_w}\right) \cdot gh}$$

$$u = 1.8 \text{ m/s } (5.9 \text{ ft/s})$$

The critical speed ratio $(\frac{U}{u})_{crit}$, which is corresponding to coincident bubble leading edge to ice failure position at the instant of ice failure, is given by:

$$(\frac{U}{u})_{crit} = (1 - \frac{w}{p_c})^n, \quad n = \tfrac{1}{2} \text{ for a wedge-type ice fragment.}$$

"w" is the distributed weight of the unbalanced ice sheet and is given by:

$$\rho_I h = 21.5 \text{ kPa } (3.12 \text{ psi})$$

$$(\frac{U}{u})_{crit} = 0.435$$

and with u = 1.8 m/s (5.9 ft/s), therefore:

$$U_{crit} = 0.8 \text{ m/s } (2.6 \text{ ft/s}).$$

Now, with the ship speed U, say, 2.0 m/sec (4 knots), i.e., $U > U_{crit}$ and $(\frac{U}{u}) > 1$, then the ice wedge will deflect downward and failure will occur ahead of the bubble leading edge.

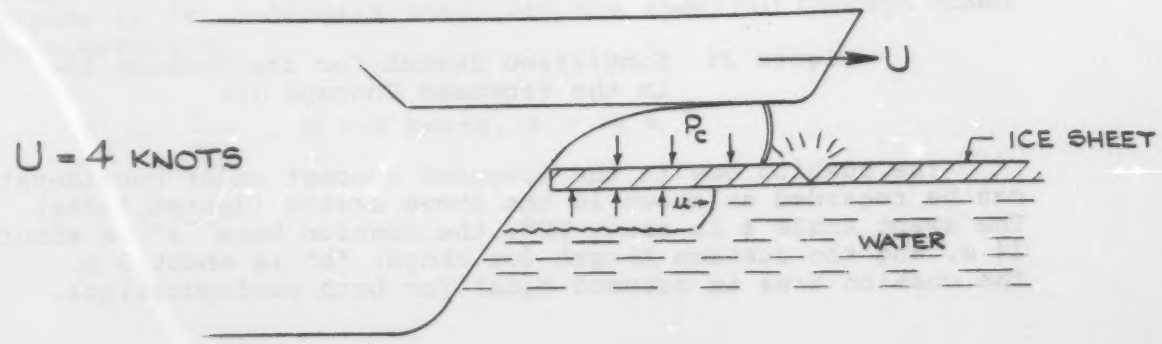

Figure 24 Ice Failure Ahead of the Bubble Leading Edge

It is worth noting that if the required speed is about 1.54 m/sec (3 knots), i.e., $U > U_{crit}$ and $\frac{U}{u} < 1$, then ice failure will still occur ahead of the cushion bow but within the air bubble, that is to say, the leading edge of the cavity is ahead of the circumferential crack at the instant of ice failure.

Some correlation may be made from the data published on the 60° swept ACIB model (4,9). The geometrical features of the concept under consideration and those of the swept model are closely related.

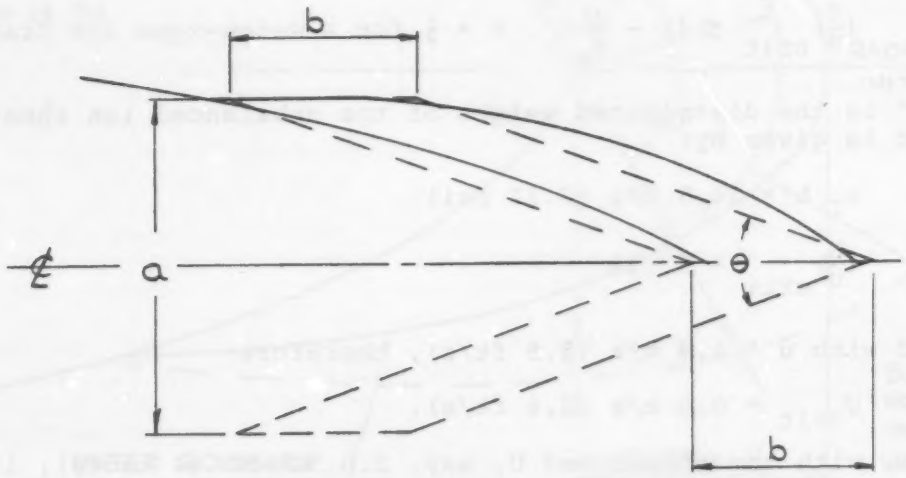

Figure 25 Simplified Sketch for the Cushion Bow in the Proposed Concept (I)

The cushion bow in the proposed concept under consideration, can be regarded as shown in the above sketch (dotted lines). The swept angle θ is about 60°, the cushion beam "a" is about 24 m, and the cushion length (or chord) "b" is about 3 m. The cushion area is assumed equal for both configurations.

Now, for a given cushion dimensions, the "cushion" power is a function of the cushion area or simply of the perimeter "c". On the other hand, observations on the icebreaking performance of model and full scale ACIBs indicated that icebreaking capability is related to the cushion beam "a". Therefore the ratio $\gamma = \frac{\text{perimeter } c}{\text{beam } a}$ represents the cushion power requirement for a given icebreaking capability. The lower the ratio, the better the design. Figure 25 shows the ratio versus the chord/beam ratio from which it is clear than an optimum design (minimum γ) can be achieved with a minimum chord/beam ratio. The actual minimum dimensions, however, will be dictated by the length of unsupported ice required to induce ice fracture for a given ice thickness.

The minimum over-hanged length of the integrated cushion bow may be obtained by applying the ice fracture theory either to a wedge type section (Carter) or to a constant-section cantilever beam (Milano), in a specific ice fracture mode. In addition, structural and strength requirements must be considered simultaneously so that a best compromise can be reached.

The bow cushion configuration proposed here seems to fulfill another design requirement, namely, minimum overall drag of the integrated hull. The additional drag consists basically of two components, viz., the aerodynamic drag and wave drag.

With regard to the first component, the above water extended bow is made reasonably streamlined, and therefore minimum additional aerodynamic drag can be expected.

With regard to the second component, it has been shown in reference (4) that the wave drag of a 60^{o} swept configuration is substantially less on average up to Froude number $F_n = 0.5$ compared with the rectangle and the double module configuration. Figure 26 (4) indicates that, for the specific concept under consideration:

$$F_n = \frac{U}{\sqrt{ga}} \quad , \; U = 4 \text{ knots}, \; a = 24 \text{ m}$$

$$= 0.15$$

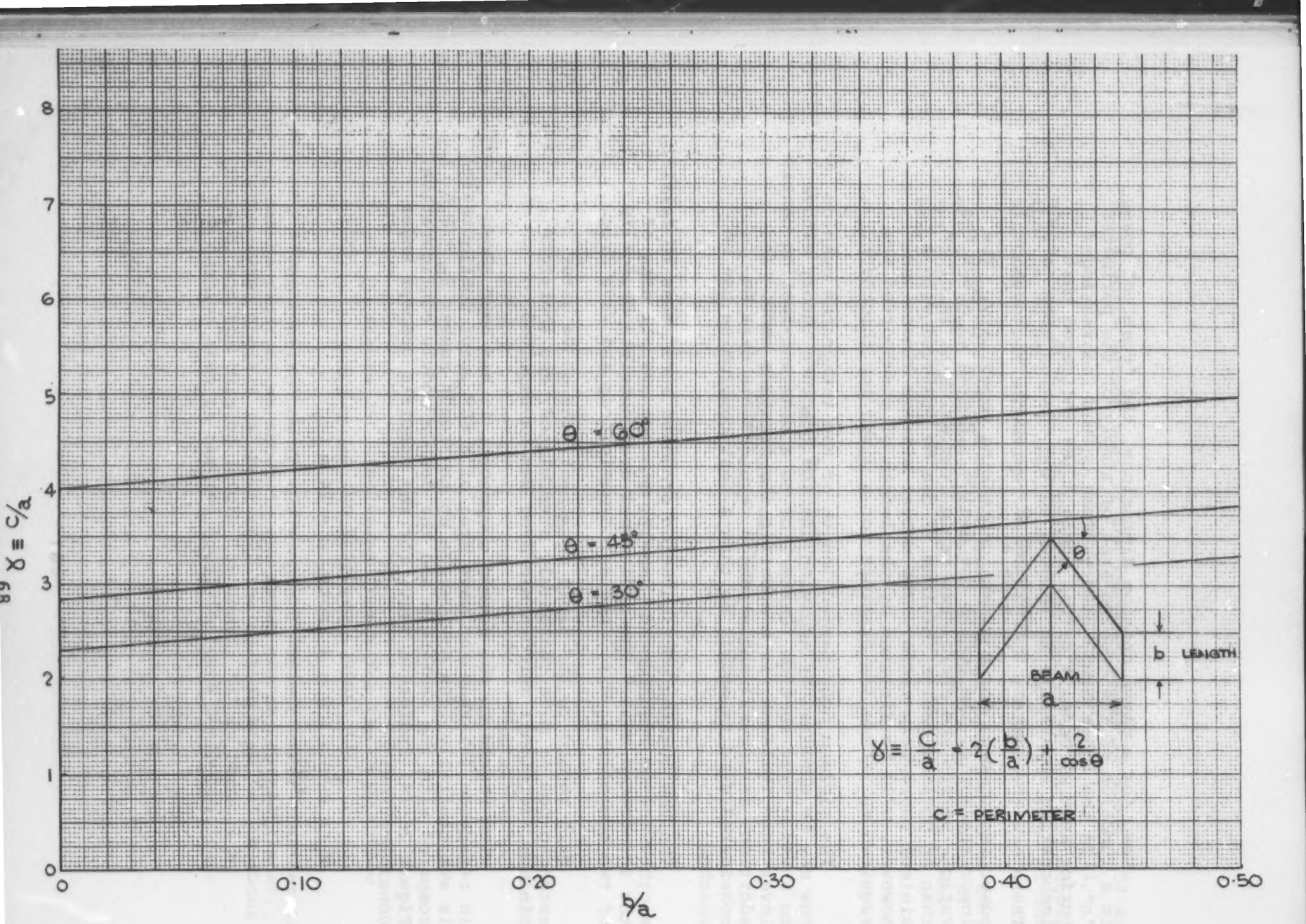

Figure 26 Perimeter/Beam Ratio Vs. Chord/Beam Ratio for the Cushion Bow as a Swept Module

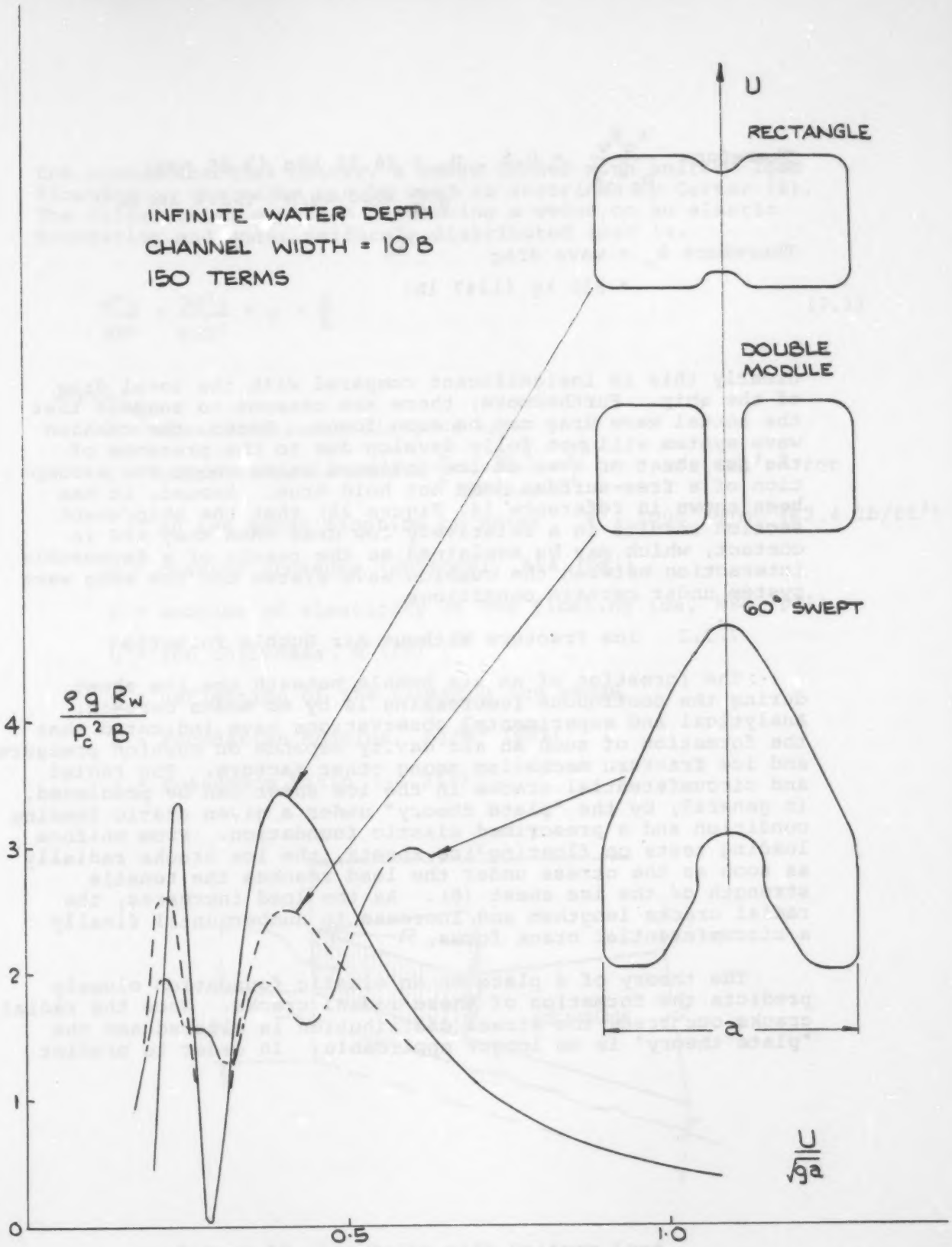

Figure 27 WAVE DRAG OF THREE ACV PLANFORMS

Therefore $\frac{\rho_g R_w}{p_c^2 . a} = 0.5$, $p_c = 26.55$ kPa (3.85 psi)

$\rho_g = 1000$ kg/m^3 (62.4 lb/ft^3)

Therefore R_w = wave drag

= 610 kg (1347 lb)

Clearly this is insignificant compared with the total drag of the ship. Furthermore, there are reasons to suggest that the actual wave drag may be even lower. First, the cushion wave system will not fully develop due to the presence of the ice sheet or even in ice-infested water where the assumption of a free-surface does not hold true. Second, it has been shown in reference (4, Figure 28) that the ship/swept section results in a relatively low drag when they are in contact, which may be explained as the result of a favourable interaction between the cushion wave system and the ship wave system under certain conditions.

7.3.2 Ice Fracture Without Air Bubble Formation

The formation of an air bubble beneath the ice sheet during the continuous icebreaking is by no means certain. Analytical and experimental observations have indicated that the formation of such an air cavity depends on cushion pressure and ice fracture mechanism among other factors. The radial and circumferential cracks in the ice sheet can be predicted, in general, by the "plate theory" under a given static loading condition and a prescribed elastic foundation. From uniform loading tests on floating ice sheets, the ice cracks radially as soon as the stress under the load reaches the tensile strength of the ice sheet (6). As the load increases, the radial cracks lengthen and increase in number until finally a circumferential crack forms.

The theory of a plate on an elastic foundation closely predicts the formation of these radial cracks. Once the radial cracks occurred, the stress distribution is altered and the "plate theory" is no longer applicable. In order to predict

the circumferential cracks, a wedge loaded with uniform load floating on the water can be used as described by Carter (6). The differential equation describing a wedge on an elastic foundation and under uniformly distributed load is:

$$\frac{d^4y}{d\bar{x}^4} + \frac{2d^3y}{\bar{x}d\bar{x}^3} + y = \frac{p}{k} \qquad (7.1)$$

where:

$\bar{x}$ = non-dimensional distance x/L

L characteristic length $\left[\frac{Eh^3}{12k(1-\mu^2)}\right]^{\frac{1}{4}} \approx 0.312\ (Eh^3)^{\frac{1}{4}}$ for an ice wedge floating on water $k = 1000\ kg/m^3\ (62.4\ lb/ft^3)$

p = cushion pressure (uniform), kPa (psi)

E = modulus of elasticity of the floating ice, kPa (psi)

h = ice thickness, m (ft)

y = deflection of the floating ice wedge

k = Foundation Modulus, kg/m^3 (psi)

μ = Poisson's Ratio (~0.317)

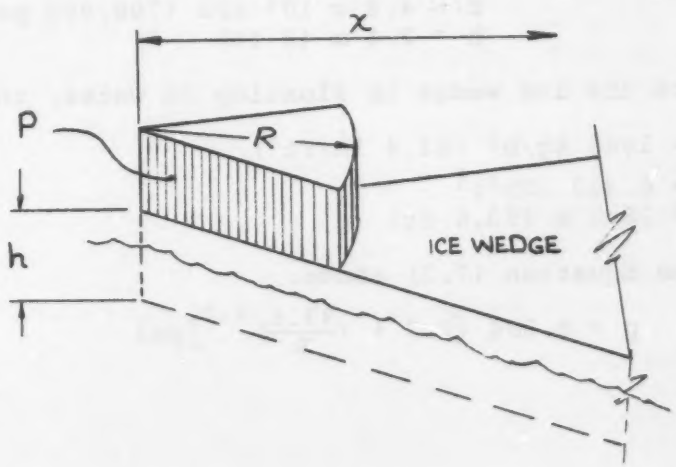

Figure 28 Ice Wedge with Uniform Load - No Air Bubble Formation

The solution of Equation (7.1) will determine the deflection of the ice wedge at a distance $\bar{x}$.

Consequently, the distribution of the bending stresses can be obtained. Carter (6), has represented the function

$$g\left(= \frac{\sigma h^2}{3pR^2}\right) \text{ by the approximate form:}$$

$$\frac{1}{g(R/L)^2} = \left[2.7 + (L/R)^{2.5}\right]$$

Therefore

$$\frac{3pR^2}{\sigma h^2 (R/L)^2} = \left[2.7 + (L/R)^{2.5}\right]$$

or $$p = \frac{\sigma h^2}{3L^2}\left[2.7 + (L/R)^{2.5}\right] \qquad (7.2)$$

The cirsumferential crack will occur when the maximum bending stress σ reaches the flexural strength of the ice sheet σ_F. If we assume that $\sigma_F \simeq 860$ kPa (125 psi)

$E = 4.8 \times 10^6$ kPa (700,000 psi)
$h = 2.4$ m (8 ft)

and since the ice wedge is floating in water, then

$k = 1000$ kg/m^3 (62.4 lb/ft^3)

$L \simeq 0.312\,(Eh^3)^{\frac{1}{4}}$
$= 28.5$ m (93.6 ft)

Then from Equation (7.2) above:

$$p = 0.304\left[2.7 + \left(\frac{93.6}{R}\right)^{2.5}\right] \text{psi}$$

Now, to estimate the required pressure to break the ice in the absence of the air bubble, one can assume that the radius of load R is equal to the length of the cushion b{≈6.0 m (20 ft)}.

Thus:

$$p = 105 \text{ kPa } (15.22 \text{ psi})$$

which is outside the practical application of the concept.

With the cushion pressure equal to that required for icebreaking with an air bubble {i.e., p ≈ 36.5 kPa (3.85 psi)}, the cushion length (radius of load) would have to be about 11.4 m (37.3 ft) which is again impractical due to its structural implications.

It is clear that icebreaking as a result of air cavity formation beneath the ice sheet is an efficient and economic way to break ice compared with that of increasing the bearing load of the ice sheet.

Finally, the determination of the position of the circumferential crack is analytically possible by using a simple two-dimensional plate theory.

8. PROPOSAL FOR A FEASIBILITY STUDY OF AN ICEBREAKER WITH AN INTEGRAL FLUID CUSHION BOW

The main objective of the study will be to investigate the technical feasibility of the proposed concepts for an integrated fluid cushion bow. This will include detailed analysis of the concepts, which will then be substantiated by experimental model studies. The water curtain, in particular, will require considerable research effort to substantiate the concept.

8.1 Work Plan

In the following subsections, the tasks required to evaluate the concepts are presented.

TASK 1.0 - ANALYTICAL STUDY

Sub-Task 1.1 - "WATER CURTAIN" Device (Concepts I & II)

It is essential that a quantitative understanding of the jet flow, and its interaction with the air cushion flow precede the implementation of the device.

Basically, the flow field of the jet is determined by three parameters: the jet velocity V_j, the jet thickness t_j, and the diameter (or characteristic length) of the enclosed area B_j.

When a water curtain is used to enclose a high air pressure, then we must add parameters such as air cushion pressure and the traversing ship speed to the above jet parameters. Therefore, if the water jet is characterized by V_j, t_j, B_j, ρ_j, and ν_j, the ship speed is V_s, the air cushion pressure is p_c with mass density ρ_c, at temperature T_c, and the gravitational acceleration "g", then we have:

$$V_j,\ t_j,\ B_j,\ \rho_j,\ \nu_j,\ V_s,\ p_c,\ \rho_c,\ T_c,\ g$$

as the main parameters of the problem.

One fairly obvious method to group these ten parameters in dimensionless ratios is as follows:

$\Pi_1 = \rho_j/\rho_c$ density ratio

$\Pi_2 = V_j/V_s$ velocity ratio

$\Pi_3 = t_j/B_j$ thickness/beam ratio

$\Pi_4 = \frac{P_c}{\rho_c T_c}$ gas constant

$\Pi_5 = \frac{V_j t_j}{\nu}$ Reynold's number

$\Pi_6 = V_j^2/t_j g$ Froude number

In addition to the above non-dimensional ratios, there are some other design parameters which will have to be investigated as well. Parameters such as the orientation of the water jets and the water pressure required to maintain minimum deformation on the water curtain are very critical in the evaluation of the effectiveness of the concept. Elevation of the jet nozzles and effects of multi-directional winds on the jet flow fields will be investigated.

Sub-Task 1.2 - Cushion Perimeter and Dimensions

As clearly indicated in the text, the required cushion power is proportional to the perimeter, while the icebreaking capability of the air cushion is a function of the maximum beam for a specific ice fracture mode. The length of the cushion strongly affects the "explosion" or the "overload cracking" of the ice sheet, depending on the unbalanced length of the wedged section.

With the forward section of the L.W.L. representing the ice edge, it is possible, analytically, to predict and study the formations of the air bubbles and their static and dynamic characteristics along the "ice edge".

Then, based on a finite element ice fracture technique, (similar to that, for example, developed by DeHavilland), and with presumed radial cracks, one can predict the pattern of ice failure under different loadings.

Sub-Task 1.3 - Crack Initiation and Propagation

The ice sheets crack radially when the stresses in the sheet reach the tensile strength. Increasing the load (i.e., pressure) causes these cracks to increase in length, as well as in number. Whether these radial cracks result in wedged sections, constant beam sections, or take a form of centre crack will depend on previous experimental observations on similar arrangements.

Circumferential cracks occur when the maximum bending stress exceeds the flexural strength of the ice sections under consideration. This can simply be predicted by a two-dimensional wedge or plate theory, as the case may be. With these tools, (sub-tasks 1.1, 1.2, and 1.3), the analytical simulation of the IFCB, with the water curtain technique, will enable the designers to carry out parametric studies for optimization or examination of a specific design or concept. The air bubble propagation theory will relate the ice fracture potential, the forward speed, the cushion pressure and ice thickness.

In addition, in view of the high cost of full scale prototype tests and the potential limitations in scaling up the model test results directly (as we will indicate later), it is hoped that this approach (i.e., analytical simulation) would be the most sensible course. The methodology of the analytical simulation will be devised in such a way that almost any range of parameters may be examined for a vessel with an IFCB.

Such a simulation will be validated by appropriate experiments.

Sub-Task 1.4 - Hydrostatic Stability

Roll and pitch stability do not possess any real danger for operations in ice. Conventional icebreakers are normally designed with a relatively high metacentric height as a result of the low centre of gravity due to the heavy underwater scantlings.

For the proposed CONCEPT I, the extended bow above water level, its weight, fan motors, nozzles and piping will result in shifting the CG of the original ship forward and upward. For a given design, using weights, moments, and required trim, the new metacentric height can be calculated. For free water cruising, the approximate period of roll may be estimated from the approximate formula (added virtual mass has been ignored, as it is likely to be small in the case of rolling):

$$T_\phi = 2\Pi \frac{K}{\sqrt{g\ GM_T}}$$

with the value of K (i.e., transverse radius of gyration) given by:

$$\left(\frac{K^2}{B}\right) = F\left[C_B\ C_u + 1.10\ C_u(1 - C_B)\left(\frac{H}{T}^{-2.20}\right) + \frac{H^2}{B^2}\right]$$

C_u = upper deck area coeff. = $\frac{1}{LB}$ x (deck area)

which is also affected by the extended bow (CONCEPT I)

H = effective depth of ship = $D + A/L_{pp}$

A = projected lateral area of erections
T = draft
F = constant*
  ≈ 0.133 for oil tankers
  ≈ 0.177 for large war ships
    (we take it ≈ 0.15 for icebreakers)

A formula for pitching period can be developed similar to that for rolling, but in this case, added virtual mass cannot be neglected. The formula, neglecting damping is:

$$T_p = \frac{2\Pi K}{\sqrt{gGM_L}} \sqrt{\frac{V + V^1}{V}}$$

---

*"Basic Ship Theory", by K. J. Rawson, 1979.

where K = longitudinal radius of gyration
V = volume of displacement
V^1 = volume of entrained water

The rolling period of a ship is much more under control than the pitching period and is affected by adding substantial weights, as for example in the case of CONCEPT I, if the extended bow happened to be within that category of "substantial" weights. The change in the natural pitching period will be investigated as a result of the extended bow. The resultant increased height of the centre of gravity will have a negligible influence on the T_p since GM_L is usually so high (of the order of the length of the ship or more). On the other hand, additional weight to the forward end of the ship would increase K and, thus, lengthen the period.

It is anticipated, however, that the extended bow concept will only have marginal effects on both roll and pitching stability in open water compared with the original hull.

For CONCEPT II, roll and pitch stability (periods) in open water will be calculated according to the above approximate formulae.

For CONCEPT III, since there are no changes in the under water or above water hull forms, the motion response will be identical to the original ship.

Sub-task 1.5 - Hydrodynamic Flow

The wave pattern and the potential flow about the submerged hull will be investigated for the three concepts. A three-dimensional potential flow program can be used to predict ice block paths. The analysis will include a usable Froude number range, equivalent to 3 - 10 knots at prototype scale.

Good seakeeping is clearly desirable, but the difficulty lies in determining how far other design features must, or should, be compromised to improve seakeeping. For example, an improved icebreaking performance may be acceptable at the expense of increasing the natural

rolling period. A particular aspect of seakeeping, that is the beached intact stability for icebreakers, will be studied for the three concepts. It is essential to ensure adequate stability when the ship is beached on an ice shelf during "ramming" mode operation. The problem can be further aggravated by the pressure of topside icing and high winds. The initial stability in the beached condition will be estimated for the three concepts from approximation of weights and centres.

Sub-Task 1.7 - Ice Trajectories

The manner in which the ice and the near surface water layers are distorted by the passage of the ship will be investigated through potential flow theory, as already indicated under sub-task 1.5. Ship parameters and cushion dimensions may have to be changed slightly to minimize flow disruption about the bow during icebreaking and to predict the ice floe trajectories along the hull.

TASK 2.0 - EXPERIMENTAL STUDY

Sub-Task 2.1 - Water Curtain Device

The results of the analytical analysis pursued under sub-task 1.1 will be validated through experimental data. First of all, the practicality of using a "water curtain" to maintain a high air pressure will be investigated. The simplest approach will be to test a platform with simple configuration (such as a circular or rectangular platform) fitted with water jet nozzles on its perimeter and high air pressure inside. The tests can be carried out on NRC experimental tanks or on UTIAS facilities*, with the tested platform rigidly clamped to the carriage. The fan or the compressor required to supply the high pressure air, and the circulating pumps required for the water jets, can be mounted on the carriage itself, which makes the construction of the tested platforms very simple indeed. The tests will be carried out under static and dynamic conditions, with the wind being simulated by an adjustable blower attached to the traversing carriage.

---

*University of Toronto, Institute for Aerospace Studies.

As indicated in sub-task 1.1, there are six dimensionless ratios affecting the performance of the water curtain concept. These Π terms are quite useful in achieving proper dynamically similar systems. The six dimensionless ratios will have to be the same for the model and the prototype. However, such a task is practically impossible since the requirements for some of these ratios are in contradiction with each other. For example, the jet thickness has to be directly proportional to the jet velocity vide supra Π_2, while it has to be inversely proportional to the jet velocity squared vide supra Π_6.

In practice, however, the phenomenon under investigation usually determines the most effective ratios to be considered in the study. For example, in the present study of the water curtain, it is safe to suggest that the Reynold's number Π_5 is probably more important to achieve dynamic similarity than the Froude number Π_6.

Additional parameters to be considered in the study:

* effect of the jet elevation on the structure of the water curtain flow; and,
* effect of the jet exit angle on both the water curtain flow and the pressurized area.

Sub-Task 2.2 - Validation

Results of the experimental task 2.1 will be used to validate the analytical analysis of the water curtain device pursued under sub-task 1.1. Discrepancies between results will be identified and explained.

TASK 3.0 - CRITIQUE OF CONCEPTS

As a result of the extensive analytical and experimental investigation, a recommendation for a specific system will be made to TDC. Alternatively, a development pattern will be suggested for continued investigation. This will take the form of an interim report forwarded to TDC.

At this point, TDC may choose to pursue the recommended concept, suggest another development route, or curtail the project.

TASK 4.0 - MODEL TESTING

The recommended concept, once approved by Transport Canada, will be adapted to an icebreaker model, whose characteristics will be supplied by TDC. Towing tank tests will then take place in open water and in ice sheets, in order to confirm the results obtained in Tasks 1 and 2.

Sub-Task 4.1 - Open Water Tests

Open water resistance tests will be carried out if the under water hull form of the recommended concept is different from a conventional hull; such as Concept II for example. Power curves will be obtained for the required sea state, with the fluid cushion device inoperative.

Sub-Task 4.2 - Stability

At Beaufort Sea state 6, roll stability of the ship for a following sea, following quartering sea, and beam sea will be checked experimentally. Roll stability in waves will also be checked, if required.

Sub-Task 4.3 - Model Ice Tests

Tests in model ice will be conducted for the recommended concepts. Indoor model tests under controlled conditions are preferable for the continuous icebreaking tests. Open water tank with natural ice formed at the top may be used for the experimental investigation of the water curtain concept in icebreaking.

In accordance with the icebreaker class chosen for the prototype installation, ice thickness and strength will be equivalent to maximum ice thickness and half of this thickness for fresh water ice (80 cm and 40 cm), or for Arctic ice (3 and 1.5 m). In addition, parameters, such as ice strength, elasticity and plasticity, skirt material properties and skirt/ice friction characteristics will be properly modelled.

Ice properties will be checked before each run to improve correlation between test runs. The model scale will be chosen in such a way that all parameters, which significantly

affect the model behaviour, will be correctly modelled. Ice resistance, under controlled ice conditions, with the fluid cushion bow in operation, will be measured and dimensionalized. Visual operation and film recording will be useful to understand the fluid cushion fracture mechanism of the tested concept under different conditions. Underwater camera and good lighting will be required to observe the air bubble and crack initiation and propagation. Ramming tests will be done only as a check on the ship's stability, and will be done on a rigid floating template, and not on model ice.

TASK 5.0 - VALIDATION

Performance criteria developed in Sections 2 and 4 will be applied to the measurements in model ice. Justification of its use for the full scale ship will be made. The validation will include crack initiation and propagation, speed and cushion pressure, water curtain configuration under static and dynamic conditions, ice properties (ice thickness, strength and modulus) and air bubble observation.

TASK 6.0 - REPORTS

Results of the study will be presented to TDC as a series of interim reports at the end of each study phase. The work plan, summarizing the foregoing tasks, is given in Figure 29.

8.2 Project Team

The Project Manager will be Mr. F.R. Livingstone, P.Eng., a Vice President of Davis Engineering Limited. During his ten years employment with the Department of National Defence, Mr. Livingstone conducted both full scale and model testing programs using the Netherlands Ship Model Basin and the National Research Council Tank. He is currently managing a contract for the Transportation Development Centre related to the protection of propellers in ice. Mr. Livingstone managed the ACV/SES contract and brings that experience to this project.

Figure 29 Proposed Work Plan for Follow-on Study

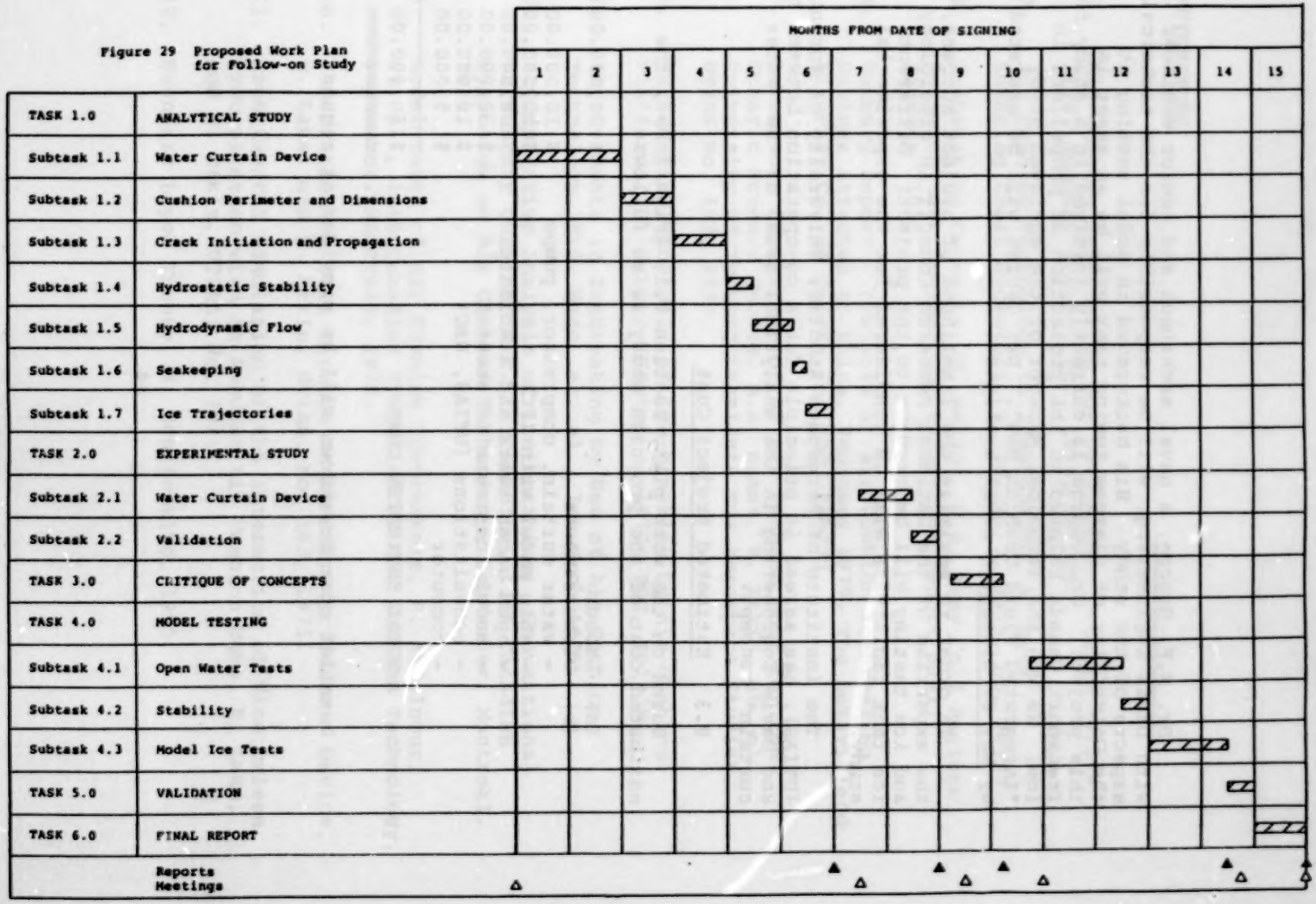

Figure 29 Proposed Work Plan for Follow-on Study

Dr. M.F. George, a naval architect and senior engineer with Davis Engineering, will be responsible for the technical aspects of the study. His background in model testing at the University of Glasgow towing tank will be an asset in this project. Dr. George is currently involved in a study for Transport Canada related to the protection of propellers in ice. He was the Technical Manager of the enclosed study "Integrated Fluid Cushion Bow". Dr. George will be assisted by Mr. D. Gibson, a naval architect.

In order to maximize the likelihood of project success, the expertise of the National Research Council in glaciology and ice testing will be brought to the project. Different ice tank facilities will be considered for the experimental study.

The Institute of Aerospace Studies, University of Toronto, (UTIAS), has agreed in principle for a co-operation between them and Davis Engineering in the analytical study of the "water curtain" concept.

8.3 Estimated Project Cost

Based on the work plan, Section 8.1, (Figure 29), the estimated cost of the proposed study is as follows:

(a)	Labour	$ 70,000.00
(b)	Disbursements	
	- water curtain, compressor, pumps	$ 10,000.00
	- ship model with IFCB	$ 10,000.00
	- open water tests and stability	$ 8,000.00
	- model ice tests (8 sheets)	$ 32,000.00
	- consultations (UTIAS, NRC)	$ 15,000.00
	- computer	$ 5,000.00
	TOTAL ESTIMATED COST	$150,000.00

Detailed cost breakdown will be provided at request.

REFERENCES

1. Air Cushion Icebreaking Bow Development Program 1975 - 1978, Summary Report, TDC, 1980, TP1924.

2. Air Cushion Technology in Icebreaking, R. Wade, Hovering Craft Hydrofoil, V. 14, N. 3, 1975, pp. 20-23.

3. Icebreaking Concepts, M. Mellor, U.S. Army Cold Regions Research and Engineering Laboratory Report 80-2, Hanover, 1980.

4. Summary Report - Analysis of Air Cushion Icebreaking Devices Attached to Ships, February 1979, The DeHavilland Aircraft Co. of Canada for TDC, TP1773.

5. Laboratory Simulation of An Air Cushion Roof for the Ontario Science Centre, A.A. Haasz, B. Etkin, et. al., University of Toronto Institute for Aerospace Studies, UTIAS No. 192, 1975.

6. Mathematical Analysis of Ice-breaking by Air Cushion Platforms, D. Carter, September 1977, TDC, TP1238.

7. Improvements in Icebreaking by Use of Air Cushion Technology, R.G. Wade, et. al., Ice Tech 1975.

8. A Comparative Analysis of Ice-breaking: Conventional Versus Air Cushion, J.E. Laframboise, 13th Canadian Symposium on Air Cushion Technology, September, Montreal, 1979.

9. Model Tests of Air Cushion Icebreakers, R. Abdelnour, et. al., 13th Canadian Symposium on Air Cushion Technology, September, Montreal, 1979.

10. Penetration of Rain Through an Annular Air Curtain Device, R. Lake, and B. Etkin, UTIAS, No. 163, 1971.

11. Experimental Simulation of the Interaction of Wind Driven Precipitation with an Annular Air Cushion Dome, R. Lake, and B. Etkin, UTIAS, No. 182.

12. Boundary Layer Theory, H. Schlichting, 1955.

APPENDIX A

Estimation of Water Jet Velocity and Power Required for Water Curtain

APPENDIX A

Estimation of Water Jet Velocity and Power Required for Water Curtain

As indicated in Section 6.2.2.2 (expression 6.27), the jet velocity V_{jet} at the exit of the jet is required as a boundary condition in the analysis of the dynamics and shape of the water curtain. Little is known about the detailed structure of the jet flow enclosing a pressurized zone. Extensive analytical and experimental studies are therefore required before qualitative and quantitative understanding can be achieved. However, with the lack of such understanding on water curtain behaviour, the following are some ideas to estimate the jet velocity and consequently the power required.

Consider a water jet of unit length perpendicular to the plan of the jet flow. From momentum considerations in y and z directions for regions I and II respectively (Figure A.1) one obtains:

$$z \omega h = \rho Q (V_{jet} \cos \alpha) \quad (A.1)$$

$$y \omega h = \rho Q (w_1 - V_{jet} \sin \alpha) \quad (A.2)$$

$$z_1 \omega h = \rho Q (v_2) \quad (A.3)$$

and $$y_1 \omega h = \rho Q (-w_1) \quad (A.4)$$

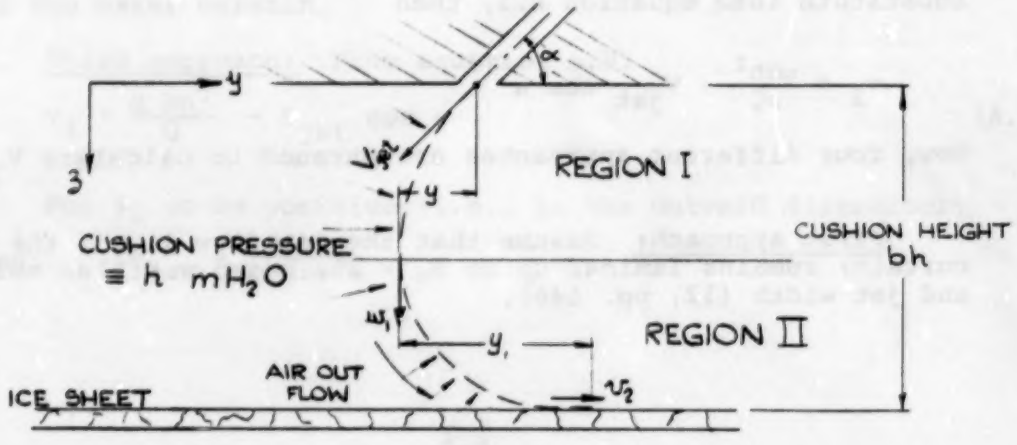

Figure A.1 Water Curtain Configuration

where h = cushion pressure head, m H_2O

Q = water volume flow rate (assumed contant), m^3/s

ω = water specific weight, N/m^3

ρ = water mass density, ω/g

v, w = water jet velocity in y and z directions, m/s

$$z + z_1 = bh \quad (\equiv \text{cushion height}) \tag{A.5}$$

Now, to ensure a perfect water curtain, let us assume that v_2 (i.e., the jet velocity at the bottom end) would be lower than that acquired by a free laminar jet flow. In practice, however, the flow becomes turbulent at a short distance from the point of discharge (12, pp. 483). Let us also assume that the jet is basically two-dimensional and the pressure is constant along the curtain.

Although the motion of the jet flow is in the absence of solid boundaries, it is nevertheless permissible to apply the boundary layer theory due to the friction between the water particles and the air.

If we assume that $y = y_1$, then from equations A.2 and A.4 one obtains:

$$w_1 = \frac{V_{jet} \sin \alpha}{2} \tag{A.6}$$

with $z_1 = bh - z$, then from equation A.3,

$$z = bh - \frac{\rho Q}{\omega h} v_2 \tag{A.7}$$

Substitute into equation A.1, then

$$v_2 = \frac{\omega b h^2}{\rho Q} - V_{jet} \cos \alpha \tag{A.8}$$

Now, four different approaches are pursued to calculate V_{jet}.

First approach: Assume that the jet flow (i.e., the water curtain) remains laminar up to $R_e \approx 30$, based on efflux velocity and jet width (12, pp. 146).

At the bottom end of the curtain, the width of the jet flow is t_2, then,

$$R_e = \frac{v_2 t_2}{\gamma}, \text{ with } \gamma = 0.18 \times 10^{-5} \text{ m}^2/\text{s for water at } 0^\circ$$

and since we assumed a constant volume flow rate then:

$$v_2 t_2 = V_{jet}\, t_o \sin \alpha \quad \text{where } t_o \text{ is the width of the jet}$$

at the point of discharge.

Therefore

$$30 > \frac{V_{jet}\, t_o \sin \alpha}{0.18 \times 10^{-5}}$$

With t_o, say, 0.05 m (2") and α, say, 60° (from Hℓ)

then $V_{jet} < 1.24 \times 10^{-3}$ m/s

which is clearly impractical due to the fact that the "stiffness" of the water curtain would not be sufficient to withstand either the inward-outward force resulting from the cushion pressure or the wind effects.

Second approach: Consider the critical $R_e = 2000$ as a limit for the laminar jet flow. Then:

$$\text{therefore } V_{jet} < \frac{2000 \times 0.18 \times 10^{-5}}{0.05 \times 0.866}$$

$$< 8. \times 10^{-2} \text{ m/s}$$

which is again impractical to provide a reasonable stiffness for the water curtain.

Third approach: From equation A.8:

$$v_2 = \frac{g\, bh^2}{Q} - V_{jet} \cos \alpha \qquad \text{(A.9)}$$

For v_2 to be positive (i.e., in the outward direction)

then: $$V_{jet} < \frac{g\, bh^2}{Q \cos \alpha}$$

With b = 0.5, h = 1.0 m, slot width t_o = 0.05 m and jet inclination $\alpha = 60^o$, then for a unit slot length:

$$Q = V_{jet} \times 0.05 \ m^3/s$$

Therefore

$$V_{jet} < 14 \ m/s$$

In order to provide adequate curtain "stiffness" the velocity of the water jet at the bottom end would have to be about, say, 0.25 V_{jet}. From expression A.8, then:

$$0.25 \ V_{jet} = \frac{g \ bh^2}{Q} - V_{jet} \cos \alpha$$

With the same parameter as chosen above, one obtains:

$$V_{jet} = 11.4 \ m/s$$

If, however, one could maintain a constant jet velocity along the curtain, then:

$$V_{jet} = 8 \ m/s$$

Fourth approach: The above condition which resulted in $V_{jet} = 8$ m/s is practically not possible. This impracticality is based on the characteristic behaviour of a jet flow. A "free jet flow" is known to increase in width and decrease in velocity in the downstream direction. In this aspect, the water curtain may be regarded as "forced" jet flow, in the sense that the cushion pressure exerts a force on the curtain. Although the dynamics of the "free" and "forced" jet flows may be different, it is permissible, at this stage at least, to assume that their general proportionality laws are similar in nature, but possibly with different constants. Now, for a "free" turbulent two-dimensional jet flow, the width of the jet increase in proportion to ℓ and the centreline velocity decreases in proportion to $\ell^{\frac{1}{2}}$, where ℓ is taken along the centreline of the jet in the downstream direction. As indicated in the text, the water curtain is curved inward first before the cushion pressure sends it in the outward direction. Depending on the geometry and pressure of the air cushion, the position of the jet slots, the jet discharge velocity and inclination and the height of cushion above the ice surface, the jet length along the curtain is, say, 20% in excess of the cushion height.

The velocity at distance ℓ along the centreline of the water curtain is given by (12, pp. 499 and 500):

$$v_2 = \frac{\sqrt{3}}{2} \sqrt{\frac{K\sigma}{\ell}}$$

where $\sigma = 7.67$ (obtained from experiments on free turbulent two-dimensional jet flows)

K = kinematic momentum per unit length perpendicular to the jet flow, and assumed constant and independent on ℓ

$= J/\rho$

and $J = \frac{4}{3} \rho v_2^2 \ell/\sigma$

Then $K = 0.104\ v_2^2$ (A.11)

and is assumed constant as mentioned above. The kinematic momentum of the jet flow at the point of discharge is given by:

$$K = J/\rho,\ J = \rho \int_{-t_o/2}^{-t_o/2} V_{jet}^2 \sin^2 \alpha\ dy$$

$$= \rho t_o V_{jet}^2 \sin^2 \alpha$$

with the assumption that the jet velocity V_{jet} is uniform across the jet at the slot exit.

Therefore $K = t_o\ V_{jet}^2 \sin^2 \alpha$ (A.12)

From A.11 and A.12, then:

$$V_{jet} = 1.67\ v_2 \quad \text{(A.13)}$$

One must remember that the volume rate of discharge in the jet flow, whether laminar or turbulent, increases in the downstream direction because air particles are carried away with the jet owing to friction on its boundaries. This effect is more appreciable of course in the case of turbulent jet flows.

CA1
DTC 801
81
C53
C.2

Library and Info... Centre
RECEIVED
NOV 9 1982
...da / Transports Canada

Now, if one substitutes the derived approximate relation A.13 into equation A.9, then:

$$V_{jet} = 9.5 \text{ m/s}$$

The net jet power is given by:

$$P = t_o \omega V_{jet}^3 / 2g$$

$$= \frac{0.05 \times 1000 \times 9.5^3}{2 \times 9.81 \times 75}$$

$$= 29 \text{ hp per 1 m slot length}$$

$$= 21.5 \text{ kW per 1 m slot length}$$

If one assumes a half elliptical cushion of 16 m wide and 16 m long, the slot length is about 40 m, and the net power required is:

$$P_{net} \simeq 865 \text{ kW (1150 hp)}.$$

With a pumping efficiency of about 0.7, the installed power for the water jet will be:

$$P_{inst} \simeq 1250 \text{ kW (1700 hp)}.$$

The power level of an ACIB (with say 50% increase in the pressure required (say 1 m H_2O) to compensate for the relatively low pumping efficiency due to leakages) is about 500 kW. The air loss in the water curtain concept is expected to be, say, half the 50% margin used above. Therefore, the power required for the air cushion for an equivalent IFCB will be about, say, 400 kW which would result in an estimated total power requirement of (water jets and air cushion):

$$P = 1650 \text{ kW}.$$

Savings in the power required for the water jets can be affected by optimizing the jet thickness, exit velocity, exit angle, and water flow temperature. Analytical predictions for such optimization must be validated experimentally as outlined, for example, in the Work Plan proposed in Section 8.1, Sub-Task 2.1.